

# *HYDROMORPHOLOGICAL LABORATORY MODEL*



University of Natural Resources and Life Sciences, Vienna  
WPT2/A.T2.1/D.T2.1.1, 2022

## **IMPRESSUM**

### **Authors:**

Mario Klösch, Johannes Schobesberger, Julia Sandberger, Fabian Franta, Lorenz Nagl,  
Christine Sindelar, Helmut Habersack

University of Natural Resources and Life Sciences, Vienna, Department of Water,  
Atmosphere and Environment, Institute of Hydraulic Engineering and River Research

### **Date:**

March 2022

### **Project Manager:**

Kerstin Böck

World Wide Fund for Nature Austria - WWF Austria

## Contents

I.	Introduction .....	6
•	General introduction.....	6
•	Problem statement .....	7
•	Experiences from the study site.....	8
•	State of general knowledge .....	17
•	Measures planned within lifelineMDD.....	19
•	Study aims .....	21
II.	Basics for physical modelling .....	23
III.	Methodology .....	28
•	Used scales for pilot site .....	28
•	Construction of the model .....	31
•	Measurement equipment.....	34
•	Modelled scenarios .....	37
•	Sediment transport calculation.....	40
•	Data analyses.....	41
IV.	Results .....	42
•	Status quo .....	42
•	Smaller-scale measure .....	46
•	Larger-scale measure .....	51
V.	Summary, conclusions & recommendations for action.....	63
VI.	References .....	67

## List of Figures

Figure 1. Map of the 5-country Biosphere Reserve Mura-Drava-Danube according to UNESCO designation in September 2021 (WWF Austria) -----	6
Figure 2. Mura River along the border between Austria and Slovenia in the TBR MDD and location of the pilot measure to be implemented in lifelineMDD -----	8
Figure 3. Mura River between the cities of Mureck and Bad Radkersburg in its historical state and in the state in the year 2000 (Habersack et al., 2001)-----	9
Figure 4. Hydropower plants in the catchment of the study site (Wagner et al., 2015).-----	9
Figure 5. Comparison of the areas per length of different types of watercourse (river km 108 – 110) in the years 1876 and 2000) (Jungwirth et al., 2001).-----	10
Figure 6. Riverbed incision in a cross section directly downstream of the pilot site at Gosdorf. -----	10
Figure 7. River restoration implemented at Gosdorf with its measure components (based on Klösch et al., 2011).-----	12
Figure 8. Bed level changes in and downstream of the restored section in Gosdorf between July 2008 and December 2009 (Habersack et al., 2013).-----	12
Figure 9. Bank erosion in a straight section of the Gosdorf measure during the flood event on July 22nd, 2012, five years after measure implementation (Habersack et al., 2013).-----	13
Figure 10. Change of mean bed elevation along the entire border section (Austria-Slovenia) of the Mura River, and in the cross section with greatest incision. -----	14
Figure 11. Types of measures for the Mura River along the border between Austria and Slovenia, taking into account the spatial constraints, all aiming at a dynamic equilibrium of the sediment balance through sediment replenishment and increased permeability of upstream barriers, with type C consuming the least amount of sediment while providing the greatest ecological benefit (Klösch et al., 2021).-----	15
Figure 12. goMURra-measure type C exemplified for a river section near Apace/Halbenrain. -----	16
Figure 13. Bedload efficiency increasing with size of the restoration measure, illustrated for the different measure variants developed in goMURra. The bedload efficiency is represented by the duration of effect of the sediment from one kilometre of construction as a supply to a section of the respective measure type and the duration of stay of a transported grain in the Grenzmur when implementing the respective measure type along the entire Grenzmur. -----	16
Figure 14. Measure types developed in goMURra, distributed along the river to achieve ecological and technical goals.-----	17
Figure 15. Dependency of morphology and channel stability from the amount of bedload supply and grain size (Church, 2006) -----	17
Figure 16. Development from a multiple channel system to a narrow channel after reduction of sediment input (Marti and Bezzola, 2009).-----	18
Figure 17. Dependence of morphology on bedload concentration according to Mueller and Pitlick (2014). $Q_{bf}$ is the bankfull discharge, $Q^*$ is a dimensionless flow, $s$ = the specific density of the sediment ( $\rho_s/\rho$ ) and $D_{50}$ the median grain diameter. The bedload concentration $C$ is calculated from the relation between the volumetric bedload transport at bankfull discharge and the bankfull discharge. $C_t$ is the bedload concentration at the transition between single-thread and braided channels. -----	18
Figure 18. A drafted target state including the Gosdorf section, a section on the southern Slovenian side, and another section already restored at the northern Austrian side.-----	19
Figure 19 a) Present state of the Gosdorf section, b) suggested measures of implementation, and c) exemplified target state after restoration. -----	20

Figure 20. Measures planned for implementation within the lifelineMDD project. Note that these measures were subject to changes during the process of approval by the authorities. -----	21
Figure 21. Shields diagram (Kobus 1984) -----	25
Figure 22. a) Plan view of the laboratory at BOKU University, b) detail of the model including the installed boundaries-----	31
Figure 23. a) Steel frame and b) sandwich panels -----	32
Figure 24. Grain size distribution of the sediments used in the model-----	32
Figure 25. a) Waterproof foil and b) sediment layer -----	33
Figure 26. Fixed river banks out of concrete and stones -----	33
Figure 27. Sediment feeder at the inlet of the model section. -----	34
Figure 28. Overview of the measured quantities/parameters and the used measurement systems. a) measurement of discharge with an IDM, b) measurement of water levels with a manual gauge and an ultrasonic sensor, c) survey of morphology using cameras for photogrammetry and a point laser -----	35
Figure 29. Used measurement device (Leica TS07) for surveying control points (b). -----	36
Figure 30. Overview of control points and three-dimensional surface points created by the photogrammetric software.-----	36
Figure 31. Overview of the Status quo based on the DEM of the initial state -----	38
Figure 32. Overview of laboratory model representing the smaller-scale measure. -----	39
Figure 33. Overview of the initial condition of the larger-scale measure. -----	40
Figure 34. Polygons used for the “zonal statistics” which overlay a DEM -----	41
Figure 35. Cumulative sediment input and output for the status quo. -----	43
Figure 36. Differences in the mean bed elevation expressed in nature scale for different model time periods per profile for the status quo-----	43
Figure 37. Differences in the cumulative volumes expressed in nature scale along the river for different model time periods in the status quo scenario.-----	44
Figure 38. Erosion and deposition in the status quo scenario, displaying the onset of incision when no sediment is supplied. -----	44
Figure 39. The wetted width at the discharge of 513 m <sup>3</sup> s <sup>-1</sup> in nature scale remaining relatively constant in the status quo scenario.-----	45
Figure 40. The mean bed elevation lowering in the status quo scenario at lacking bedload supply, analysed in the wetted width of mean discharge for definition of the riverbed. -----	46
Figure 41. Bed level changes when all bedload was supplied (model time 315min). -----	47
Figure 42. Bed level changes in the last recorded time step (255 min – 315 min).-----	47
Figure 43. The wetted width at the discharge of 513 m <sup>3</sup> s <sup>-1</sup> in the smaller-scale scenario in the period between the start and end of bedload supply. -----	48
Figure 44. The change in bed elevation between the start and end of bedload supply, analysed within the wetted width of mean discharge for definition of the river bed.-----	49
Figure 45. Application of the tool HyMoLink (Klösch et al., 2019) in a cross section of the smaller-scale measure: a) Systematic analysis of morphodynamic changes in a cross section, b) diagram relating elevation above water surface to elevation differences and counting the frequency of occurrence of each combination of classes.-----	50
Figure 46. Frequency of occurrence of elevation changes in different elevations for the investigated smaller measure. -----	51
Figure 47. Cumulative sediment input and output for the large measure, with volumes at nature scale related to model minutes. -----	53
Figure 48. Differences in the mean bed elevation $\Delta h$ for different time periods per polygon for the large measure -----	53
Figure 49. Differences in the cumulative volumes $\Delta V$ along the profiles for different time periods for the large measure. -----	54

Figure 50. Morphological changes between the beginning of the model run and the point in time, when the excavated sediment used as supply was consumed.-----	54
Figure 51. Morphodynamics in the large measure towards the end of sediment supply in the model time span between 1860 min and 1920 min.-----	55
Figure 52. Change of the average wetted width in the restored section following the implementation of the larger-scale measure.-----	55
Figure 53. change of the mean bed elevation in the wetted width of the restored section following implementation of the larger-scale measure.-----	56
Figure 54. Morphodynamics in a cross section displayed in cross-sectional view and in a diagram showing the frequency of elevation changes in different vertical positions in relation to the water table, for the model time intervals a) 540 min – 660 min, b) 660 min – 780 min, and c) 780 min – 900 min.-----	57
Figure 55. Morphodynamics in a cross section displayed in cross-sectional view and in a diagram showing the frequency of elevation changes in different vertical positions in relation to the water table, for the model time intervals a) 900 min – 1020 min, b) 1020 min – 1140 min, and c) 1140 min – 1260 min.-----	58
Figure 56. Morphodynamics in a cross section displayed in cross-sectional view and in a diagram showing the frequency of elevation changes in different vertical positions in relation to the water table, for the model time intervals a) 1260 min – 1380 min, and b) 1380 min – 1500 min.-----	59
Figure 57. Frequency of occurrence of elevation changes in different elevations for the investigated larger-scale measure.-----	60
Figure 58. Cumulative provision of habitats potentially of increased usability for rejuvenation of riverine species in the larger-scale measure.-----	61
Figure 59. Bare sediment surfaces created annually in the status quo, in the smaller-scale measure and in the larger-scale measure, calculated for a period corresponding to one year of bedload supply. Note that in the smaller-scale measure, all bedload supply may eventually be consumed within one year only.-----	62

## List of Tables

Table 1. Relationships of scales (Kobus 1984).-----	27
Table 2. Relationship of scales by neglecting the viscosity (Kobus 1984).-----	27
Table 3. Relationship of scales by neglecting the roughness condition (Kobus 1984).-----	28
Table 4. Main parameters or natural quantities of the Mura river at the pilot site in Gosdorf. Hydrologic data was obtained from the Hydrographic Service Styria-----	29
Table 5. Summary of the main scale numbers.-----	30
Table 6. Natural quantities transferred to mode scale:-----	30
Table 7. Hydraulic and sedimentological conditions for status quo.-----	38
Table 8. Hydraulic and sedimentological conditions for smaller-scale measure-----	39
Table 9. Hydraulic and sedimentological conditions for the larger-scale measure-----	40
Table 10. Summarized results of sediment input and sediment output under model and natural scales for the status quo-----	42
Table 11. Summarized results of sediment input and sediment output under model and natural scales for the smaller-scale measure.-----	46
Table 12. Summarized results of sediment input and sediment output under model and natural scales for the larger-scale measure-----	52

## I. Introduction

### • General introduction

The present report is the result of a study conducted within the DTP3-308-2.3 lifeline MDD, financed by the European Union’s Interreg Danube Transnational Programme. The area analysed in lifelineMDD comprises river sections in the 5-country Biosphere Reserve Mura-Drava-Danube (TBR MDD, Figure 1), shared between Austria, Slovenia, Hungary, Croatia and Serbia. Spanning Austria, Slovenia, Hungary, Croatia and Serbia, the lower courses of the Drava and Mura Rivers and related sections of the Danube are among Europe’s most ecologically important riverine areas. The three rivers form a “green belt” 700 kilometres long, connecting almost 1.000,000 hectares of highly valuable natural and cultural landscapes, including a chain of 13 individual protected areas and 3.000 km<sup>2</sup> of Natura 2000 sites. This is the reason why, in 2009, the Prime Ministers of Croatia and Hungary signed a joint agreement to establish the Mura-Drava-Danube Transboundary Biosphere Reserve across both countries. Two years later, in 2011, Austria, Serbia and Slovenia joined this initiative. Together with Croatia and Hungary, the five respective ministers of environment agreed to establish the world’s first five-country Biosphere reserve and Europe’s largest river protected area. Step by step the TBR MDD was realized: Hungary and Croatia (in 2012), Serbia (in 2017), Slovenia (in 2018) and Austria (2019) achieved UNESCO designation. The pentilateral designation was submitted in 2020 and designation finally achieved in September 2021.

#### 5-country Biosphere Reserve Mura-Drava-Danube (TBR MDD)\*

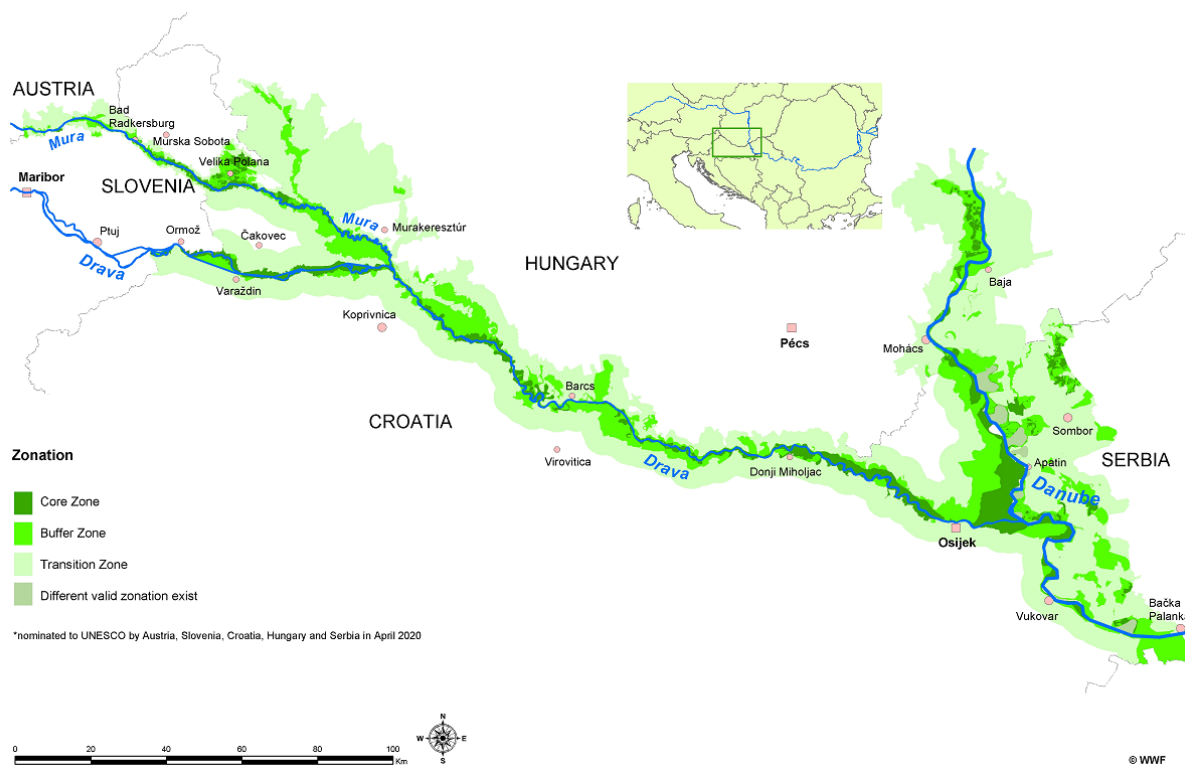


Figure 1. Map of the 5-country Biosphere Reserve Mura-Drava-Danube according to UNESCO designation in September 2021 (WWF Austria)

The aim of the project's work package for Cross-sectoral restoration of connectivity (Work Package T2) is to strengthen transboundary cross-sectoral cooperation between nature protection and water management and develop an integrated TBR MDD River Restoration Strategy. In this context, the Hydromorphological Laboratory model presented in this deliverable provides insights for consideration in restoration actions in the TBR MDD. The model investigates the conditions at the Mura River at the border between Austria and Slovenia, where the reduction of sediment supply is most noticeable given the short distance from the upstream chain of hydropower plants, while the large natural floodplain would allow lateral dynamics to occur. These boundary conditions are representative for most of the entire project region, hence should provide basic knowledge useful for future restoration actions in the TBR MDD.

- **Problem statement**

Historically, the Mur along the present-day border between Austria and Slovenia was a dynamic river landscape, which consisted to a large extent of several river branches and constantly changed its shape. The dynamics of the former anabranching and braided river morphology increasingly came into conflict with the human uses (agriculture, settlement, milling). Starting in the Middle Ages, local regulations were carried out until the Grenzmur was finally subjected to systematic channelization at the end of the 19<sup>th</sup> century.

While an increase in bedload transport capacity was initially desirable in order to cause a lowering of the bed to increase the discharge capacity between the riverbanks, the progressive erosion of the riverbed - intensified by the construction of hydropower plants and torrent control structures in the catchment area - increasingly became a problem for the fauna and flora as well as for the people living along the Mura River at the border between Austria and Slovenia. River managers increasingly became confronted with scouring and the resulting destabilisation of the bank protection structures. The reduced supply of groundwater from the incised Mura River caused problems in part for the drinking water supply and for agriculture. The narrowing and straightening caused an immediate loss of habitats for fauna and flora, and with progressing incision the situation aggravated given the progressive disconnection of the floodplain from the main channel through poorer connection of the mill channels, less frequent flooding and a lower groundwater level. Boreholes revealed a small thickness of the gravel layer, and the risk of a "riverbed breakthrough" into the finer sediment of the Tertiary.

The basic water management concept completed in 2001 (Austrian-Slovenian Standing Committee for the Mur River, 2001) designed countermeasures that were intended to stabilise the bed, at least temporarily, by artificially introducing gravel and allowing lateral erosion. In addition to the artificial addition of bedload, particular expectations were assigned to the erosion of the gravel-rich banks after bank restoration, which should have supplied the Mura River with bedload over a longer period of time and counteracted the bed incision. The positive effect of the subsequently implemented measures could be confirmed, but turned out to be smaller than expected, and the incision of the riverbed continued. The low thickness of the remaining gravel bed and the measured erosion rates indicate an urgent need for action.

Restoration actions implemented in the TBR MDD, such as the measure which is to be implemented at Gosdorf, need to consider the insights gained so far, and require further investigations on measure initiation and on the demand on sediment supply.

- **Experiences from the study site**

### Site characteristics

The studied site of pilot implementation at the Mura River is situated at the border between Austria and Slovenia near the village of Gosdorf (Figure 2).

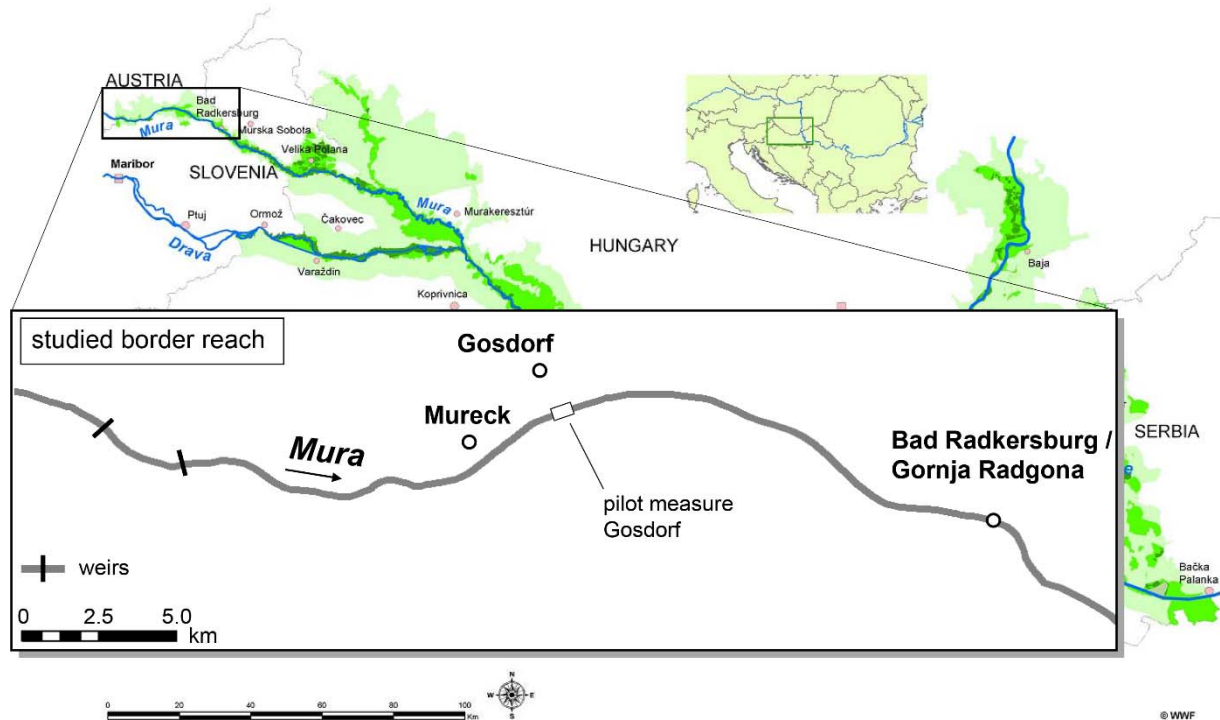


Figure 2. Mura River along the border between Austria and Slovenia in the TBR MDD and location of the pilot measure to be implemented in lifelineMDD

The Mura River along the border between Austria and Slovenia, once a river that was divided into up to seven adjacent channels and reached a width of up to 1.2 km, was

systematically channelized towards the end of the 19<sup>th</sup> century. The width was narrowed to 76 m and the course was straightened (Figure 3). All banks were protected by riprap.

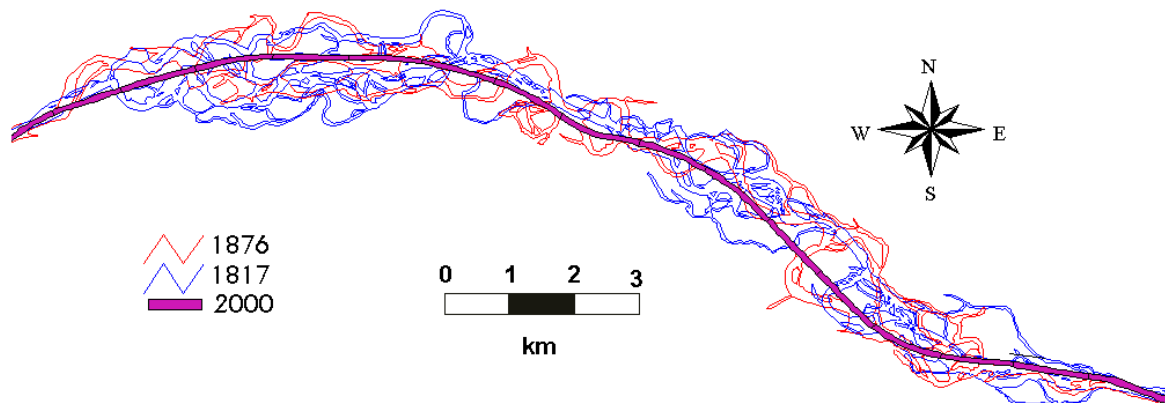


Figure 3. Mura River between the cities of Mureck and Bad Radkersburg in its historical state and in the state in the year 2000 (Habersack et al., 2001)

In addition, shortly afterwards, at the end of the 19<sup>th</sup> century, the construction of power plants was started on the Mura River, which, together with torrent control structures, interrupted the sediment connectivity. The study site is at the upstream end of the TBR MDD in close proximity to a series of hydropower plants (Figure 4).

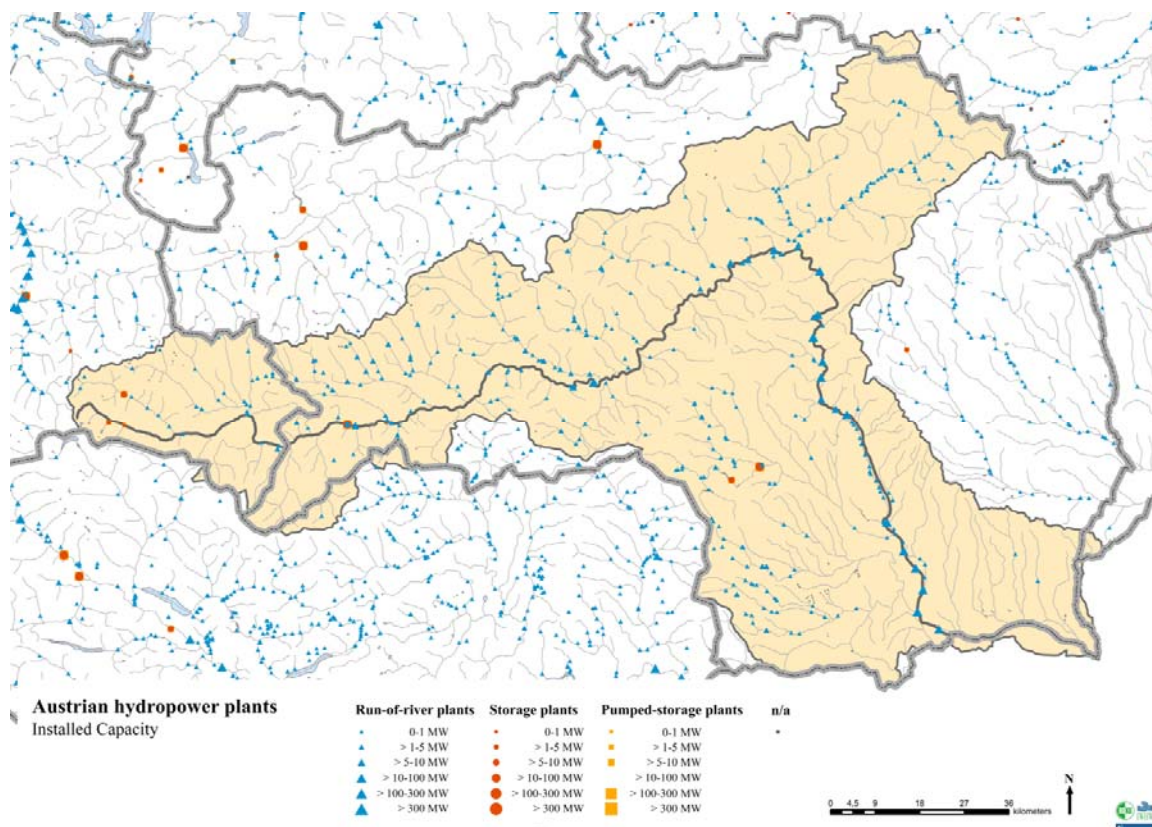


Figure 4. Hydropower plants in the catchment of the study site (Wagner et al., 2015).

The channelization had immediate ecological effects through the narrowing and the protection of the banks, but together with the increased bedload transport capacity in the channel and with the retention of bedload in the catchment area, the conditions for ecology even worsened through bed incision, as the floodplain and the mill channels increasingly disconnected from the main channel and from the groundwater. Figure 5 shows the change of the different types of surface water from the historical state to the state in the year 2000.

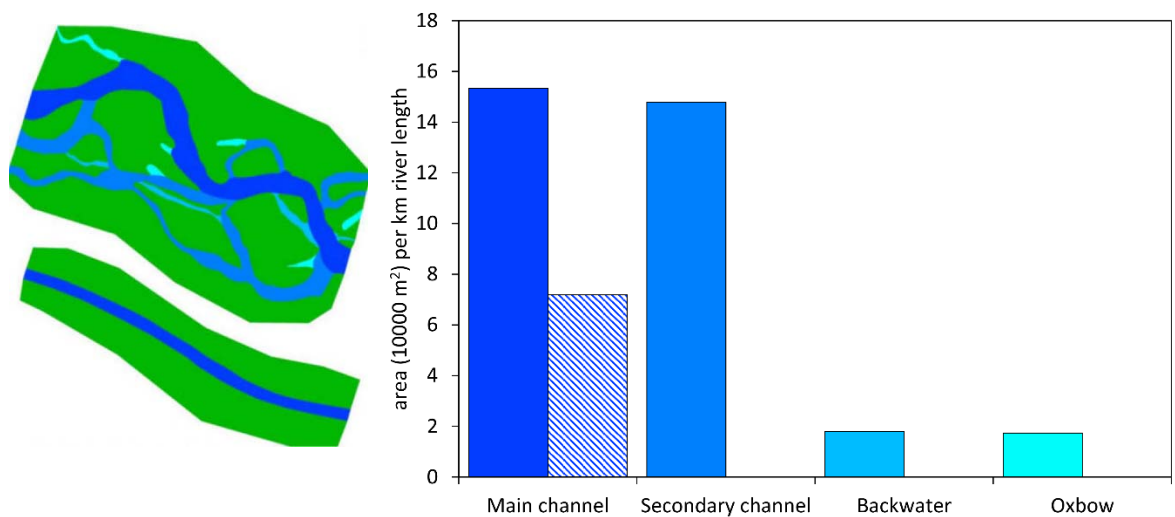


Figure 5. Comparison of the areas per length of different types of watercourse (river km 108 – 110) in the years 1876 and 2000) (Jungwirth et al., 2001).

In addition, the incision of the riverbed also had a negative impact on human uses along the Grenzmur, as well as on the stability of the bank protection structures themselves. Last but not least, the shallow gravel layer threatened with a complete loss of the gravel bed and a riverbed breakthrough into the finer tertiary (Figure 6).

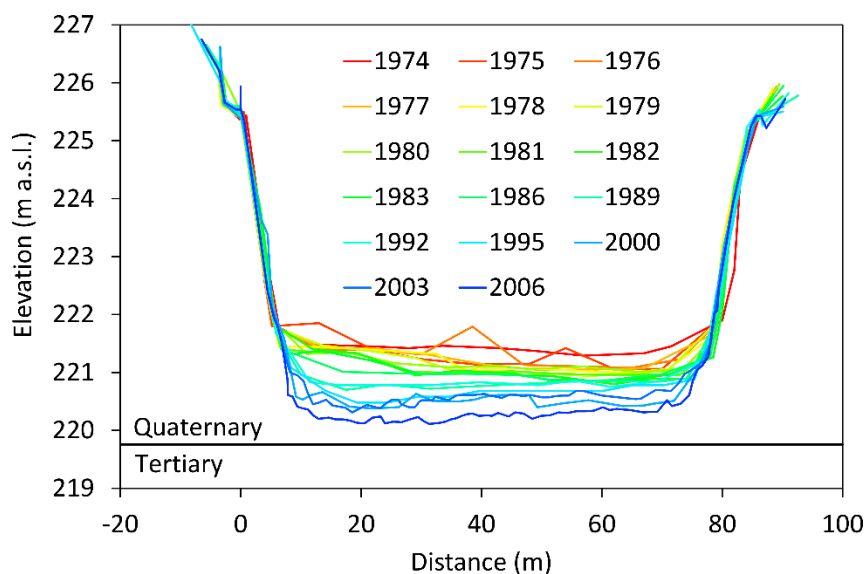


Figure 6. Riverbed incision in a cross section directly downstream of the pilot site at Gosdorf.

## **Restoration in 2006/2007**

To counter the adverse development, a basic water management concept was created on behalf of the Austrian-Slovenian Standing Committee for the Mura River in the period between 1998 and 2001, which, based on detailed investigations, also contained a draft of countermeasures.

In 2006 and 2007, a respective major measure was implemented at Gosdorf in the section between river kilometre 114.980 and 116.040 (Figure 7). The basic water management concept saw the greatest urgency for the implementation of a measure in this section, as the distance to the tertiary was very short there. The bank protections were removed from the Austrian bank over a length of one kilometre, and an excavation of 150,000 m<sup>3</sup> of sediment served as an immediate supply for a local increase of the bed levels and for dotation of the channelized section downstream. In addition, the Mura River was supposed to widen dynamically, to supply its bed with the eroded bank sediment and to reduce its transport capacity by increasing the channel width. In the bedload transport modelling (Hengl. et al., 2001) applied within the framework of the basic water management concept, which served to optimise the implementation of measures in the Austrian-Slovenian border section of the Mura River, it was assumed that the Mura River would widen to 150m within 17 years and would be supplied with sediment from bank erosion over this period. According to the calculations in the basic water management concept, further measures would have stabilised the riverbed for a period of 60 years, thus bridging a long period of time until a possible solution for the restoration of the sediment connectivity from upstream.

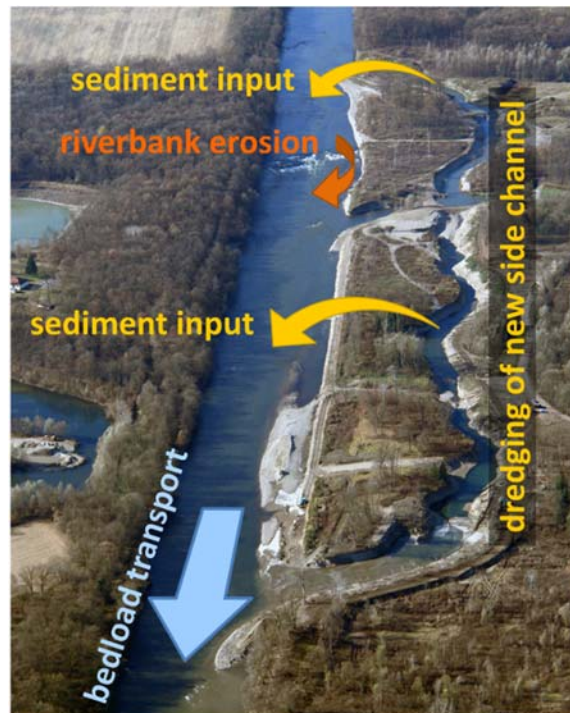


Figure 7. River restoration implemented at Gosdorf with its measure components (based on Klösch et al., 2011).

The countermeasure initially had a stabilising effect, also on the channelized section downstream (Figure 8).

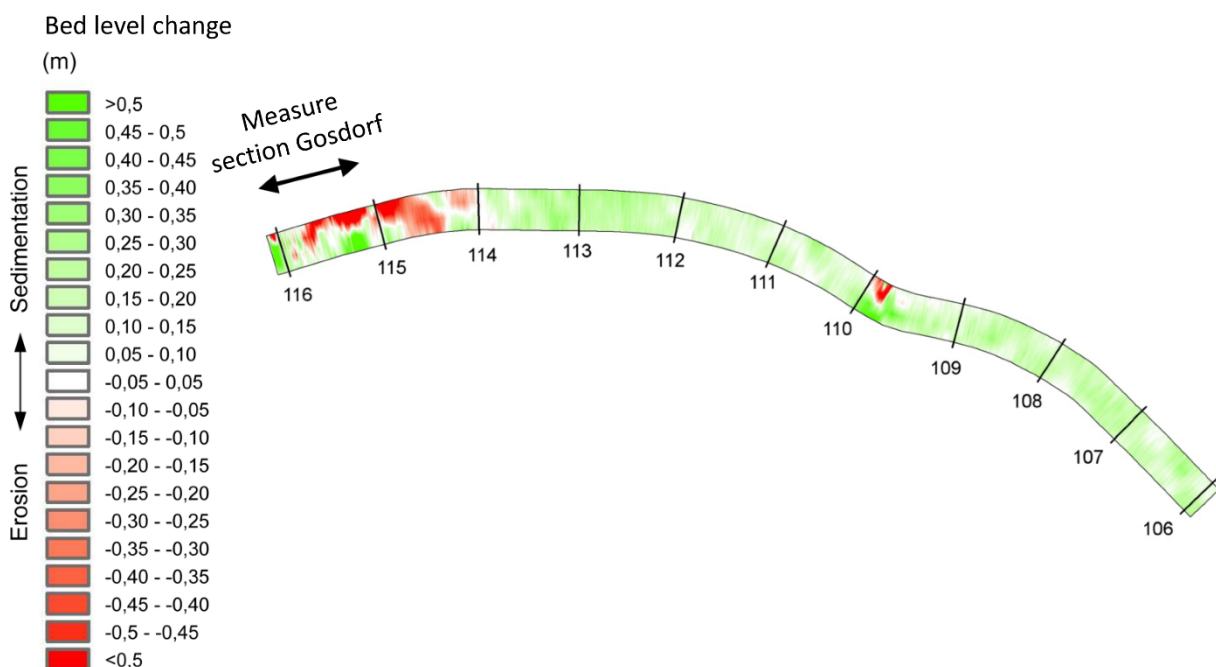


Figure 8. Bed level changes in and downstream of the restored section in Gosdorf between July 2008 and December 2009 (Habersack et al., 2013).

However, due to the negligible bedload input from upstream in the widening section at Gosdorf, there were no bars forming in the channel which would have deflected the flow

towards the banks. As a result, there was only little widening pressure and only little bedload was introduced from the banks by the river's own dynamics, so the effect of the measure lasted for a shorter time than expected. During a flood almost reaching the discharge of a 10-years flood, a straight bank section revealed a bank retreat of only about 1 m (Figure 9).

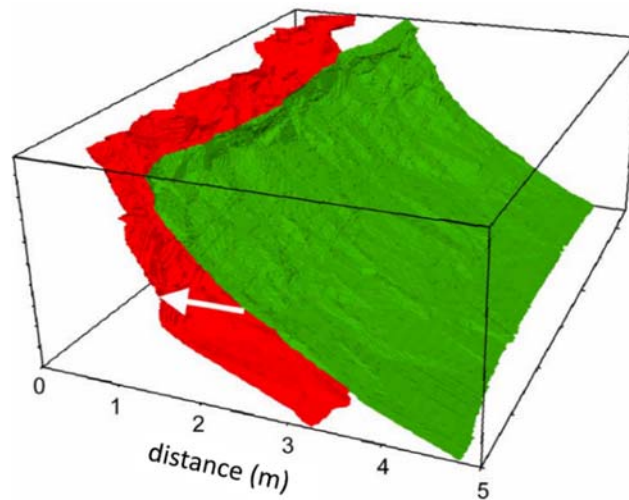


Figure 9. Bank erosion in a straight section of the Gosdorf measure during the flood event on July 22<sup>nd</sup>, 2012, five years after measure implementation (Habersack et al., 2013).

An updated analysis of the development of the river bed elevations along the border between Austria and Slovenia, carried out in the course of the parallel study in lifelineMDD (D.T1.2.3), showed that the incision of the river bed resumed unexpectedly quickly. Currently, the average height of the riverbed is below the level before the implementation of the countermeasures (Figure 10). From the now even smaller distance to the Tertiary as well as from the overall even higher pressure on biodiversity, an urgent need for restoration was derived.

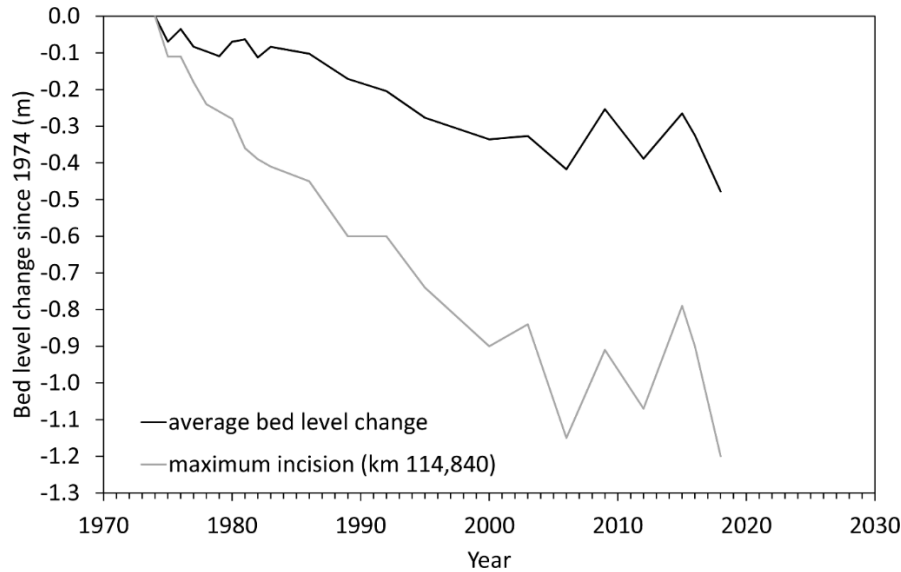


Figure 10. Change of mean bed elevation along the entire border section (Austria-Slovenia) of the Mura River, and in the cross section with greatest incision.

## Measures recommended by the goMURra project

In the bilateral EU Interreg V-A SI-AT project goMURra new measure types were developed as a part of a 'Management Plan 2030'. These measure types account for the need of bedload supply from upstream, while aiming to reduce the transport capacity and hence the bedload requirement of the river. Based on analyses of spatial demands and space availability (Senfter et al., 2021), three types of measures were defined (Klösch et al., 2021). All three types of measures address the parameters crucial for bed stabilisation (channel width and slope) to varying degrees, depending on the size of the space provided. It was hypothesised that as the size of the measure type increases, the bedload transport capacity decreases, so that the bedload requirement for stabilising the bed elevations decreases. The three types of measures can be characterised as follows (and are summarised in Figure 11):

**Measure type A:** Here, the channel is widened to an average of approx. 150 m by widening the main branch or by creating a side branch. The increase in channel width causes a small reduction in bedload transport capacity. The gradient is not changed, or only to a very limited extent, so that the contribution of a reduction in gradient remains small. The amount of bedload required to stabilise the bed elevations remains high. The length of the widening is limited, but extends over at least one kilometre. This minimum length ensures that the morphology can also make use of the width provided.

**Measure type B:** Here, a continuous corridor of approx. 220 m width is provided, which, in addition to the increased channel width, also allows for a slight oscillation of the river course and slightly reduces the gradient due to the sinuosity made possible. A medium bed stabilising effect of the measure is assumed, and a medium amount of bedload supply would be necessary to maintain the bed heights.

**Measure type C:** In this case, the channel width is unconstrained (and estimated to reach approx. 220 m), hence able to migrate to a certain extent within a corridor of greater width, as well as greater curvature, which reduces the gradient. Banks are protected only along the outer banks of bends, if necessary. The greatest bed stabilising effect can be assumed from the strong increase in channel width with simultaneous strong reduction of the gradient, which necessitates the smallest bed load. Due to the low degree of constraints, the largest areas of different morphological units and the expected morphodynamics, this type can be assumed to have the greatest ecological effect.

For comparison, a **measure type 0** was also defined, in which the geometry corresponds to the current state, but a corresponding supply of bedload stabilises the bed. According to the hypothesis, it is assumed that type 0 requires the most bedload supply to maintain the bed levels. Measure type 0 is not to be confused with the actual state, as there is currently no such bedload input and the riverbed is incising.

The functionality of these measure types was then confirmed in numerical investigations. Depending on the availability of space, intermediate forms can also be chosen for implementation in the Grenzmur.




	Channelized reference	Restoration type A	Restoration type B	Restoration type C																
Planform																				
Space need	Channelized width (~80m bank top width)	Small (150m)	Medium (220m)	Large (220m, if possible larger corridor)																
Width	Channelized width	Small channel widening or side channel	Large channel widening, but with side and mid-channel bars	River channel 220m, Corridor > 220m – higher morphodynamics, more bank erosion, bars																
Sinuosity and slope	Only „sinuosity“ of channelized course, higher slope	No/Little sinuosity added to channelized course, no slope change	Minor increase of sinuosity, minor decrease of slope	Higher sinuosity, lower slope																
Bank protection	All banks protected	Higher percentage of fixed banks	Frequent existence of bank protection	Bank protection focuses on outer banks where necessary																
Parameter setting	<table border="0"> <tr> <td>Channel width</td> <td>Sinuosity</td> </tr> <tr> <td></td> <td></td> </tr> </table>	Channel width	Sinuosity			<table border="0"> <tr> <td>Channel width</td> <td>Sinuosity</td> </tr> <tr> <td></td> <td></td> </tr> </table>	Channel width	Sinuosity			<table border="0"> <tr> <td>Channel width</td> <td>Sinuosity</td> </tr> <tr> <td></td> <td></td> </tr> </table>	Channel width	Sinuosity			<table border="0"> <tr> <td>Channel width</td> <td>Sinuosity</td> </tr> <tr> <td></td> <td></td> </tr> </table>	Channel width	Sinuosity		
Channel width	Sinuosity																			
																				
Channel width	Sinuosity																			
																				
Channel width	Sinuosity																			
																				
Channel width	Sinuosity																			
																				
Effect on river bed stabilisation	Zero	Minor	Mean	High																
Required sediment input	Very high	High	Medium	Low																

Figure 11. Types of measures for the Mura River along the border between Austria and Slovenia, taking into account the spatial constraints, all aiming at a dynamic equilibrium of the sediment balance through sediment replenishment and increased permeability of upstream barriers, with type C consuming the least amount of sediment while providing the greatest ecological benefit (Klösch et al., 2021).

In Figure 12, the morphology of type C is exemplified for a river section near the villages Apace/Halbenrain.

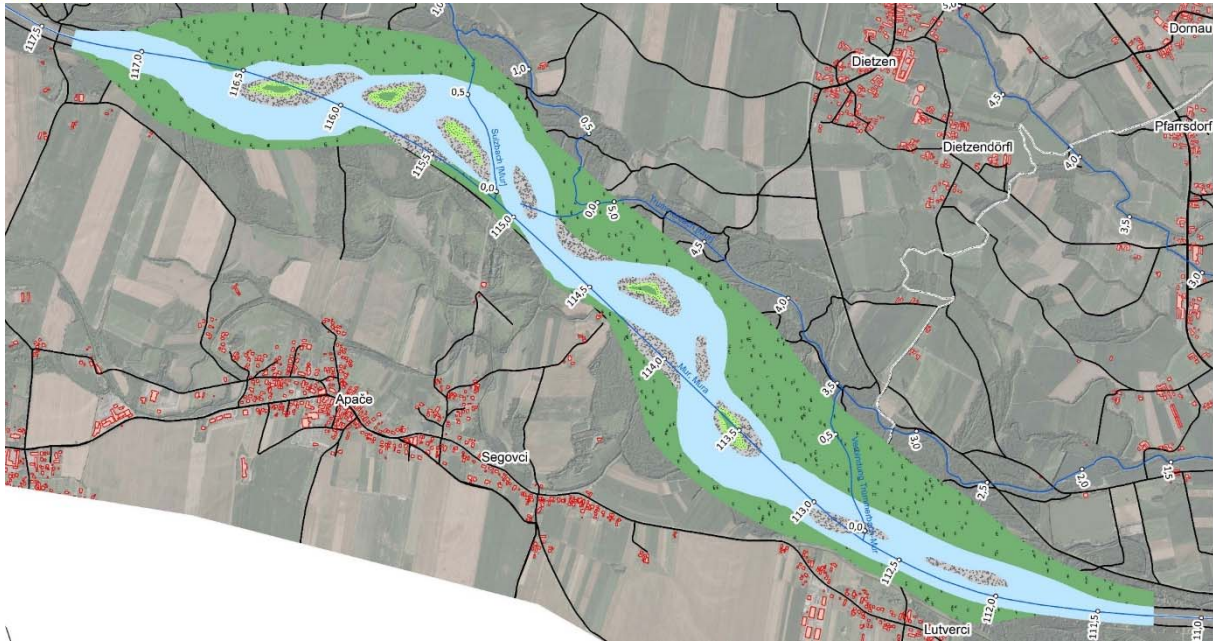


Figure 12. goMURra-measure type C exemplified for a river section near Apáče/Halbenrain.

With increasing measure size, more material becomes available which may be supplied from upstream. Together with the reduced transport capacity, the duration of effect of the measure increases. The reduced transport capacity is also evident from the longer residence time of bedload in the Grenzmur (Figure 13).

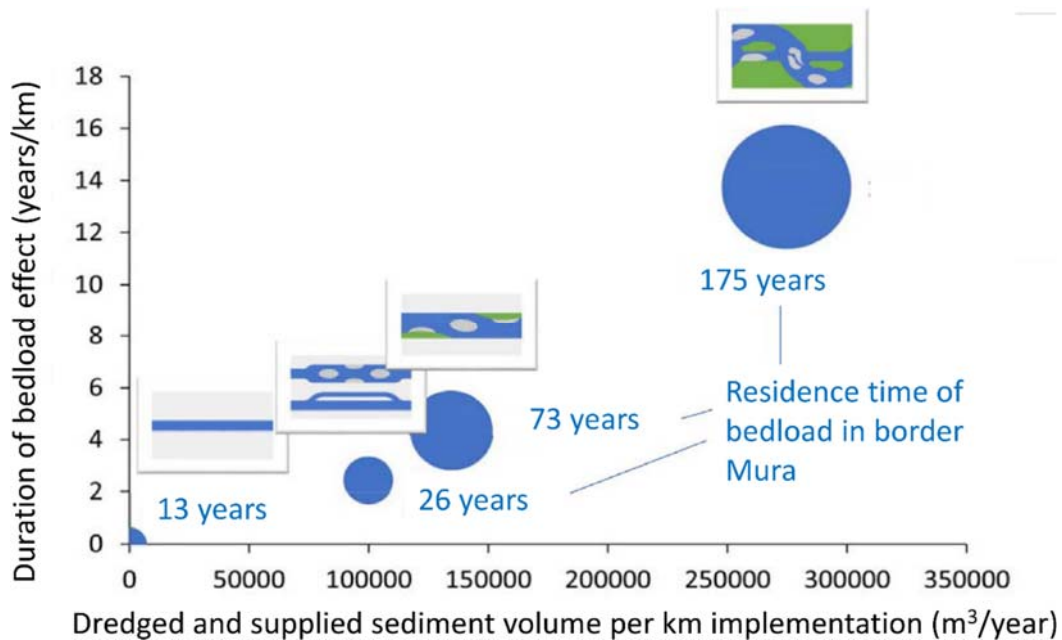


Figure 13. Bedload efficiency increasing with size of the restoration measure, illustrated for the different measure variants developed in goMURra. The bedload efficiency is represented by the duration of effect of the sediment from one kilometre of construction as a supply to a section of the respective measure type and the duration of stay of a transported grain in the Grenzmur when implementing the respective measure type along the entire Grenzmur.

Depending on the availability of space along the river, the measure types can be put in sequence, which would achieve ecological as well as technical goals which were defined in goMURra (Zupancic et al., 2021).

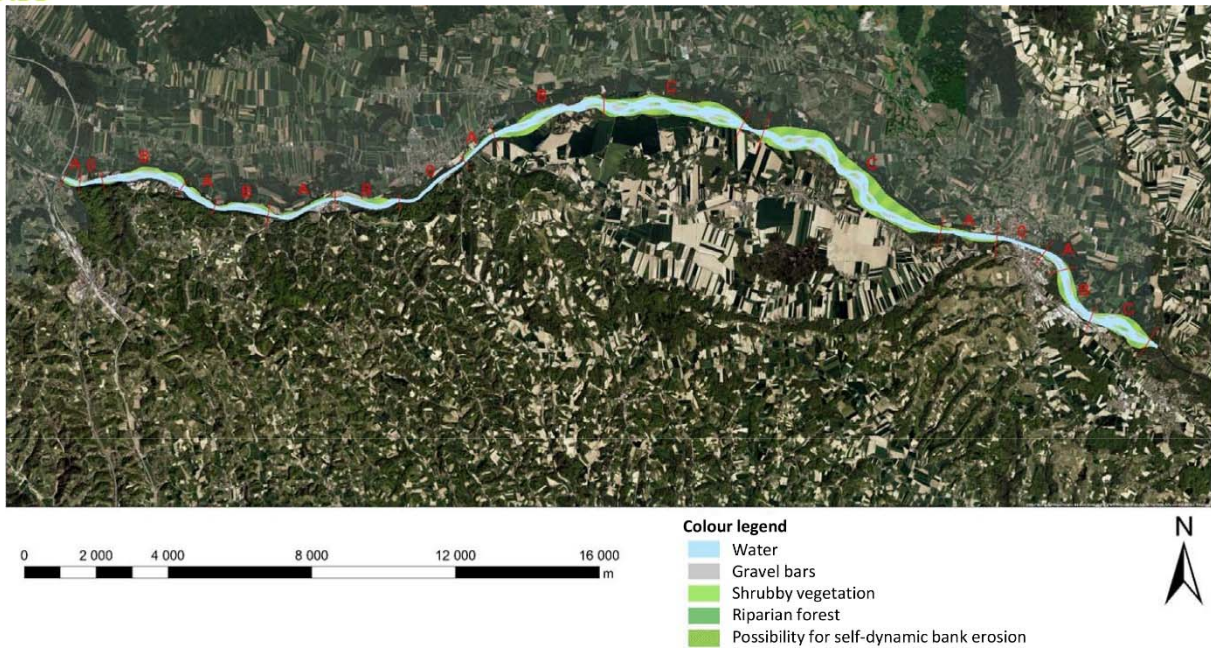


Figure 14. Measure types developed in goMURra, distributed along the river to achieve ecological and technical goals.

● **State of general knowledge**

In addition to the knowledge gained at the study site, general knowledge is compiled that deals with the interactions between sediment supply and morphology.

From observations, Schumm (1985) and Church (2006) derived correlations between sediment quantity, grain size and the emerging morphology. According to their findings, the emerging morphology is strongly dependent on sediment input. For a river that can form its bed in its own alluvium, greater sediment input means a greater channel width and/or a more pronounced curvature, as well as greater lateral dynamics and a greater tendency to divide into multiple branches (Figure 15).

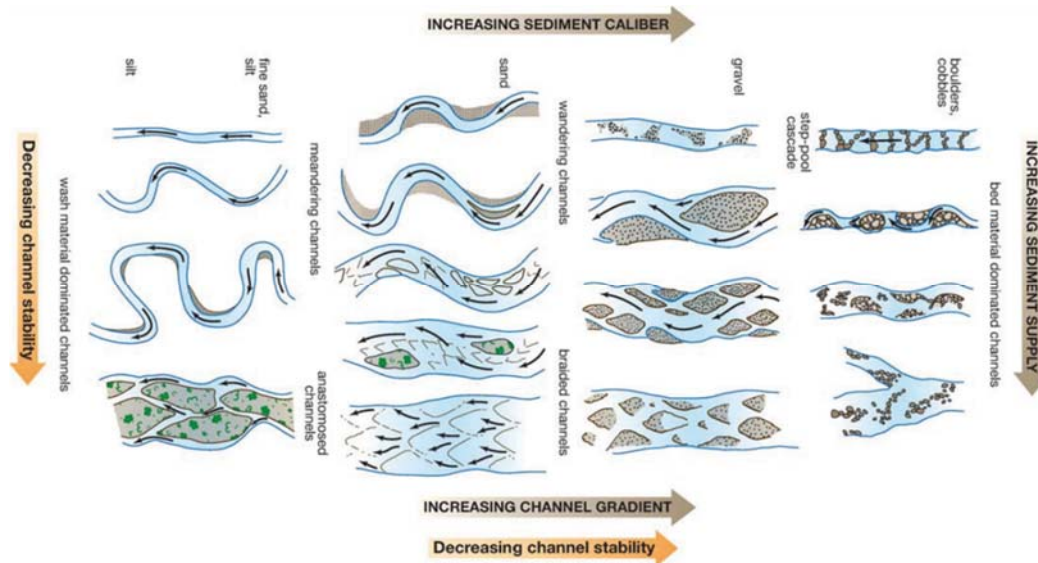


Figure 15. Dependency of morphology and channel stability from the amount of bedload supply and grain size (Church, 2006)

Conversely, channel width and lateral dynamics decrease strongly when sediment input is reduced. Marti and Bezzola (2009) confirmed this morphological relationship in a laboratory experiment (Figure 16).

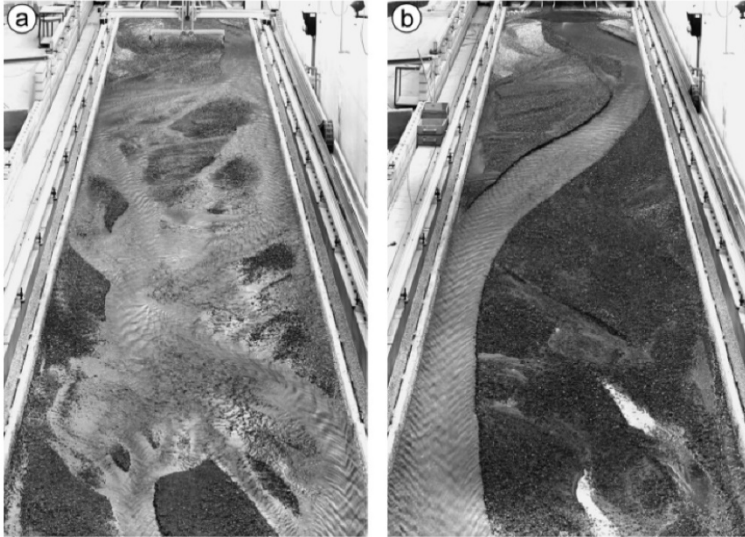


Figure 16. Development from a multiple channel system to a narrow channel after reduction of sediment input (Marti and Bezzola, 2009).

Mueller and Pitlick (2014) were also able to establish the dependence of morphology on bedload concentration. They classified rivers with known bedload transport according to their morphology and were able to define a threshold value for a transition from single-thread channels to braided channels (Figure 27). The threshold value depends on the discharge of the respective channel.

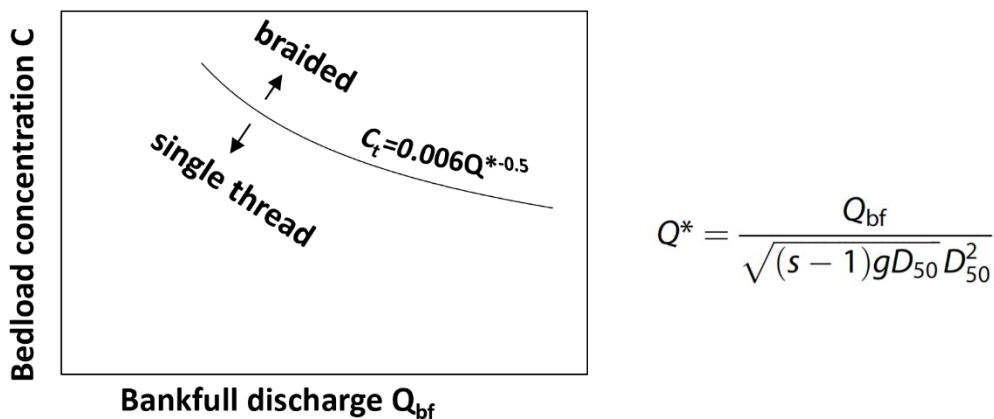


Figure 17. Dependence of morphology on bedload concentration according to Mueller and Pitlick (2014).  $Q_{bf}$  is the bankfull discharge,  $Q^*$  is a dimensionless flow,  $s$  = the specific density of the sediment ( $\rho_s/\rho$ ) and  $D_{50}$  the median grain diameter. The bedload concentration  $C$  is calculated from the relation between the volumetric bedload transport at bankfull discharge and the bankfull discharge.  $C_t$  is the bedload concentration at the transition between single-thread and braided channels.

Note that the rivers studied by Schumm (1985), Church (2006) and Mueller and Pitlick (2014) were in a dynamic equilibrium, while a river before and after restoration actions usually is in a strong disbalance, and the initial reaction of the river differs from a state in dynamic equilibrium. This needs to be considered when monitoring the effectiveness of

measures. To reach a dynamic equilibrium, in rivers such as in the TBR MDD a sustaining bedload supply is required next to removing channel constraints.

- Measures planned within lifelineMDD**

Considering the lack of dynamics in the Gosdorf section, one recognised option for restoration was to ‘re-restore’ the section based on the insights gained since the last restoration action in 2006 and 2007. The advantage in selecting this section was that the floodplains near Gosdorf along the left bank have already been purchased from the private property owners in the course of the last measure implementation in 2006 and 2007, and that the space available allowed a measure of significant size.

The types developed in goMURra were used to draft a target state at Gosdorf. One such drafted target state included sections downstream, which would allow increased curvature over a length of approximately 2 km (Figure 18).

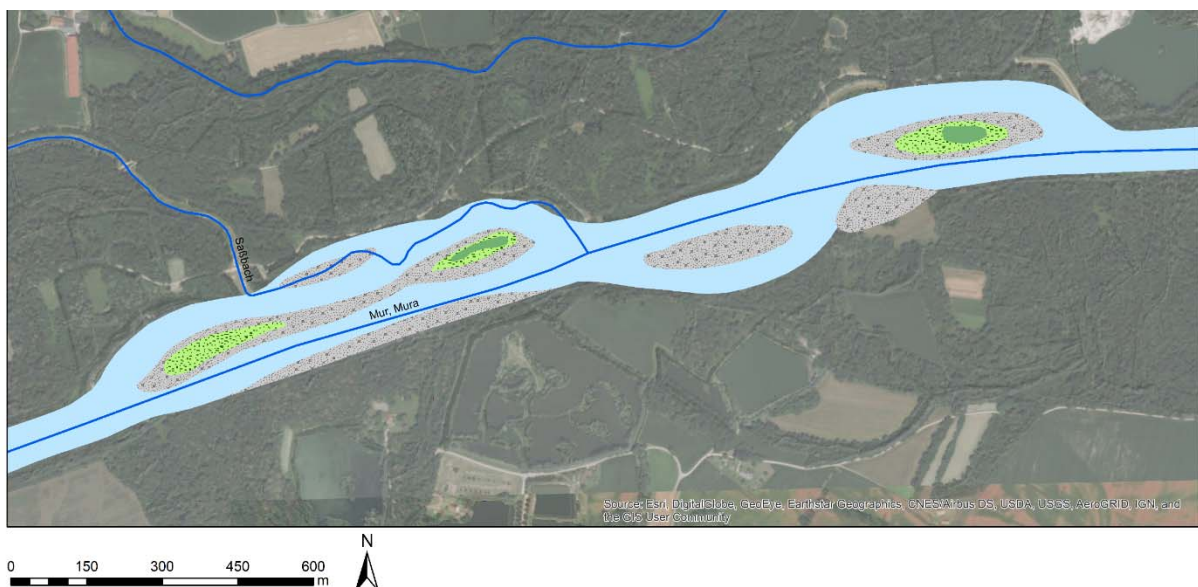


Figure 18. A drafted target state including the Gosdorf section, a section on the southern Slovenian side, and another section already restored at the northern Austrian side.

Considering the time constraints of the project, investigations were then limited to the section at Gosdorf 1 km in length as a first step of a larger-scale implementation (Figure 19). As initiation measure, the excavation of a new main channel should cause an immediate increase of curvature, but also an immediate increase in width, both following recommendations from the goMURra-project. An inlet structure protecting the island head from erosion should help deviating the main channel flow into the left floodplain (Figure 19b).

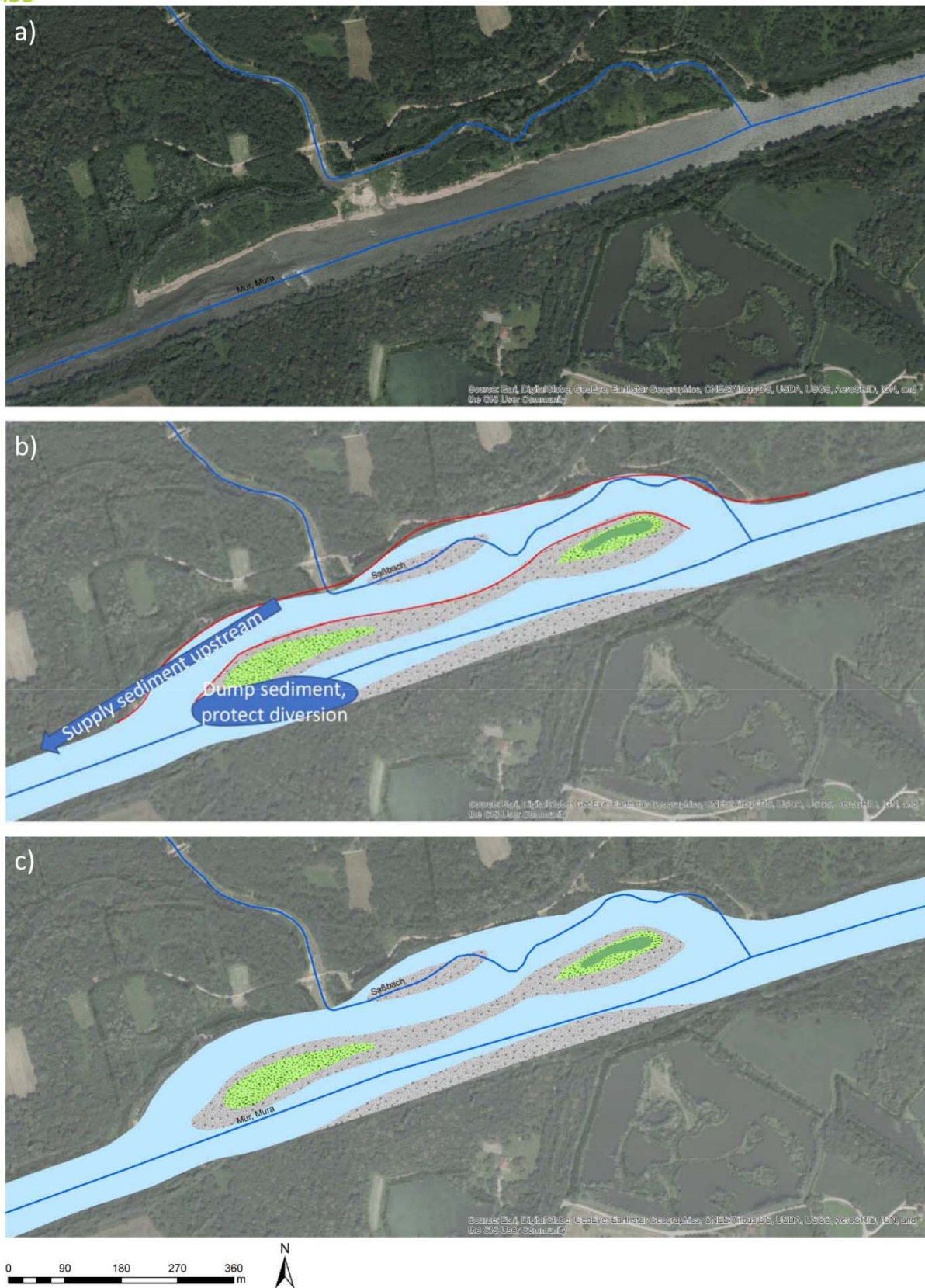


Figure 19 a) Present state of the Gosdorf section, b) suggested measures of implementation, and c) exemplified target state after restoration.

Finally, the planning process showed that the costs of this measure would exceed the project budget, and the planner had to restrict the implementation to a smaller measure as a first step, which can be extended to finally obtain the larger target state. The planned measure is restricted to the upstream part of the Gosdorf section, and included the excavation of a side-channel, the construction of an inlet structure and the excavation of an embayment in the bank line of the main channel. Importantly, the excavated sediment is reinserted upstream and hence made available as sediment supply to trigger morphodynamics in this section.

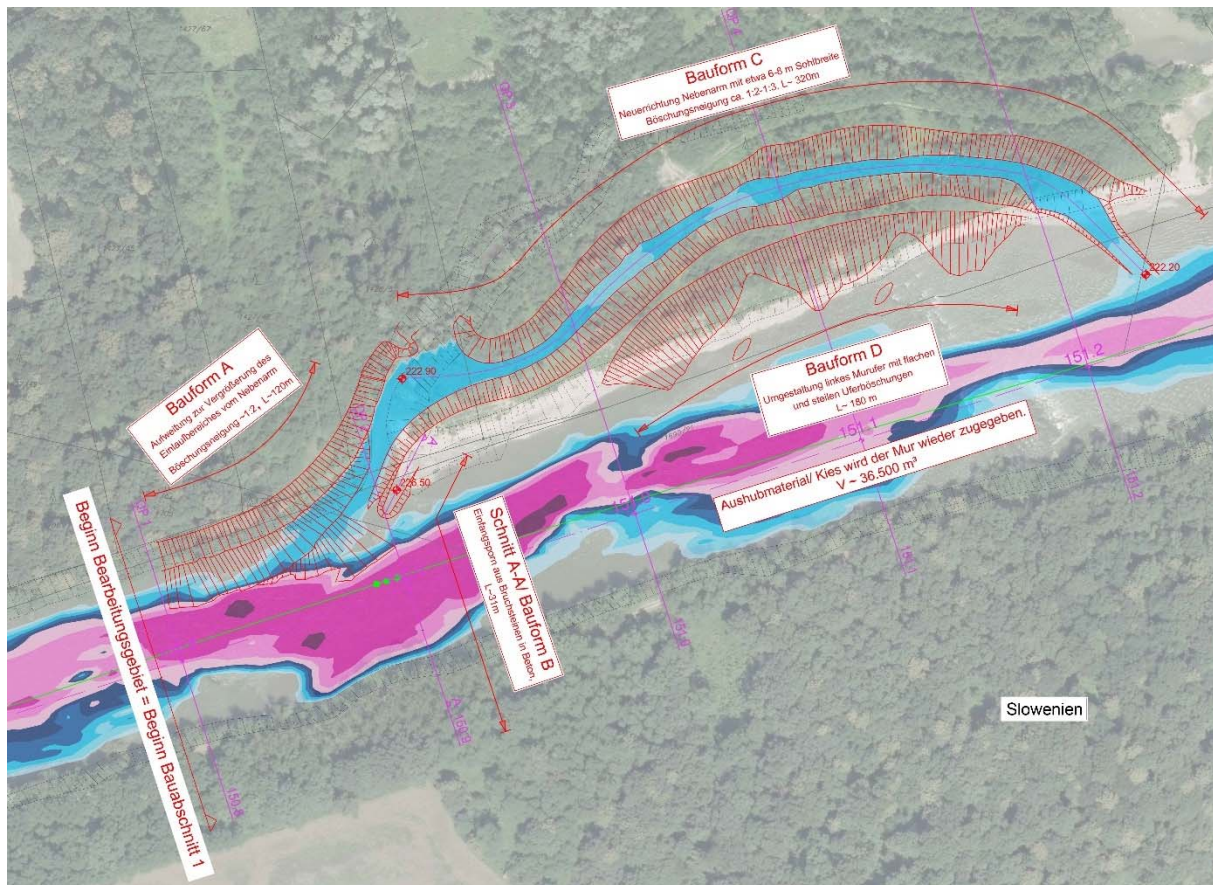


Figure 20. Measures planned for implementation within the lifelineMDD project. Note that these measures were subject to changes during the process of approval by the authorities.

While this state of the planning documents was considered in the laboratory experiments, the plan slightly changed as it went through the process of approval at the authorities.

- Study aims**

The undiminished risk of riverbed breakthrough, as well as the urgent need to restore biodiversity requires the implementation of measures on the new knowledge of cause and effect. In this context, consideration of sediment transport is of central importance. The present study aims to support measure implementations with additional knowledge gained from the application of a physical hydromorphological laboratory model. The aims are to investigate the role of channel width, channel curvature, sediment supply and measure size for the exemplified pilot site at Gosdorf. The data analyses focus on the success in countering bed incision and in the provision of critical habitats for rejuvenation

of riverine species. Finally, the aim is to provide basic knowledge useful for future restoration actions in the TBR MDD.

## II. Basics for physical modelling

Physical modelling is used to simulate mostly complex problems in hydraulic engineering. For that purpose, the natural processes are typically down-scaled. The controlled conditions in the laboratory setting allow repeatable experiments. For the correct design and implementation of the experiments, it is important to consider similitude and model laws. Based on the consideration of the similitude, processes can be transferred between nature and the model. In following chapters natural parameters and model parameters are indicated with the subscripts “n” and “m” respectively.

The similarity of models can be divided into geometric, kinematic and dynamic similarity. If the geometric lengths between nature and the model are in a constant ratio, the model can be considered geometrically similar. This ratio describes the scale number  $L_r$  which is calculated as follows:

$$L_r = \frac{L_n}{L_m} \quad (1)$$

In kinematically similar models, the time intervals between natural and model processes are put into a ratio, resulting in the time scale number  $t_r$ :

$$t_r = \frac{t_n}{t_m} \quad (2)$$

Dynamic similarity is defined by constant force ratios between forces occurring in nature and in the model. The force scale number  $F_r$  is calculated as follows (Kobus 1984):

$$F_r = \frac{F_n}{F_m} \quad (3)$$

Several important model laws for hydraulic engineering experiments can be derived from the similarity laws. Euler's model law, Reynolds' model law, Weber's model law, Cauchy-Mach's model law and Froude's model law should be mentioned here. It has to be mentioned that not all natural quantities can be scaled with reasonable effort e.g., the water mass density,  $\rho$ , gravitational acceleration,  $g$ , kinematic viscosity,  $\nu$ , specific weight,  $\gamma$ , and dynamic viscosity,  $\mu$ , of water, hence the scale ratios are constrained to be 1:

$$\rho_r = \frac{\rho_n}{\rho_m} = 1; \quad g_r = \frac{g_n}{g_m} = 1; \quad \nu_r = \frac{\nu_n}{\nu_m} = 1; \quad \gamma_r = \frac{\gamma_n}{\gamma_m} = 1; \quad \mu_r = \frac{\mu_n}{\mu_m} = 1 \quad (4)$$

Therefore, a complete similitude between natural and model processes is not possible and an approximation of the similarity based on the main quantities and forces should be achieved (Kobus 1984).

Since this study focuses on a free water flow which is a gravity governed process the so-called Froude model law was used based on Kobus (1984). The basic requirement here is that the Froude numbers  $Fr$ , as defined in equation (5), correspond to each other in nature

and in the model. Here  $v$  is the flow velocity and  $L$  a characteristic length (usually the water depth).

$$Fr = \frac{v}{\sqrt{g \cdot L}} ; Fr_r = \frac{Fr_n}{Fr_m} = 1 \quad (5)$$

Using  $Fr$ , it is possible to differentiate the flow conditions between sub critical ( $Fr < 1$ ) and super critical ( $Fr > 1$ ). In water flows, the internal viscous frictional forces always act simultaneously with gravity, so that the ratio of inertial and viscous forces, the so-called Reynolds number,  $Re$ , must also be considered (Kobus 1984):

$$Re = \frac{L \cdot v}{\nu} \quad (6)$$

However, without changing the viscosity of the fluid it is not possible to achieve the equality of the Froude and Reynolds number in scaled models. This was mentioned here, for the sake of completeness.

Since one of the main objectives of this study was the investigation of the sediment transport and further of the morphodynamic processes it was crucial to ensure similarity of the grain Froude number  $Fr^*$ .  $Fr^*$  represents the Shields number, which is recognised as the variable determining bedload in most bedload formulas. Further, the particle Reynolds number  $Re^*$  also has to be considered.

$$Fr^* = \frac{\rho}{\rho_s - \rho} \cdot \frac{v_*^2}{g \cdot d} ; Re^* = \frac{v_* \cdot d}{\nu} \quad (7)$$

Here,  $\rho_s$  is the sediment density,  $\rho$  the water density,  $v_*$  the shear velocity and  $d$  the particle diameter. The shear velocity can be further calculated based on equation (8), where  $\tau_0$  the boundary shear stress and  $I$  the slope.

$$v_* = \sqrt{\tau_0 / \rho} = \sqrt{g \cdot h \cdot I} \quad (8)$$

The described parameters define the threshold to motion in the Shields diagram (Figure 21).

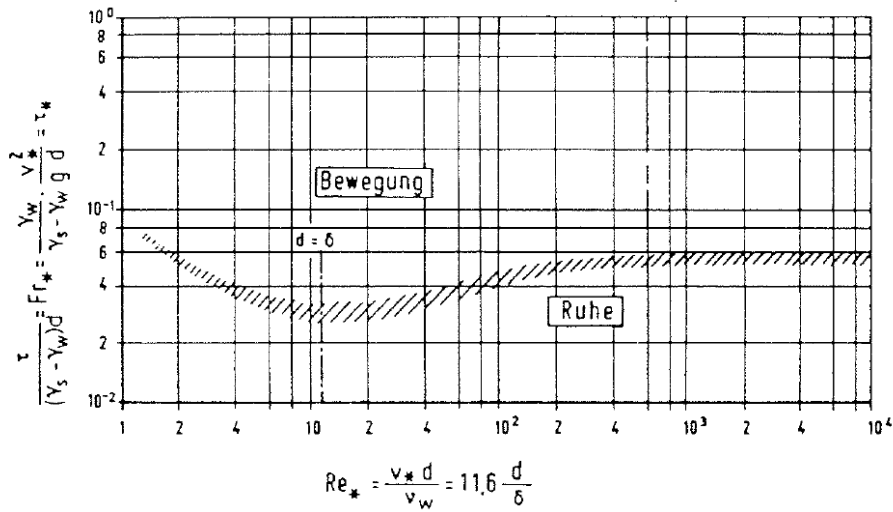


Figure 21. Shields diagram (Kobus 1984)

If the values of the grain Froude number  $Fr^*$  are set equal between nature and model, the following applies:

$$Fr^*_r = \frac{Fr^*_n}{Fr^*_m} = 1 \quad (9)$$

The same can be applied for the particle Reynolds number:

$$Re^*_r = \frac{Re^*_n}{Re^*_m} = 1 \quad (10)$$

In addition to the geometric scale numbers such as the lengths  $L_r$  and the heights  $h_r$ , two more are used for models with mobile sediments, namely the grain scale number  $d_r$  and the scale number for the sediment density weighed under water (Kobus 1984). The following applies to the grain scale number  $d_r$ :

$$d_r = \frac{d_n}{d_m} \quad (11)$$

The scale number for the sediment density weighed under water is defined as  $\Delta\rho_r$ :

$$\Delta\rho_r = \frac{\Delta\rho_n}{\Delta\rho_m} = \frac{(\rho_s - \rho)_n}{(\rho_s - \rho)_m} \quad (12)$$

If it is assumed that the specific weight and the kinematic viscosity are the same between nature and the model, the following relationship results for the Reynolds number of the grain:

$$Re_{*r} = \frac{\sqrt{g_r \cdot h_r \cdot l_r} \cdot d_r}{\nu_r} = \frac{\sqrt{h_r} \cdot d_r}{\sqrt{n}} = \frac{h_r \cdot d_r}{\sqrt{L_r}} = 1 \quad (13)$$

According to Kobus (1984), the grain Froude number between nature and model can be determined in a similar way by setting the specific weight of the water equal:

$$Fr_{*r} = \frac{\rho_{wr} \cdot g_r}{\Delta\rho_r \cdot g_r} \cdot \frac{h_r}{d_r} \cdot L_r = \frac{h_r}{\Delta\rho_r \cdot d_r \cdot n} = \frac{h_r^2}{\Delta\rho_r \cdot d_r \cdot L_r} = 1 \quad (14)$$

Combining ( 13 ) and ( 14 ),  $h_r$  is eliminated and the following relationship can be determined (Kobus 1984):

$$h_r^3 = \Delta\rho_r \cdot L_r^{3/2} \text{ and } d_r^3 = \frac{1}{\Delta\rho_r} \quad (15)$$

Using the Strickler equation ( 16 ), a relationship between roughness and grain diameter can be determined ( 17 ) with respect to the model scale. Using an empirical relationship, the Strickler coefficient  $k_{st}$  on open channels with a mobile sediment bed can be calculated as follows:

$$v = k_{st} \cdot R_h^{3/2} \cdot I^{1/2} \quad (16)$$

$$k_{st} = \frac{26}{d_{90}^{1/6}} \quad (17)$$

Here  $R_h$  is the hydraulic radius and  $d_{90}$  is the characteristic grain diameter where ninety percent of the grain size distribution has a smaller particle size. Further  $k_{st}$  can be written according to the Froude model law as:

$$k_{st,r} = \frac{L_r^{1/2}}{h_r^{2/3}} = d_r^{-1/6} \rightarrow d_r = \frac{h_r^4}{L_r^3} \quad (18)$$

According to Kobus (1984), by using equations 13 and 18 the following relationship between the scale of length and the scale of height can be derived:

$$h_r = L_r^{0.7} \quad (19)$$

On the basis of this equation ( 18 ) it can be seen that maintaining the roughness condition between nature and model always results in an distortion of the model (Kobus 1984). Moreover, the time scale ratio for sediment transport  $t_{s,r}$  and for hydraulic processes  $t_{h,r}$  can be written as:

$$t_{s,r} = \frac{L_r^{5/2} \cdot \Delta p_r}{h_r^2} \text{ and } t_{h,r} = \frac{L_r}{h_r^{1/2}} \quad (20)$$

The hydraulic and the sedimentological time scale are not equal. Under certain circumstances it becomes therefore necessary to conduct so called historical experiments to avoid uncertainties regarding the sedimentological time scale (Kobus 1984).

As mentioned before the Froude model law has to be considered if sediment transport should be investigated in the experiments. Further the grain Froude number  $Fr^*$  and the

particle Reynolds number  $Re^*$  as well as the roughness condition should be complied. Considering this, a system out of three equations with four variables can be determined:

$$\text{Eq. 13 } Re^*_r = 1 \quad Re^*_r = h_r \cdot d_r \cdot L_r^{-1/2} = 1$$

$$\text{Eq. 14 } Fr^*_r = 1 \quad Fr^*_r = h_r^2 \cdot d_r^{-1} \cdot L_r^{-1} \cdot \Delta\rho_r^{-1} = 1$$

$$\text{Eq. 18 } \quad \text{roughness condition} = h_r^{-4} \cdot d_r \cdot L_r^3$$

Only one variable can be chosen, while the remaining three other variables are determined based on the equations shown Table 1.

Table 1. Relationships of scales (Kobus 1984).

Independent scale ratio	Depended scale ratio			
	$L_r$	$h_r$	$d_r$	$\Delta\rho_r$
$L_r$		$h_r = L_r^{7/10}$	$d_r = L_r^{-2/10}$	$\Delta\rho_r = L_r^{6/10}$
$h_r$	$L_r = h_r^{10/7}$	-	$d_r = h_r^{-2/7}$	$\Delta\rho_r = h_r^{6/7}$
$d_r$	$L_r = d_r^{-10/2}$	$h_r = d_r^{-7/2}$	-	$\Delta\rho_r = d_r^{-6/2}$
$\Delta\rho_r$	$L_r = \Delta\rho_r^{10/6}$	$h_r = \Delta\rho_r^{7/5}$	$d_r = \Delta\rho_r^{-2/6}$	-

However, it is not always possible to achieve the requirements shown in Table 1. This can have different reasons e.g., available space in the laboratory, sufficient discharge, sufficient water depth to avoid the influence of the water surface tension etc., or other restrictions like budget limits for constructing and running the model. All these factors play an important role by defining the possible scale and therefore the degree of freedom may be restricted. In many cases it is feasible or necessary to neglect one of the three criteria. It may be assumed that it is sufficient to replicate the condition of roughness (by creating Reynolds numbers and friction within the rough or smooth range), instead of sticking to number present in the prototype. For example, if the particle Reynolds number is large enough to cause a hydraulically rough condition as in nature (typically larger than 60) and sediment transport in form of bed load transport occurs then the criteria based on Eq. 13 can be neglected. Then two scales can be chosen. Here,  $Fr^*_r = 1$  and the roughness condition equals 1 and are considered.

Table 2. Relationship of scales by neglecting the viscosity (Kobus 1984).

Independent scale ratio	Depended scale ratio			
	$L_r$	$h_r$	$d_r$	$\Delta\rho_r$
$L_r$ und $h_r$	$L_r$	$h_r$	$d_r = h_r^4 / L_r^3$	$\Delta\rho_r = L_r^2 / h_r^2$
$L_r$ und $\Delta\rho_r$	$L_r$	$h_r = L_r / \Delta\rho_r^{(1/2)}$	$d_r = L_r / \Delta\rho_r^2$	$\Delta\rho_r$
$h_r$ und $\Delta\rho_r$	$L_r = h_r \Delta\rho_r^{(1/2)}$	$h_r$	$d_r = h_r / \Delta\rho_r^{(3/2)}$	$\Delta\rho_r$

Further, also the roughness condition can be neglected if for example the slope or the water levels are of minor importance (Kobus 1984). The regime, hydraulically smooth or

rough, should be kept between nature and the model. Again, two scales can be chosen. Here,  $Fr^*_{r} = 1$  and  $Re^*_{r} = 1$ .

Table 3. Relationship of scales by neglecting the roughness condition (Kobus 1984).

Independent scale ratio	Depended scale ratio			
	$L_r$	$h_r$	$d_r$	$\Delta\rho_r$
<b><math>L_r</math> und <math>h_r</math></b>	$L_r$	$h_r$	$d_r = L_r^{(1/2)} / h_r$	$\Delta\rho_r = h_r^3 / L_r^{(3/2)}$
<b><math>L_r</math> und <math>\Delta\rho_r</math></b>	$L_r$	$h_r = L_r^{(1/2)} \Delta\rho_r^{(1/3)}$	$d_r = 1 / \Delta\rho_r^{(1/3)}$	$\Delta\rho_r$
<b><math>h_r</math> und <math>\Delta\rho_r</math></b>	$L_r$	$h_r$	$d_r = 1 / \Delta\rho_r^{(1/3)}$	$\Delta\rho_r$

In case the influence of the particle Reynolds number and the roughness condition are neglected, then the suspended sediment and the slopes are not similar. In this case  $Fr^*_{r} = 1$ , keeping the sediment transport balanced between nature and the model, and three scales can be chosen.  $Fr^*_{r} = 1 \rightarrow Fr^*_{r} = h_r^2 \cdot d_r^{-1} \cdot L_r^{-1} \cdot \Delta\rho_r^{-1} = 1$

More information about physical scale modelling for hydrodynamic processes can be found in Julien (2002, 2010), Kobus (1984) or Novak et al. (2010).

### III. Methodology

- **Used scales for pilot site**

Based on the objectives defined for the project lifelineMDD it was required to model the pilot measure in Gosdorf, a section with freely eroding banks approximately 1 km in length, and about 1.5 km when considering inlet and outlet sections. At this section the width of the Mura River ranges between 76 m in the channelized sections up- and downstream and about 100 m in the restored reach, where the left bank retreated due to bank erosion. A total width of approximately 300 m would be available for self-dynamic processes and was considered in the model. In the next step the water depths of the Mura River at different discharges were analysed. The mean discharge  $Q_m$  of the Mura River at the pilot site is  $146.5 \text{ m}^3/\text{s}$  and the annual flood discharge  $HQ_1 = 730 \text{ m}^3/\text{s}$ . The range between these two discharges was defined to be relevant for the model runs and therefore considered for defining the scales. At a mean discharge  $Q = 146.5 \text{ m}^3/\text{s}$  at the gauging station Mureck the water depth is 2.5 m. From grain size distributions determined from floodplain samples within the establishment of the Basic Water Management Concept (2001), an average grain size of 0.0285 m was expected to develop in a restored reach when excavated sediment is supplied as bedload. The slope was determined to be 0.0014. The main parameters for deriving the scales are shown in (Table 4).

Table 4. Main parameters or natural quantities of the Mura river at the pilot site in Gosdorf. Hydrologic data was obtained from the Hydrographic Service Styria

Parameter	Nature
Length (m)	1500
Mean discharge $Q_m$ ( $m^3/s$ )	146.5
Annual flood discharge $HQ_1$ ( $m^3/s$ )	730
Mean water depth (m)	2.5
Mean grain diameter (m)	0.028
Slope	0.0014

As mentioned in the previous chapter it is not always possible to achieve all three mentioned criteria (Eq 13, Eq 14 and Eq 18). Based on the input parameters for defining the scales (Table 4) the equations or relationships shown in Table 1, Table 2 and Table 3 were used. Due to the dimensions and because of the restrictions (shown as bullet points), it was not possible to find a suitable scale using the relationships shown in the Table 1, Table 2 and Table 3. This was due to following restrictions.

Restrictions and thresholds for the application of physical hydraulic models:

- Available space in the laboratory 15 x 5 m → choice of length scale  $L_r$
- Available discharge in the laboratory 2 – 120 l/s
- Grain size diameter cannot be scaled too much given the risk of cohesive forces → choice of grain size scale  $d_r$  and particle density scale  $\Delta\rho_r$
- Water depths should not be less than 3 cm (influence of water surface tension) → choice of depth scale  $h_r$
- The duration of the experimental runs must be feasible → choice of length  $L_r$  and depth scale  $h_r$

The required space in the laboratory was limited to a length of 15 m and a maximum width of 5 m. Based on the required space in the laboratory and the dimensions of the pilot measure in nature a length scale of  $L_r = 110$  was chosen. Since at that scale the water depth and grain sizes would be too small, it was necessary to introduce a further scale, the depth scale  $h_r$ . Under the consideration of the water depths, which are 2.5 m according to Table 4 for the mean discharge a depth scale of  $h_r = 30$  was chosen. Moreover, larger water depths increase the accuracy and facilitate the operability of measurement devices. As the required sediment volume of the model is large and artificial sediments e.g. light weighted sediments are expensive compared to sand or gravel the third scale  $\Delta\rho_r$  was set to 1. This means that density of the sediments and the water is same in nature and the model. In accordance with the Froude's model law  $Fr_r = 1$  and the grain Froude number  $Fr_r^* = 1$  the grain size scale  $d_r$  has to be calculated. This was done by eliminating  $d_r$  from equation (14), resulting in  $d_r = 8.2$ . In Table 5 the main scale numbers are listed. As the depth scale  $h_r$  deviates from the length scale  $L_r \neq h_r$  the model is distorted by a factor  $n = L_r/h_r = 3.67$ .

Table 5. Summary of the main scale numbers.

Scale	Chosen/calculated	Value
$L_r$	chosen	110
$h_r$	chosen	30
$\Delta\rho_r$	chosen	1
$d_r$	(eq. 14)	8.2
$t_{s,r}$	(eq. 20)	141
$t_{h,r}$	(eq. 20)	20.1
$I_r$	$1/n$	0.273
$Q_r$	$Lr^{5/2}/n^{3/2}$	18075

In Table 6 the main parameters/quantities shown in Table 5 are transferred to model dimensions. Based on these dimensions the model was planned and constructed.

Table 6. Natural quantities transferred to mode scale:

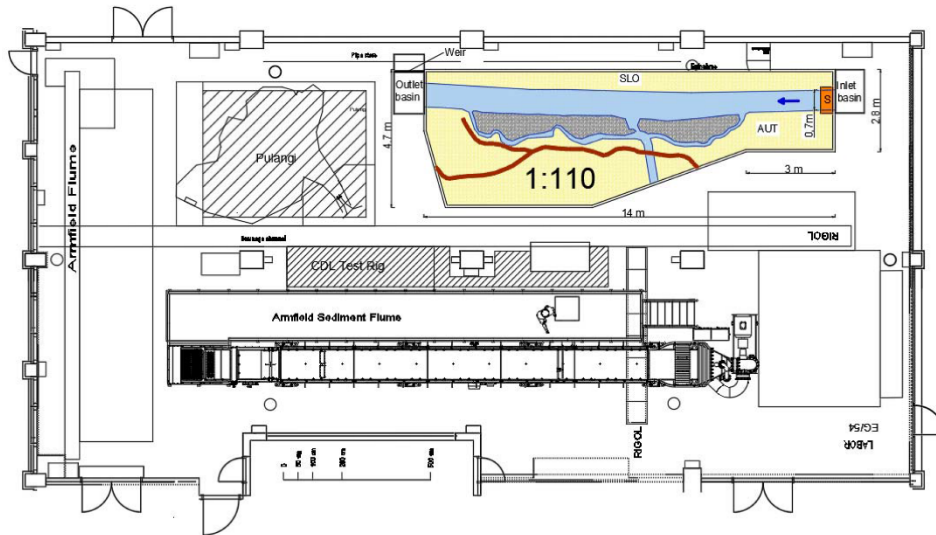
Parameter	Nature	Model
Length (m)	1500	13.6
Mean discharge $Q_m$ ( $m^3/s$ )	148	0.0082
Annual flood discharge $HQ_1$ ( $m^3/s$ )	730	0.0404
Mean water depth (m)	2.5	0.084
Mean grain diameter (m)	0.0285	0.0035
Slope	0.0014	0.0051

## • Construction of the model

Based on the calculated model dimensions shown in Table 6 and due to the available space in laboratory the model was planned with a length scale of  $L_r = 110$ . The relevant depths were calculated based on  $h_r = 30$ . Figure 22 shows the plan view of the laboratory and the location as well as the boundaries of the model. Essentially, the model consists of five main parts:

1. Model section
2. Inlet basin
3. Outlet basin
4. Sediment feeder
5. Weir

a)



b)

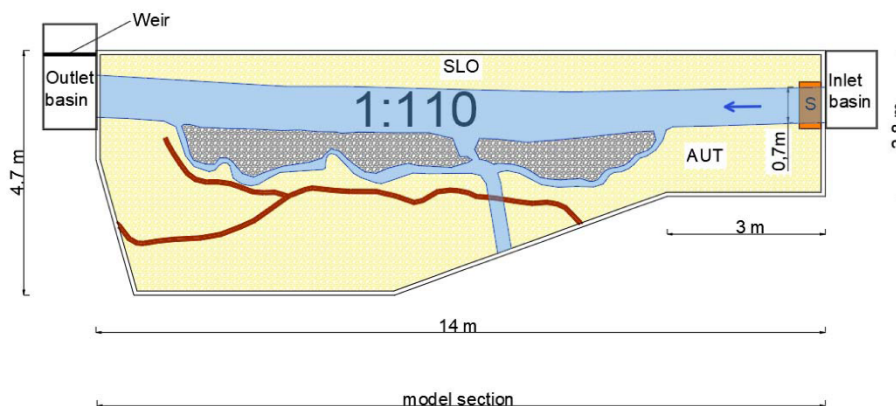


Figure 22. a) Plan view of the laboratory at BOKU University, b) detail of the model including the installed boundaries

The flow direction in Figure 22 is from right to left. On the left side of the river is Austria and on the right Slovenia. The model section has a total length in streamwise direction of 14 m and a width of 4.7 m at widest section. The model section consists out of a steel frame and sandwich panels (Figure 23). The sandwich panels (Brucha panels) have a length of

14.0 m and a width of 1.0 m and were put together. Therefore, it was possible to build the boundaries and the bed of the model, which was the basis of the model.

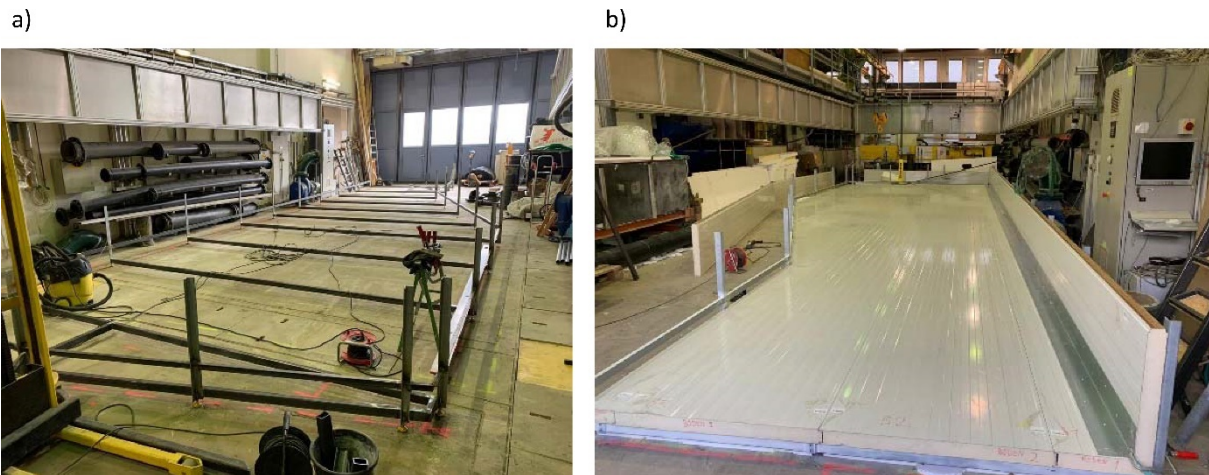


Figure 23. a) Steel frame and b) sandwich panels

In the next step the model was covered with a waterproof foil. On top of the foil sediment layers were inserted. In total 4.1 m<sup>3</sup> sediments with a diameter of 0.4 to 0.8 mm and 15.3 m<sup>3</sup> of sediments with a diameter of 2.0 to 4.0 mm were used. Based on the model laws which were previously described, the scale number for the grain sizes was  $d_r = 8.2$ . The mean grain diameter in nature is 28.5 mm and using the grain scale results in a grain diameter of 3.47 mm for the sediment under model conditions. The sediment intended for the model was analysed in advance by means of a sieve analysis (Figure 24). This resulted in a  $d_{10} = 2.3$  mm, a  $d_{50} = 3.4$  mm, a  $d_{90} = 5.0$  mm and a  $d_m = 3.58$  mm, which corresponds well to the mean in nature.

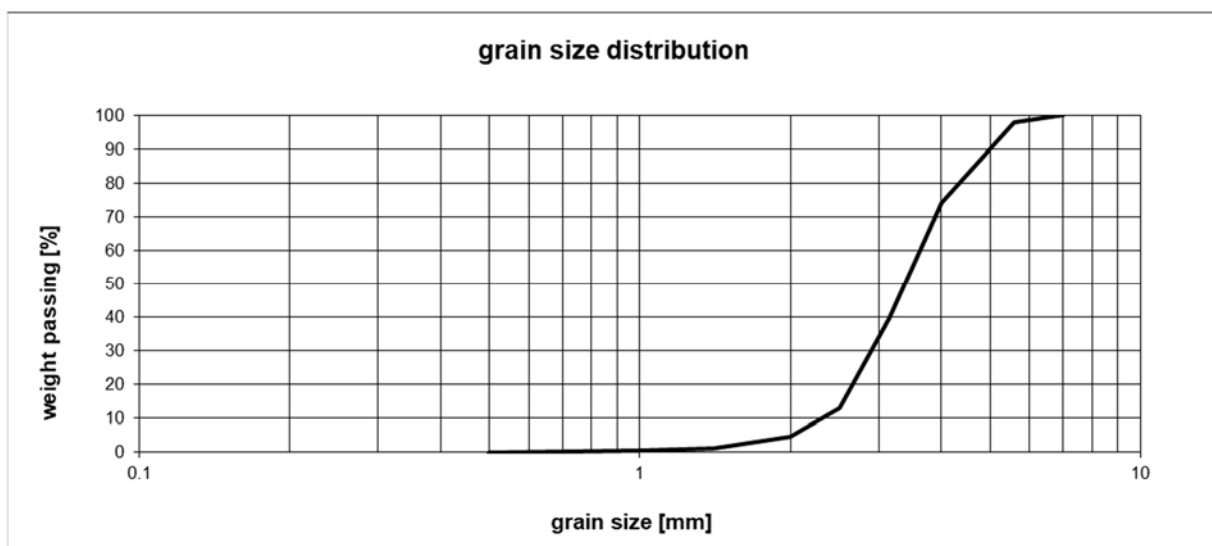


Figure 24. Grain size distribution of the sediments used in the model

In Figure 25 the waterproof foil and the sediment layers are displayed. The sediment layers were further adjusted to the scaled bed slope of the Mura River at the pilot site.

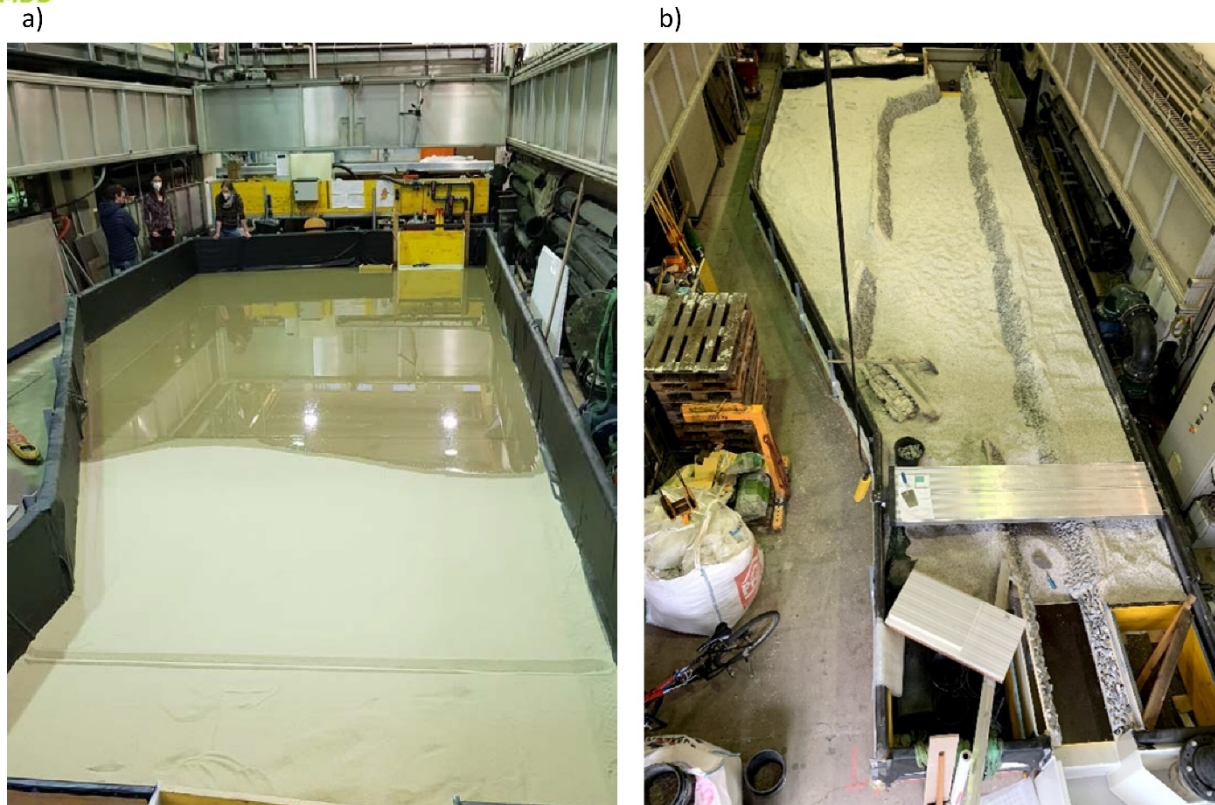


Figure 25. a) Waterproof foil and b) sediment layer

The sediment layers were the basis for creating the shape of the different scenarios. As at the pilot site of the lifelineMDD project the bank erosion is restricted due to bank protections (along the Slovenian border and along the forest road at the Austrian section) same was done for the model. Therefore, the bank areas were built out of concrete and stones with a diameter between 30 and 60 mm were added (Figure 26). This was done to avoid bank erosion at the fixed boundaries of the project site and to achieve a sufficient roughness. Between the fixed banks the model was filled with sediments which allows a flexible geometry depending on the scenarios.



Figure 26. Fixed river banks out of concrete and stones

To direct the water into the model, a plastic inlet basin was built. This serves to create uniform and steady inflow conditions. The inlet basin is connected to water cycle of

laboratory with a pipe and has length of 1.0 m and width of 1.5 m. The height is 0.8 m. After the water passes the model section, it enters the outlet basin. From there the water is guided back to the water cycle. Further the outlet basin serves as a sediment trap where the transported sediments collect during the model runs can be extracted. At the end of the outlet basin there is a weir located to control the water depths, if this is necessary (e.g. to lower flow velocities during the filling of the model with water at every run). To control the amount of sediment transport or to continuously add a certain amount of sediments during the model runs a sediment feeder was used (Figure 27). The sediment feeder is located at the beginning of the model section and supplies across the entire width. The system consists of a funnel, where the sediments are added and a horizontal steel shaft with a diameter of 6 cm. The shaft is controlled by a speed-controlled electric motor (0.75 kW power). The steel shaft has a total of eight longitudinal notches with a width and depth of 1.0 cm, which are filled with sediments and emptied into the model. The amount of sediments to be added can be controlled via the speed and the number of open longitudinal notches.



*Figure 27. Sediment feeder at the inlet of the model section.*

- **Measurement equipment**

Figure 28 shows the different measurement systems used for measuring the discharge, the water level and the morphological dynamics (such as erosion and sedimentation).

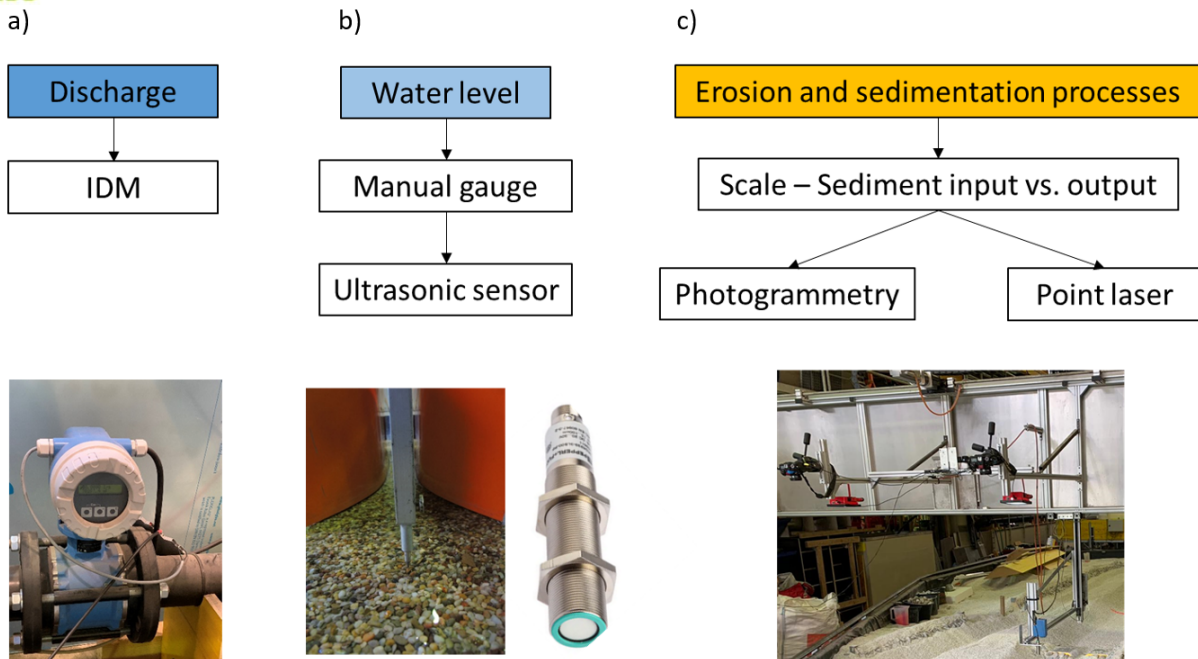


Figure 28. Overview of the measured quantities/parameters and the used measurement systems. a) measurement of discharge with an IDM, b) measurement of water levels with a manual gauge and an ultrasonic sensor, c) survey of morphology using cameras for photogrammetry and a point laser

Before the water entered the inlet basin the discharge was measured with an electromagnetic flowmeter. Further the water levels were measured with an ultrasonic sensor. One sensor was installed 1.0 m downstream of the inlet basin, to measure the water level in the channelized Mura River section. The second ultrasonic sensor was mounted at a measurement bridge, which can be seen in the lower right-hand corner of Figure 28. The measurement bridge can operate along the whole model section. With the ultrasonic sensor mounted at the measurement bridge it becomes possible to measure the water level at any point in the model section. In addition to the recording of the water level, the alteration of the bed was also measured. This was done pointwise with a distance point laser, which was also installed at the measurement bridge in addition to the ultrasonic sensor. Photogrammetry was used to repeatedly derive digital elevation models of the entire model section. Two synchronized cameras (Nikon D7100) were used and mounted on the measurement bridge to take overlapping images. An automated procedure ensured sufficient overlap in both, flow and lateral direction. In Figure 28c the camera setup is displayed. The software “Metashape” was used to derive the three-dimensional Digital Elevation Models (DEM) on basis of the overlapping camera images. By means of control points, the DEM can be transferred into an existing coordinate system. For external orientation, the control points (markers) required for evaluation were provided with a local coordinate system. Using the reflectorless measurement option offered by a theodolite (Leica TS07), 40 control points (markers) were measured, which were distributed over the entire model (Figure 30). These are automatically detected by the Metashape software via coded targets (Figure 29).

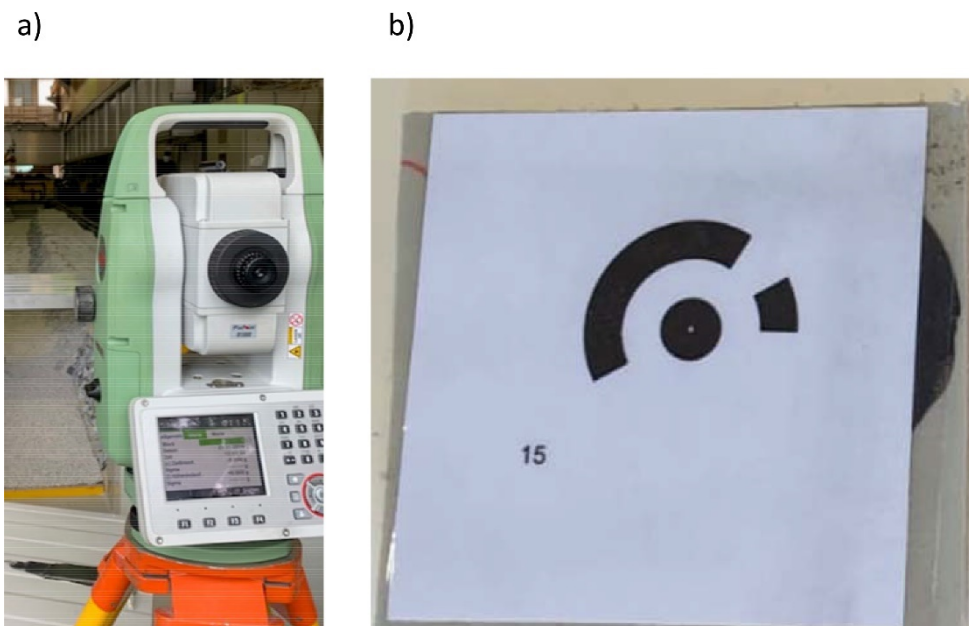


Figure 29. Used measurement device (Leica TS07) for surveying control points (b).

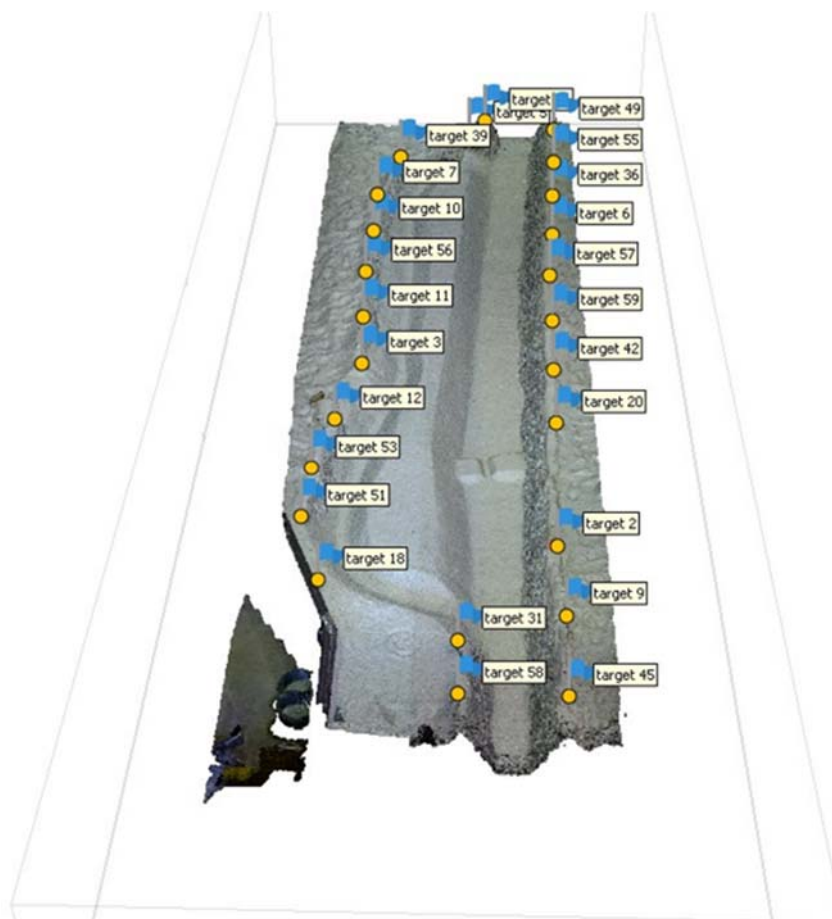


Figure 30. Overview of control points and three-dimensional surface points created by the photogrammetric software.

By using a geographic information system, it was possible to calculate differences between digital elevation models and hence to depict sedimentation and erosion processes and to determine related volumes.

- **Modelled scenarios**

The geometry of initial status of the model was adapted to the current geometry of the Mura River at the pilot site. Some simplifications regarding the geometry had to be done due to lack of data or inaccurate natural data. In the side channel, the available digital elevation model from 2019 contained Lidar data only, which reflected the water surface instead of the riverbed. In addition, the geometry of the natural bedrock sill was uncertain, as it could never be surveyed in detail in the field given the locally strong currents and therefore had to be approximated. For a better comparison of the scenarios, an initially constant bed slope upstream as well as downstream was used for the model conditions. Based on measurements in the available Digital Elevation Model, upstream of the natural bedrock sill the bed slope was adjusted to 0.0039 and downstream to 0.0021, respectively. In lateral direction the initial bed level was assumed to be horizontal. The slopes and the geometry of the natural bedrock sill were used as initial status for each scenario.

Three scenarios were investigated:

**Status quo:** The scenario ‘status quo’ reflects the current condition (obtained from the digital elevation model from 2019) at Gosdorf, which was restored in 2006/2007. Hence, in the state investigated in the model, bank protections along the left bank were already removed and the bank already showed bank retreat which occurred since the implementation of the restoration measure in 2006/2007. In the present, investigated state, the bank retreated locally by up to 28 m in the vicinity of the bedrock sill, but to a much smaller extent up- and downstream.

**Smaller-scale measure:** The measure implemented within lifelineMDD is denominated the ‘smaller-scale measure’, as it is compared to a larger-scale measure which was defined as a target implementation. It reflects the current geometry just as in the Status quo, but contains the initiation measures planned within lifelineMDD (Figure 20). Note that after completion of the model run, the original plan was subject to slight alterations as it went through the processes of approval at the authorities.

**Larger-scale measure:** The larger scale measure was designed based on outcomes of the EU Interreg V-A SI-AT project goMURra in the first step of the planning phase. As the costs showed to exceed the budget reserved for the measure, the smaller-scale measure was designed as a first step towards the targeted larger-scale measure. The larger-scale measure was additionally investigated to identify differences in the measure effects.

These representation of the measures in the hydromorphological model are described below:

### **Status quo**

The morphodynamics of the status quo were evaluated under the following hydraulic and morphological conditions described in Table 7.

Table 7. Hydraulic and sedimentological conditions for status quo.

Parameters	Model conditions	Nature conditions
Simulated discharge Q (m <sup>3</sup> /s)	0.0166	298
Total Sediment input (m <sup>3</sup> )	0.0	0.0
Sediment transport rate (m <sup>3</sup> /h)	0.0	0.0
Simulated time (hydraulic) (h)	49	989.9 (41 days)
Simulated time (sedimentological) (h)	49	6909 (287.9 days)

A constant discharge of 298 m<sup>3</sup> s<sup>-1</sup> was selected for the “status quo” measure, as this corresponds to the bed forming discharge for the investigated grain size of the channelized section (and the channel width is only slightly higher in the Gosdorf section). Figure 31 shows the geometry of the status quo based on a digital elevation model of the initial status.

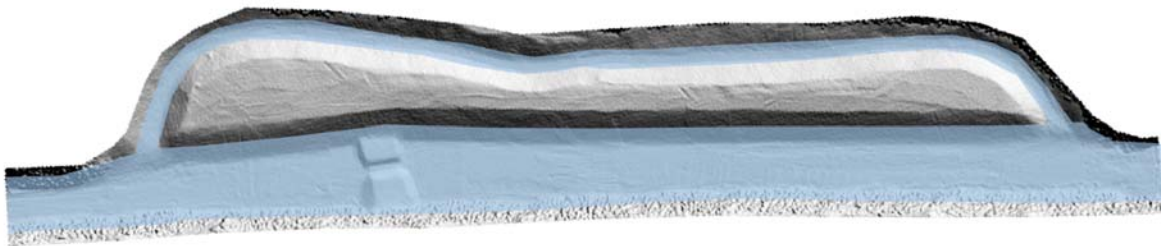


Figure 31. Overview of the Status quo based on the DEM of the initial state

### Smaller-scale measure

The smaller-scale measure was reconstructed on the basis of the planning documents available in summer 2021. It consists of a second side channel in the upper part of the Gosdorf section, including an intake structure and a widening near the bottom sill in the main channel. The entire sediment excavation (approx. 40000 m<sup>3</sup>) is to be supplied from upstream by depositing sediment in the main channel, which in the model was supplied from the sediment feeder.

Again, a discharge of 298 m<sup>3</sup>s<sup>-1</sup> was selected as the bed-forming discharge as the initial width did not much variate from the status quo (Table 8). Naturally eroding banks in the model adjust their slope to the friction angle of the laboratory sediment, which cannot follow the exaggeration of elevations which was required to meet scaling laws at the selected model scale in plan view. At a bank slope corresponding to the friction angle, the small width of the side-channel could not be reconstructed between the main channel and the old side-channel. As it was important to see the connection of the side-channel, the bed levels in the side-channel needed to correspond to those planned, so that the banks in the side-channel were protected to at least reproduce vertical morphodynamics. At the outlet of the new side-channel, these protections also affected the main channel.

Table 8. Hydraulic and sedimentological conditions for smaller-scale measure

Parameters	Model conditions	Nature conditions
Simulated discharge Q (m <sup>3</sup> /s)	0.0166	298
Total Sediment input (m <sup>3</sup> )	0.108	39236
Sediment transport rate (m <sup>3</sup> /h)	0.021	372/53
Simulated time (hydraulic) (h)	13.25	166 (11 days)
Simulated time (sedimentological) (h)	13.25	1868 (78 days)

Figure 32 shows the geometry of the smaller-scale measure based on a digital elevation model of the initial status.

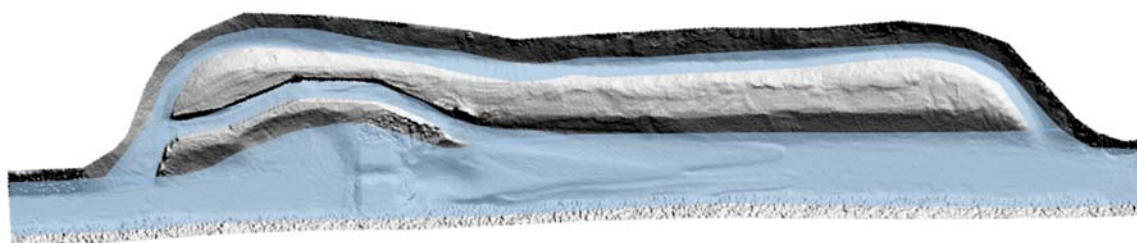


Figure 32. Overview of laboratory model representing the smaller-scale measure.

## Larger-scale measure

During construction of the larger scale measure, excavations occur over the entire length of the Gosdorf section. The increased curvature would be established by constructing a new main channel in the floodplain, which strongly increases curvature and overall width. In natural rivers without constraints, the bed forming discharge would approximately correspond to the discharge of an annual flood (Biedenharn et al., 2001). Given the presence of constraints along the boundaries of this measure, a discharge of 513 m<sup>3</sup>s<sup>-1</sup> was selected as a discharge in between the effective discharge of the channelized section and the annual flood.

The morphodynamics of the status quo were evaluated under the conditions of hydraulic and sediment discharge described in Table 9. At the model scale, in total 1.00 m<sup>3</sup> sediment were made available from the excavations for the initiation of the larger-scale measure. Most of the excavated sediment originated from the widening and deepening of the new main channel. The gained sediment was constantly fed to the model at a sediment transport rate of 0.059 m<sup>3</sup>/hm. The amount was calculated based on equation 21 and 22 for the “regulated” Mur section. Based on the calculated sediment transport rate and the used steady discharge (28.4 l/s in the model or 513 m<sup>3</sup>/s in nature) the 1.00 m<sup>3</sup> or 364068 m<sup>3</sup> under natural conditions were transported during a time period of 1920 minutes in the model or 188 days in nature, according to the sedimentological time scale.

Table 9. Hydraulic and sedimentological conditions for the larger-scale measure

Parameters	Model conditions	Nature conditions
Simulated discharge Q (m <sup>3</sup> /s)	0.0284	513
Total Sediment input (m <sup>3</sup> )	1.0	363 000
Sediment transport rate (m <sup>3</sup> /h)	0.032	584.3/83.3
Simulated time (hydraulic) (h)	72	1447.2 (60.3 days)
Simulated time (sedimentological) (h)	72	10152 (423 days)

Figure 33 gives an overview of the initial condition of the larger-scale measure. The inlet structure was constructed with larger blocks placed into concrete, representing rip-rap such as present along the fixed banks in the channelized section. The excavated sediment amounted to 1.0 m<sup>3</sup> in the model and was supplied at the transport capacity of the supplied water discharge.



Figure 33. Overview of the initial condition of the larger-scale measure.

### • Sediment transport calculation

The bedload transport capacity of the channelized section upstream was calculated with the bedload formula of Wong and Parker (2006), who conducted a reanalysis of data used by Meyer-Peter and Müller (1948). Bedload replenishment was then conducted at the rate of the obtained bedload transport capacity. The bedload formula was applied to the model conditions. The sediment transport rate was calculated for the channelized Mura River section upstream of the modelled restored section, which has a length of 3.0 m (see also Figure 22). The equation can be written as:

$$q^* = 3.97 (\tau_b^* - 0.0495)^{1.5} \quad (21)$$

Here,  $q^*$  is the dimensionless volume bed load transport rate per unit width and  $\tau_b^*$  the dimensionless boundary shear stress which is calculated according to equation (23):

$$\tau_b^* = \tau / (\rho R g d) \quad (22)$$

Here  $R$  is the submerged specific gravity of sediment and  $\tau$  boundary shear stress for the river bed.

- **Data analyses**

### **Bed levels and sediment budget**

Statistical analyses were applied to the digital elevation models and differences maps to analyse bed levels and sediment volumes for each step of the model run. Therefore, the digital elevation models were separated in 116 polygons, each with a length in flow direction of 0.1 m (model scale). For each model run and for each polygon along the model the mean bed elevation and the minimum bed elevation was extracted. This allowed the calculation of the changes regarding the mean bed elevation and the cumulative volume over time by subtracting polygons at different time steps. Figure 34 displays the locations of the polygons.

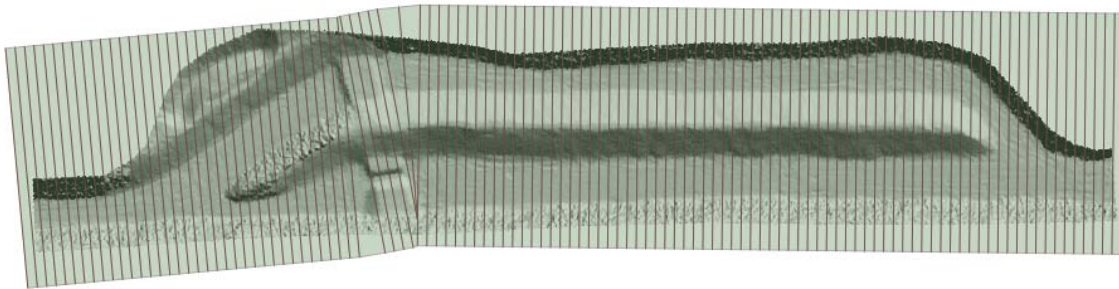


Figure 34. Polygons used for the “zonal statistics” which overlay a DEM

While the analysis described above was conducted for the entire widths of the recorded model geometry, in a second analyses the bed elevations were calculated for the wetted width in 24 cross sections.

### **Morphodynamic habitats**

The morphodynamics were analysed separately in different vertical zones of the river by using the tool HyMoLink (Klösch et al., 2019). An aquatic, semiterrestrial and terrestrial zone were separated by the water surface elevations of discharges at the 50% and 10% submergence frequency within the vegetation period. Special focus was then put on the semiterrestrial zone, as bare sediment surfaces there are suggested to provide habitat to pioneer vegetation, but also to bar-breeding birds, hence critical habitats required for rejuvenation. Bank erosion is indicated as relevant for bank-nesting birds as soon as a 1 m layer of fine sediment is eroded, which was assumed to promote the development of steep banks.

## IV. Results

The results are reported separately for the model runs in the scenarios of the status quo, the smaller-scale measure and the larger-scale measure.

- **Status quo**

As a first result, the sediment input compared to the sediment output is summarised in Table 10. In addition, the duration of the test runs under model and natural conditions is reported. For the status quo, the model was not supplied with sediment corresponding to conditions in nature, as it was of interest to observe whether the model could reproduce bed incision, as is the case in the river section of the Mur at the pilot site.

Table 10. Summarized results of sediment input and sediment output under model and natural scales for the status quo

Model			Nature			
cumulative duration (min)	cumulative sediment input (m <sup>3</sup> )	cumulative sediment output (m <sup>3</sup> )	cumulative hydraulic duration (d)	cumulative sedimentological duration (d)	cumulative sediment input (m <sup>3</sup> )	cumulative sediment output (m <sup>3</sup> )
0	0	0.000	0.0	0.0	0	0
60	0	0.000	0.8	5.9	0	0
180	0	0.000	2.5	17.6	0	0
300	0	0.000	4.2	29.4	0	0
420	0	0.002	5.9	41.1	0	649
540	0	0.003	7.5	52.9	0	1194
660	0	0.006	9.2	64.6	0	2172
780	0	0.010	10.9	76.4	0	3451
900	0	0.013	12.6	88.1	0	4621
1020	0	0.018	14.2	99.9	0	6361
1140	0	0.020	15.9	111.6	0	7429
1260	0	0.024	17.6	123.4	0	8727
1380	0	0.028	19.3	135.1	0	10083
1500	0	0.032	20.9	146.9	0	11575
1620	0	0.034	22.6	158.6	0	12501
1740	0	0.038	24.3	170.4	0	13827
1860	0	0.040	26.0	182.1	0	14399
1980	0	0.043	27.6	193.9	0	15469
2100	0	0.046	29.3	205.6	0	16583
2228	0	0.048	31.1	218.2	0	17408
2340	0	0.049	32.7	229.1	0	17765
2460	0	0.051	34.3	240.9	0	18570
2580	0	0.054	36.0	252.6	0	19613
2700	0	0.056	37.7	264.4	0	20449
2820	0	0.058	39.4	276.1	0	20945
2940	0	0.060	41.0	287.9	0	21771

It can be clearly seen that without sediment input there is a tendency towards erosion processes in the modelled area. Based on the constant discharge ( $298 \text{ m}^3/\text{s}$ ) used for the experimental runs, a total volume of  $21771 \text{ m}^3$  was eroded. Figure 14 shows the results under natural conditions and according to the time scales, such as hydraulic and sedimentological duration.

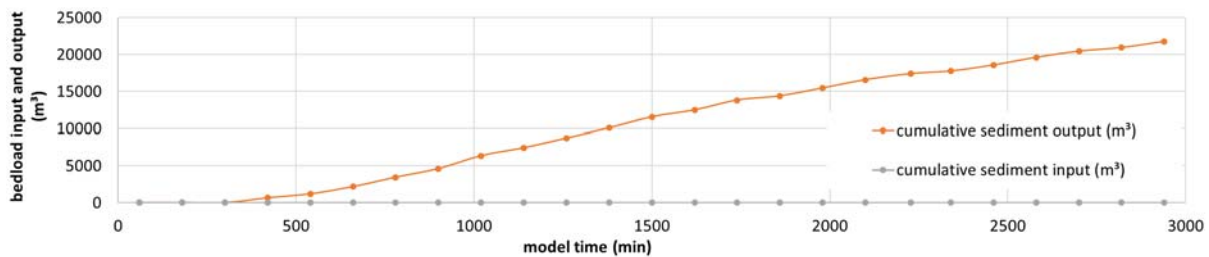


Figure 35. Cumulative sediment input and output for the status quo.

Based on the comparison between sediment input and sediment output, it could be shown that mainly erosion processes were predominant. To identify the location of the erosion processes, the morphodynamics were analysed within zones along the river. The changes in the mean bed elevation and the volumetric changes were analysed for each of the 116 zones. Figure 15 shows the differences of the mean bed elevations with respect to the initial state after certain time steps. For reasons of clarity, not every time step was used in comparison to the data displayed in Table 10. It can be seen that erosion (decreasing mean bed elevation) occurs in the first 20 zones, which represent the section of the channelized Mura River. Further decreasing mean bed elevations can be observed in the area downstream of the natural sill (scour). Decreasing mean bed elevations can also be observed in the section between profile 80 and 100. The greatest value of erosion amounted to 0.9 m (nature scale).

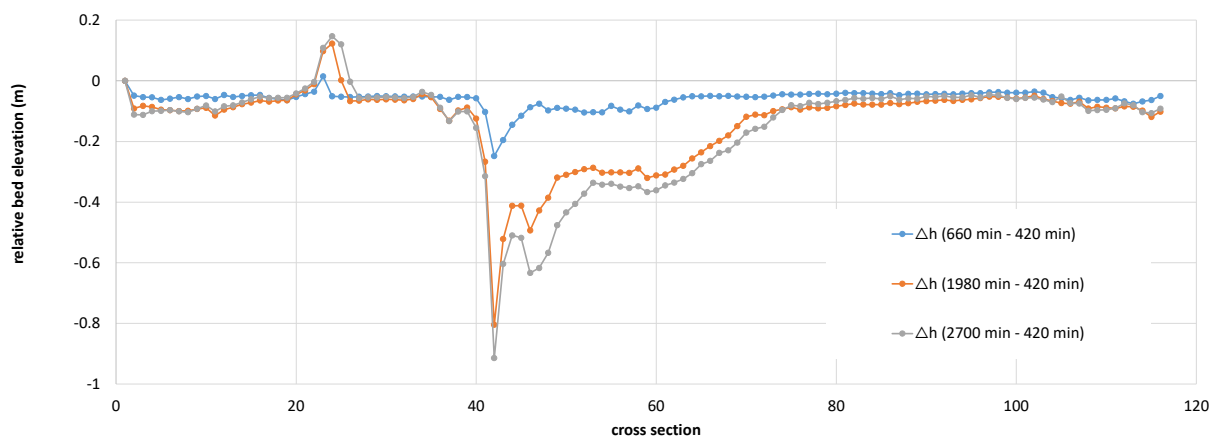


Figure 36. Differences in the mean bed elevation expressed in nature scale for different model time periods per profile for the status quo

For the same time steps like in Figure 36, the changes in volume along the river were calculated. Again, the erosion can be recognised as the experiment progresses. Here the elevation model obtained from 420 min model run time was selected as basis for comparison, to account for an initial shaping of the bed at the start of the experiment.

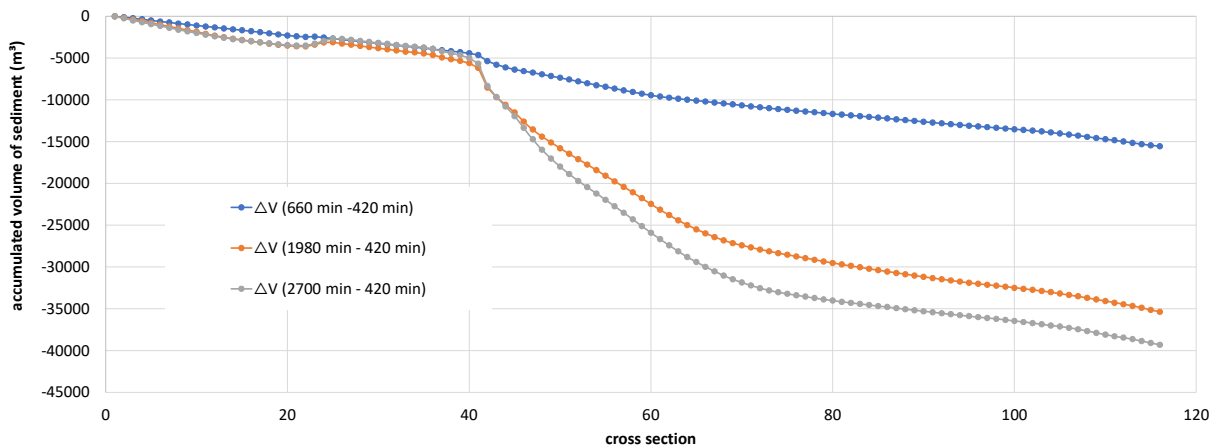


Figure 37. Differences in the cumulative volumes expressed in nature scale along the river for different model time periods in the status quo scenario.

Figure 38 displays the morphodynamics found in the status quo. In the vicinity of the bedrock sill the bank erosion is larger than observed in nature, but no bank erosion occurred up- and downstream of this eroded bank section.

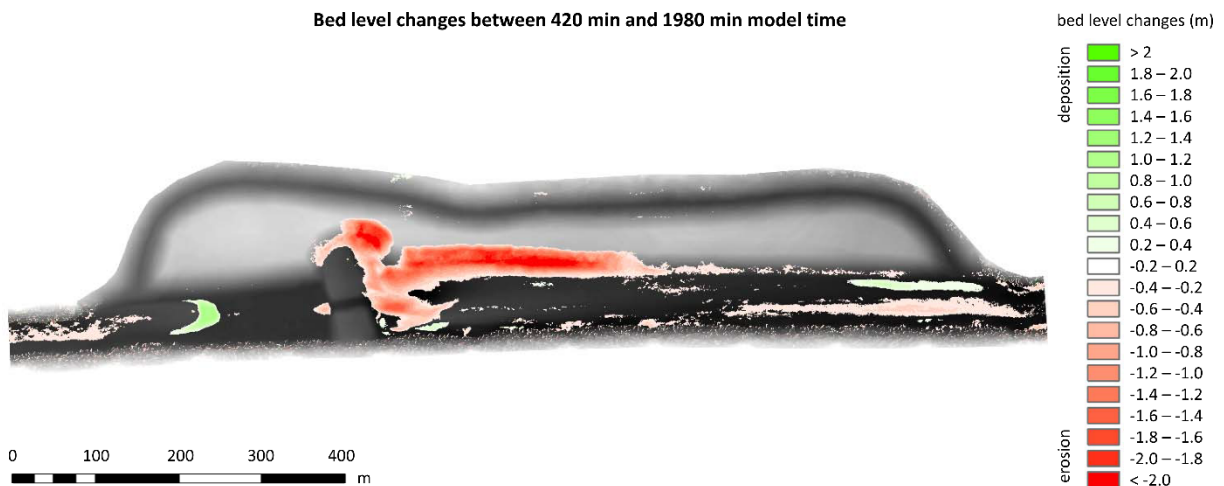


Figure 38. Erosion and deposition in the status quo scenario, displaying the onset of incision when no sediment is supplied.

After some initial reaction of the morphology to the supplied discharge in the first 420min, the average wetted width nearly remained unchanged around a value a bit larger than 100 m (Figure 39).

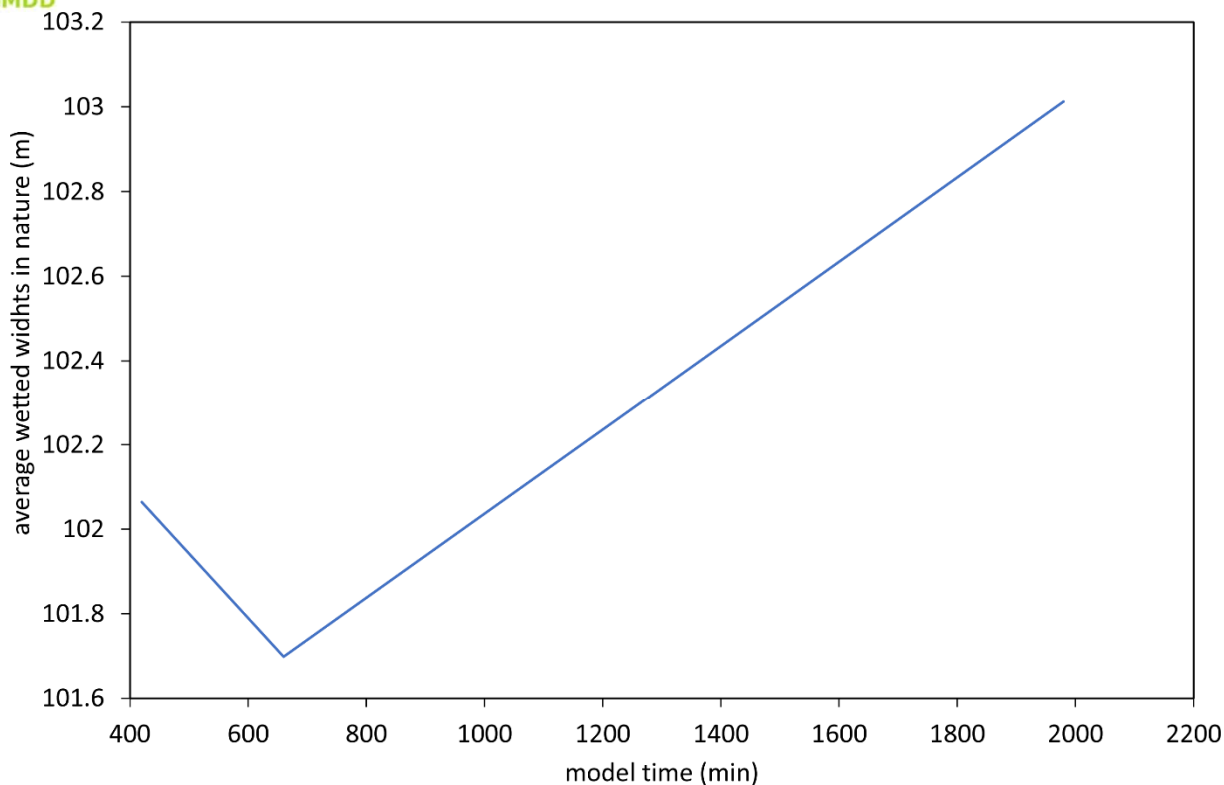


Figure 39. The wetted width at the discharge of  $513 \text{ m}^3\text{s}^{-1}$  in nature scale remaining relatively constant in the status quo scenario.

The lack of bedload supply in the status quo scenario results in an overall lowering of the river bed (Figure 40). After 1980 minutes, the bed incision reaches more than 0.12 m in nature, before the incision in the model became affected by the fixed bed level at the downstream end of the model.

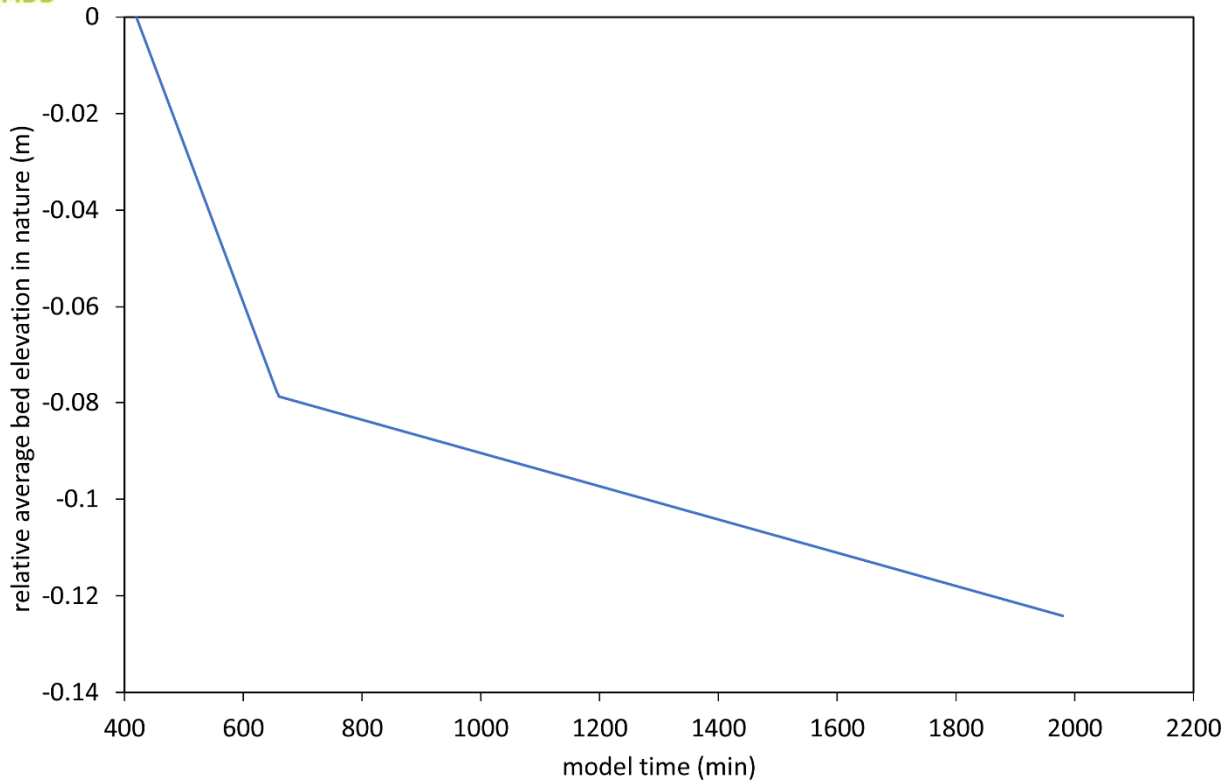


Figure 40. The mean bed elevation lowering in the status quo scenario at lacking bedload supply, analysed in the wetted width of the discharge of  $513 \text{ m}^3 \text{ s}^{-1}$  for definition of the riverbed.

- **Smaller-scale measure**

Table 11 summarizes the conditions of sediment input and sediment output for the smaller-scale measure and reports on the duration of the experimental runs under model as well as under natural conditions.

Table 11. Summarized results of sediment input and sediment output under model and natural scales for the smaller-scale measure.

Model			Nature			
cumulative duration (min)	cumulative sediment input ( $\text{m}^3$ )	cumulative sediment output ( $\text{m}^3$ )	cumulative hydraulic duration (d)	cumulative sedimentological duration (d)	cumulative sediment input ( $\text{m}^3$ )	cumulative sediment output ( $\text{m}^3$ )
60	0.021	0	0.8	5.9	7474	0
105	0.036	0	1.5	10.3	13079	0
180	0.062	0	2.5	17.6	22421	0
255	0.088	0	3.6	25.0	31763	0
315	0.108	0	4.4	30.8	39236	0

Figure 41 displays the morphological change between the start and end of the supply of sediment (approximately  $40000 \text{ m}^3$  in nature). At that point in time, the sediment reaches the bedrock sill, and a small part of the sediment enters into the new side channel, there

causing deposits. Sediment eroded downstream of the sill deposits further downstream at the centre of the channel.

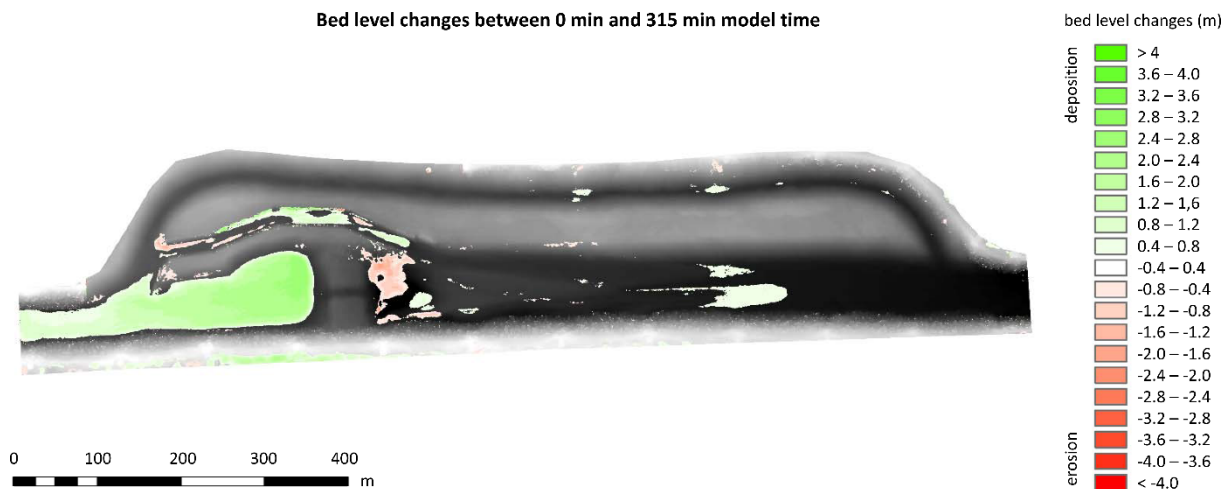


Figure 41. Bed level changes when all bedload was supplied (model time 315min).

Focusing on the latest time period during supply, the morphodynamics are restricted mainly to depositions at the front of the bedload supply upstream of the bedrock sill (Figure 42).

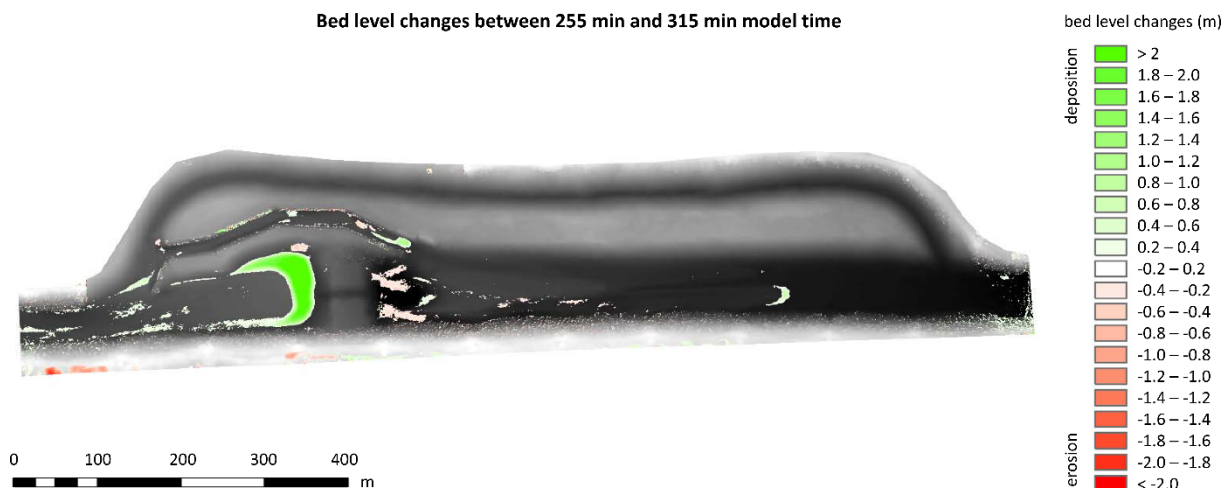


Figure 42. Bed level changes in the last recorded time step (255 min – 315 min).

The average wetted width increases slightly (Figure 43), mainly in the section where most material deposits and where it causes a rise of the water level.

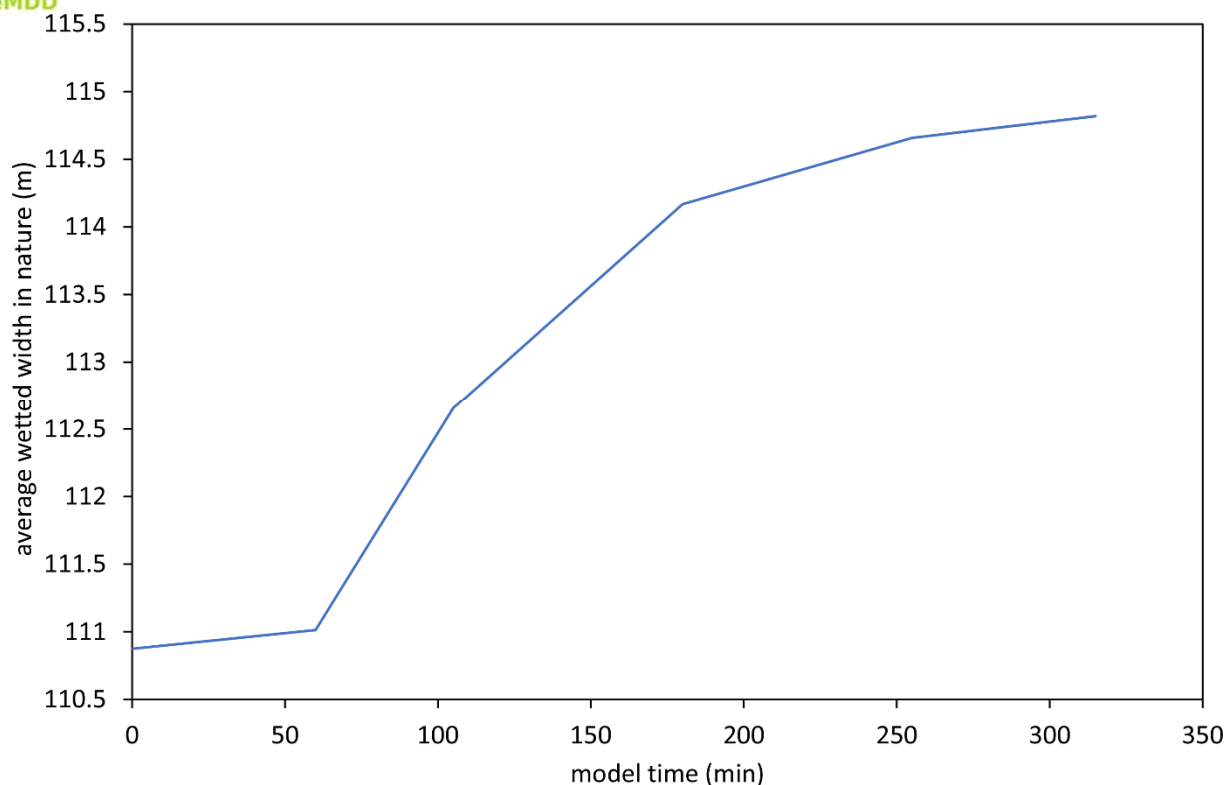


Figure 43. The wetted width at the discharge of  $513 \text{ m}^3 \text{ s}^{-1}$  in the smaller-scale scenario in the period between the start and end of bedload supply.

On average, the deposits cause an increase of bed elevation by about 0.33 m in the Gosdorf section (Figure 44), which mainly results from the local deposits upstream of the bedrock sill.

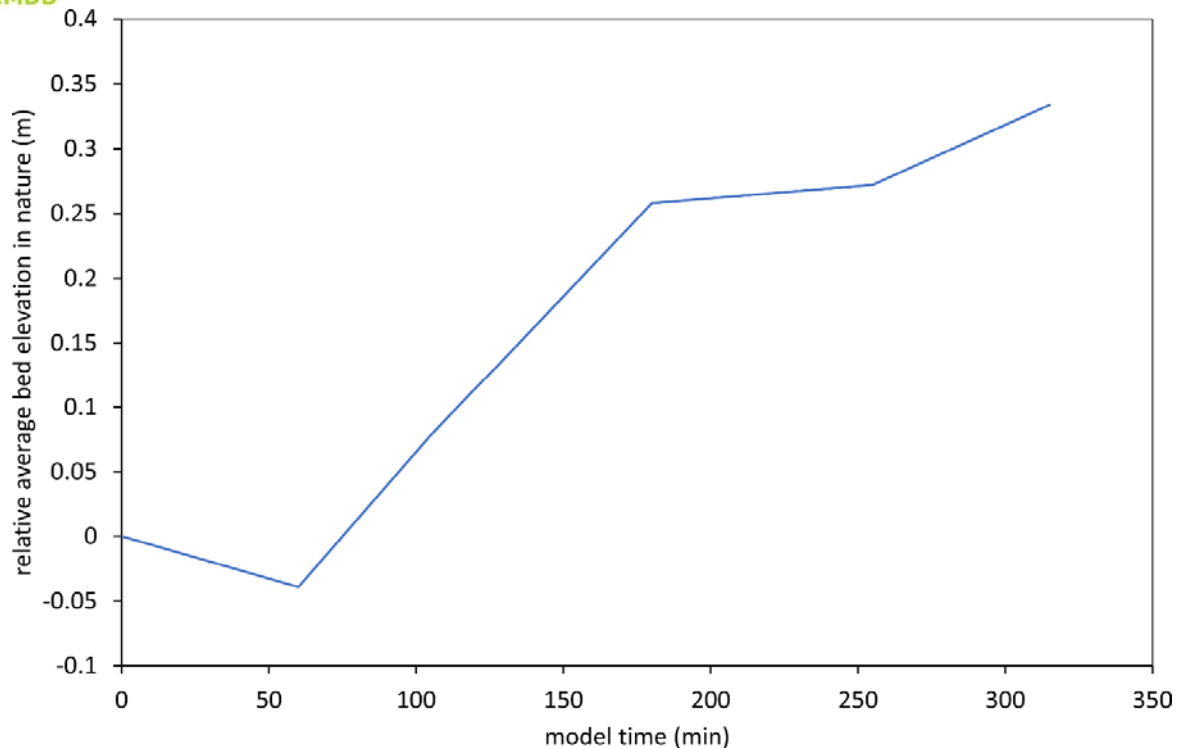


Figure 44. The change in bed elevation between the start and end of bedload supply, analysed within the wetted width of a discharge of  $513 \text{ m}^3 \text{ s}^{-1}$  for definition of the river bed.

Similarly, the cross sections mainly show aggradation in the main channel, but which does not reach into the semiterrestrial zone (Figure 45a). To a little extent, the side-channel shows aggradation along the bank, even in the semiterrestrial zone. Figure 45b displays a diagram for the morphodynamics in this cross section, which relates the elevation relative to the water surface (that of 50% submergence frequency in the vegetation period) to the elevation differences, and which displays in third dimension the frequency of occurrence of each combination. The diagram indicates regions, where morphodynamics would produce bare sediment surfaces in the aquatic and semiterrestrial zones, and where – depending on the elevation of an eventual fine sediment layer – bank erosion would create steep banks eventually suitable for birds nesting in banks.

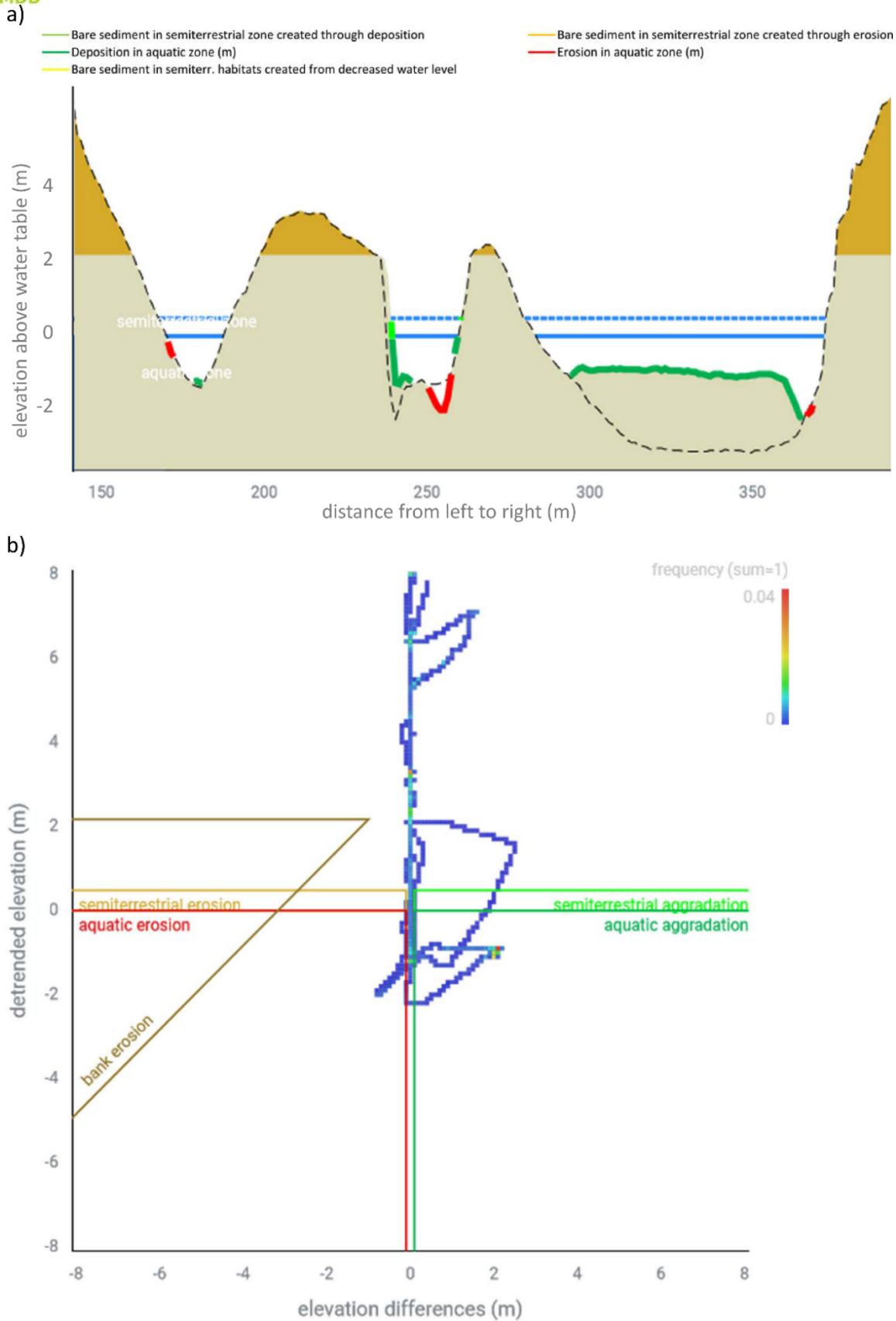


Figure 45. Application of the tool HyMoLink (Klößch et al., 2019) in a cross section of the smaller-scale measure: a) Systematic analysis of morphodynamic changes in a cross section, b) diagram relating elevation above water surface to elevation differences and counting the frequency of occurrence of each combination of classes.

Figure 46 shows the frequency diagram for all analysed 22 cross sections (50 m interval) at once for the entire time period of bedload supply, showing that larger elevation changes were caused by aggradation, to a large part in the aquatic zone. The bedload supplied in this measure approximately corresponds to the annual bedload transport capacity of the channelized Mura River upstream, hence these morphodynamics may reflect the provision of habitats after one year.

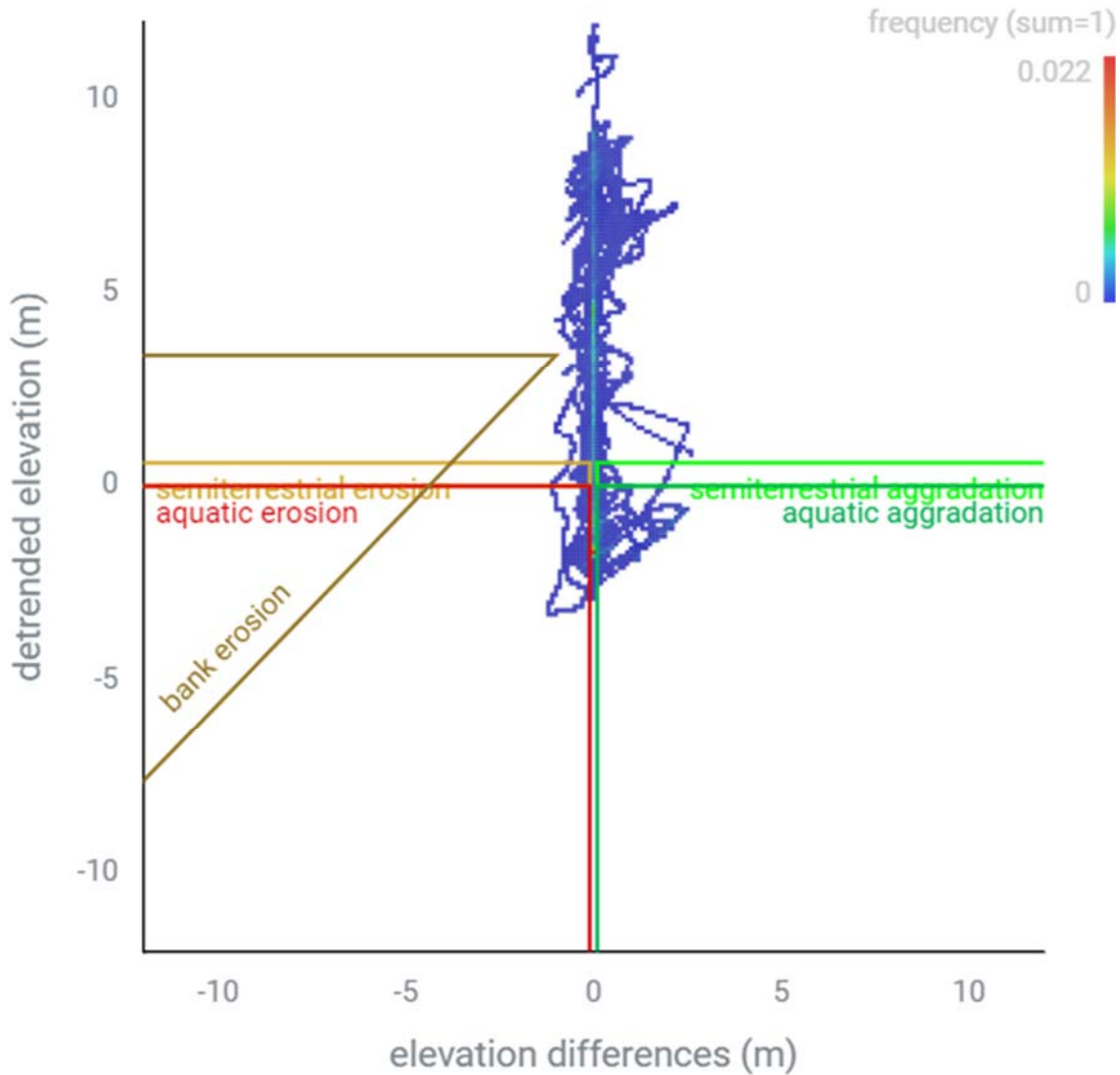


Figure 46. Frequency of occurrence of elevation changes in different elevations for the investigated smaller measure.

- **Larger-scale measure**

Sediment input vs. the sediment output is summarized in Table 12 for the larger-scale measure. In addition, Table 12 shows the duration of the experimental runs under model as well as under natural conditions.

Table 12. Summarized results of sediment input and sediment output under model and natural scales for the larger-scale measure

Model			Nature			
cumulative duration (min)	cumulative sediment input (m <sup>3</sup> )	cumulative sediment output (m <sup>3</sup> )	cumulative hydraulic duration (d)	cumulative sedimentological duration (d)	cumulative sediment input (m <sup>3</sup> )	cumulative sediment output (m <sup>3</sup> )
0	0	0	0	0	0	0
60	0.00	0.001	0.8	5.9	0	438
120	0.03	0.006	1.7	11.8	11744	2347
180	0.06	0.007	2.5	17.6	23488	2432
240	0.10	0.007	3.4	23.5	35232	2656
300	0.13	0.008	4.2	29.4	46976	2725
420	0.19	0.008	5.9	41.1	70465	2767
480	0.23	0.008	6.7	47.0	82209	2853
540	0.26	0.008	7.5	52.9	93953	2989
660	0.32	0.016	9.2	64.6	117441	5799
780	0.39	0.033	10.9	76.4	140929	11834
900	0.45	0.056	12.6	88.1	164418	20398
1020	0.52	0.084	14.2	99.9	187906	30522
1140	0.58	0.104	15.9	111.6	211394	37929
1260	0.65	0.121	17.6	123.4	234882	44023
1380	0.71	0.149	19.3	135.1	258371	53959
1500	0.78	0.202	20.9	146.9	281859	73307
1620	0.84	0.239	22.6	158.6	305347	86761
1740	0.91	0.283	24.3	170.4	328835	102573
1860	0.97	0.345	26.0	182.1	352324	125374
1920	1.00	0.378	26.8	188.0	364068	137148
1968	1.00	0.400	27.5	192.7	364068	145314
2040	1.00	0.423	28.5	199.8	364068	153481
2160	1.00	0.463	30.2	211.5	364068	168193
2400	1.00	0.565	33.5	235.0	364068	205033
2640	1.00	0.705	36.9	258.5	364068	255975
2880	1.00	0.773	40.2	282.0	364068	280467
3120	1.00	0.818	43.6	305.5	364068	297013
3360	1.00	0.848	46.9	329.0	364068	307798
3600	1.00	0.874	50.3	352.5	364068	317356
3840	1.00	0.885	53.6	376.0	364068	321402
4080	1.00	0.898	57.0	399.5	364068	325987
4320	1.00	0.906	60.3	423.0	364068	328818

Again, the sediment output was measured after each experimental run shown in Table 12 which allows a comparison to the sediment input. In Figure 47 the cumulative sediment input and output is depicted.

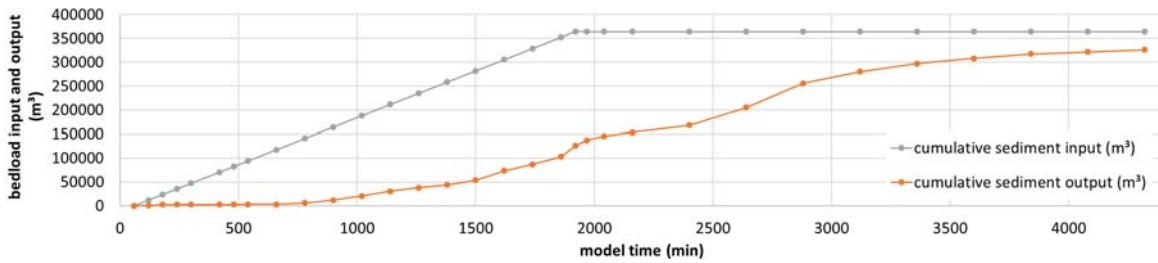


Figure 47. Cumulative sediment input and output for the large measure, with volumes at nature scale related to model minutes.

Based on Figure 47 it can be seen that notable sediment output started after approximately 600 laboratory minutes, which is shown based on the orange graph. After approximately 1500 minutes, according to the sedimentological time scale, the gradient of the cumulative sediment output becomes steeper and flattens after 3000 minutes again. From 3500 minutes on, the cumulative sediment output converges slowly towards the total amount of sediment input. Notably, this happens after about twice the time until bedload supply stopped after all bedload was supplied after 1920 min. Similar to the status quo the zonal statistics have been applied to certain time steps to give an overview of zones with sedimentation and erosion along the 116 profiles. The results for the changes of the mean bed elevations  $\Delta h$  at certain time steps during the sedimentation period (e.g. differences in mean bed elevations by subtracting the digital elevation model at 0 min run time from the model at 900 min run time) is shown in Figure 48.

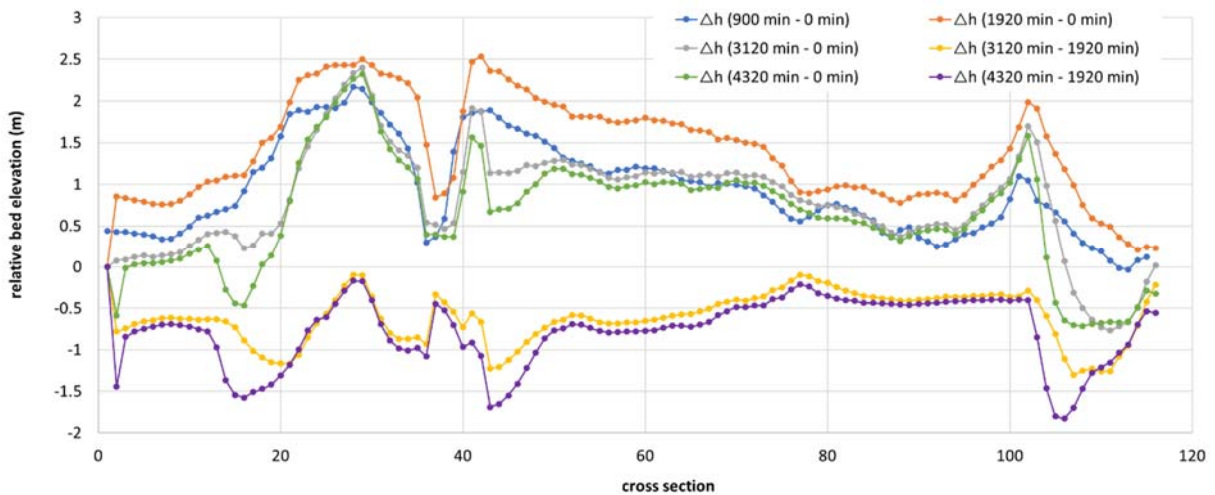


Figure 48. Differences in the mean bed elevation  $\Delta h$  for different time periods per polygon for the large measure

During the sedimentation period, as long as bedload is supplied, until after 1920 min, the mean bed elevations increase constantly in almost every profile, with a maximum of plus 2.5 m. After the entire available sediment volume was fed to the model, the erosion period began. According to Figure 48, decreasing mean bed elevations were observed compared to 1920 min (end of sediment supply), which can be seen in the grey (3120 min - 0 min) and green graph (4320 min - 0 min). Taking the 1920 min elevation model as a basis, it is

clear that the bed is decreasing again, as shown in the yellow (3120 min - 1920 min) and purple graphs (4320 min - 1920 min). The changes in the cumulative volume  $\Delta V$  were calculated for the same cases as shown in Figure 48. During the period until 900 min and until 1920 min increasing volumes were observed. Similar as displayed by the mean bed elevations, erosion occurred after the bedload supply stopped (Figure 49), but from a high intermediate storage of sediment.

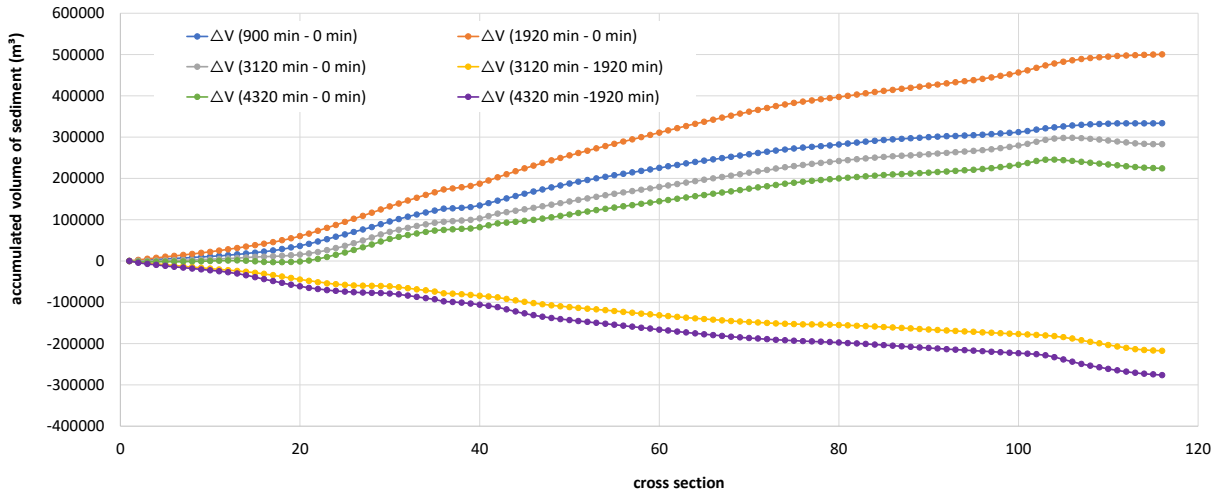


Figure 49. Differences in the cumulative volumes  $\Delta V$  along the profiles for different time periods for the large measure.

Figure 50 displays the elevation differences which occurred until the end of bedload supply at 1920 min, hence at the peak of sediment stored in the reach. The island, which separated the new left channel from the old main channel was completely eroded and sediment deposited all over the riverbed, except for the outlet section.

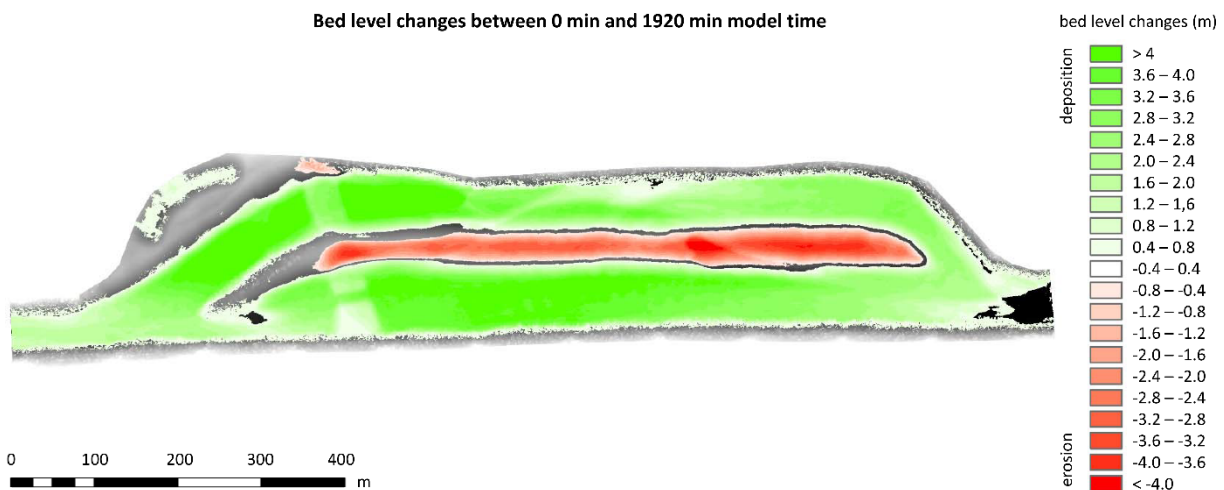


Figure 50. Morphological changes between the beginning of the model run and the point in time, when the excavated sediment used as supply was consumed.

In the differences between the elevation models from 1860 min and 1920 min, thus in the last investigated time step before bedload supply stopped, morphodynamics occur in the entire area (Figure 51).

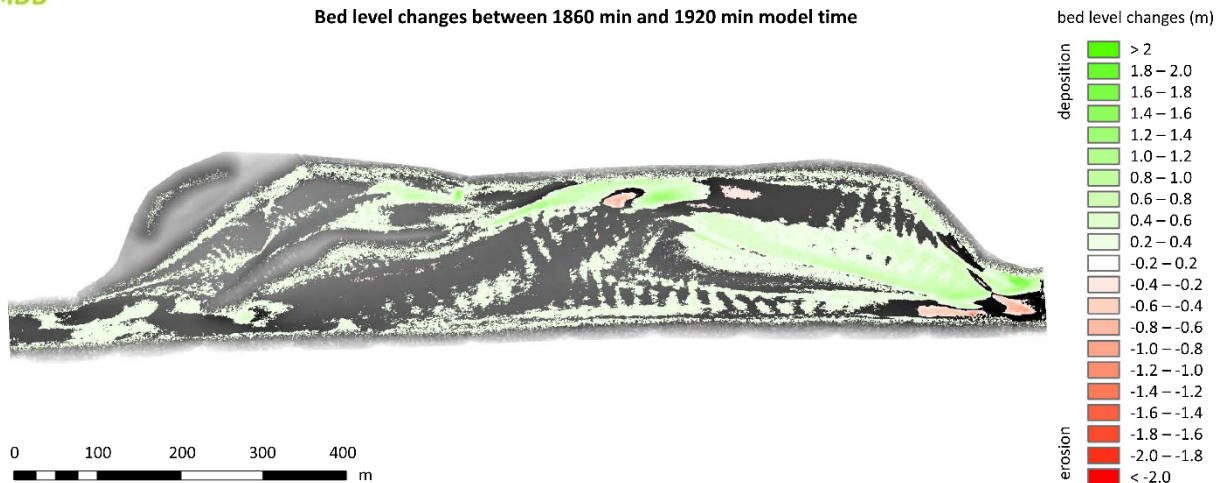


Figure 51. Morphodynamics in the large measure towards the end of sediment supply in the model time span between 1860 min and 1920 min.

As a result of the morphodynamics, the wetted width (at the investigated discharge of  $513 \text{ m}^3 \text{ s}^{-1}$  at nature scale) increases from about 120 m after measure initiation to about 160 m at the end of bedload supply (Figure 52). After the supply ended, degradation at sediment deficit tends to form narrower channels, which can be identified by a narrowing to about 140 m at the end of the experiment.

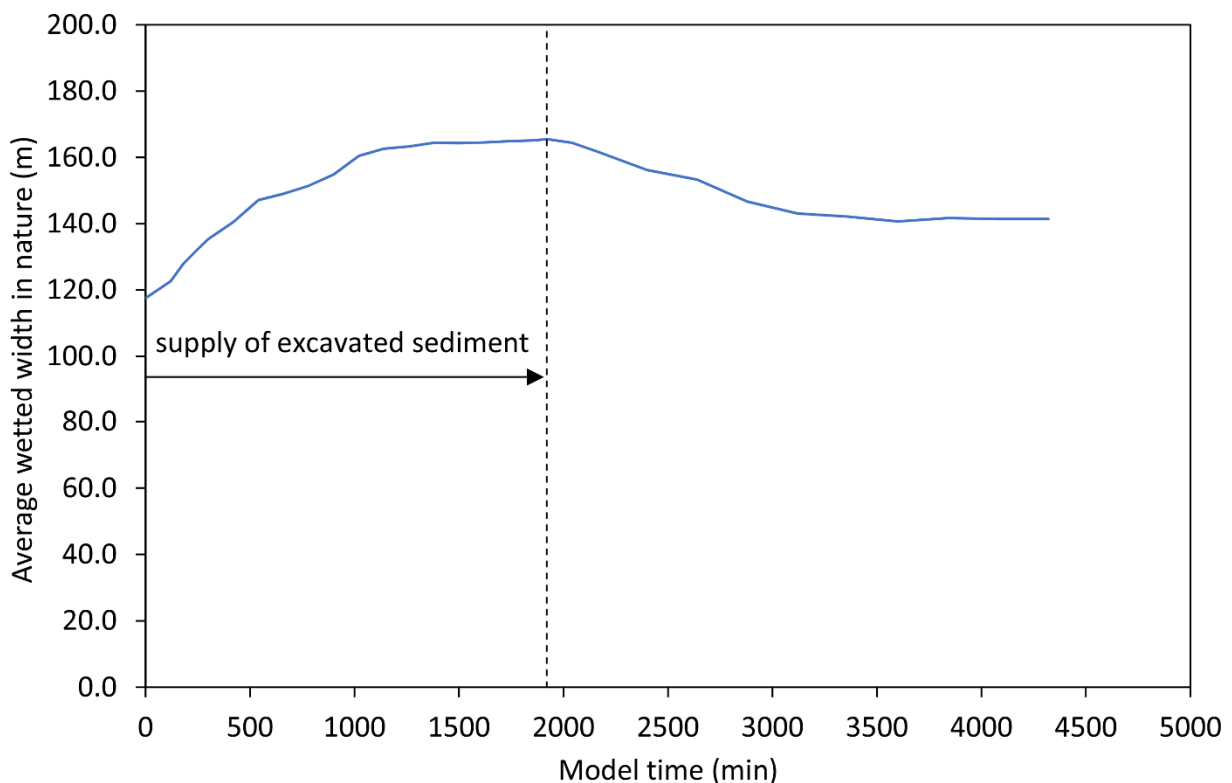


Figure 52. Change of the average wetted width in the restored section following the implementation of the larger-scale measure.

The increase in width and the excess bedload supply goes along with a strong increase of bed levels, now evaluated within the wetted width of mean discharge to define the river bed (Figure 53).

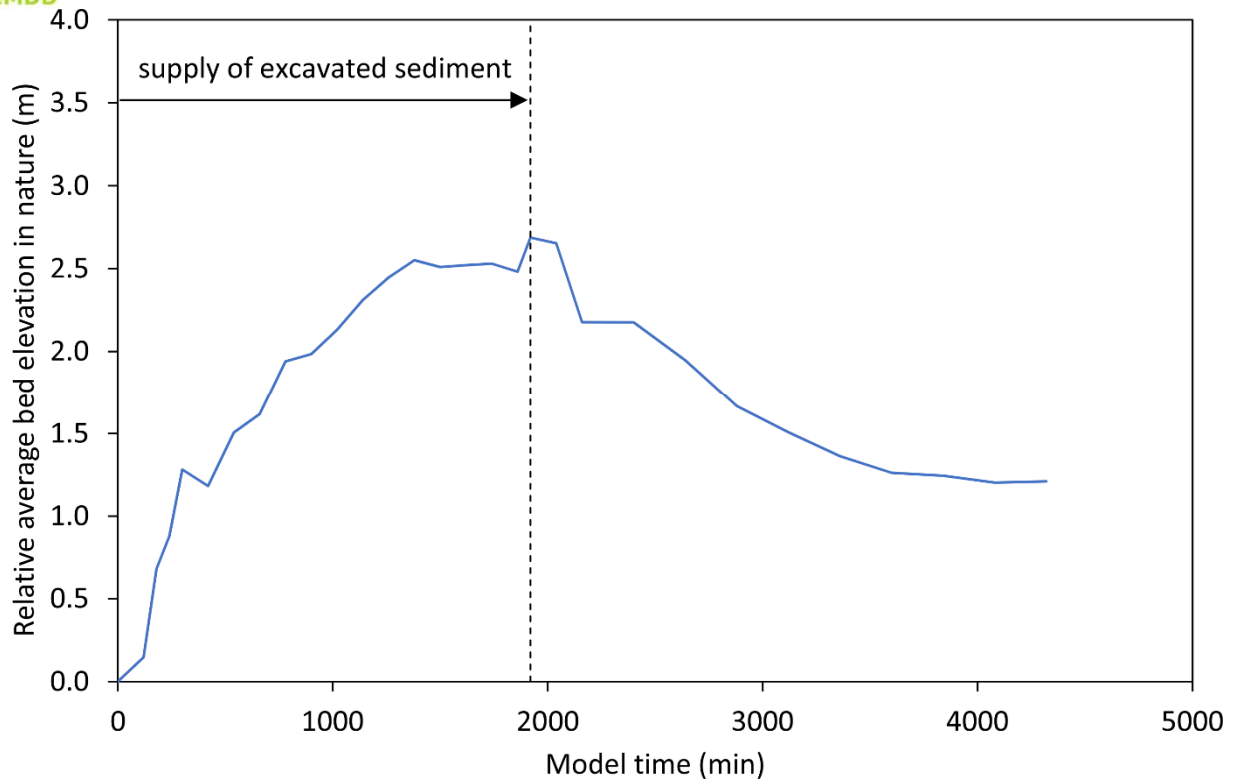


Figure 53. change of the mean bed elevation in the wetted width of the restored section following implementation of the larger-scale measure.

Figure 54, Figure 55 and Figure 56 exemplify the results for one cross section in the larger-scale measure in several time periods. The sequence shows the erosion of the bank of the island, which is then followed by depositions elsewhere which finally reach the elevation of the semiterrestrial zone, there providing habitat with bare surfaces which are unsubmerged for the larger part of the time in the vegetation period. Each cross section is accompanied by a frequency diagram (relating relative elevation to elevation changes) which summarizes the morphodynamics for each cross section and assigns morphodynamics to categories as displayed by the polyline colours in the cross sections.

- Bare sediment in semiterrestrial zone created through deposition
- Deposition in aquatic zone (m)
- Bare sediment in semiterr. habitats created from decreased water level

- Bare sediment in semiterrestrial zone created through erosion
- Erosion in aquatic zone (m)

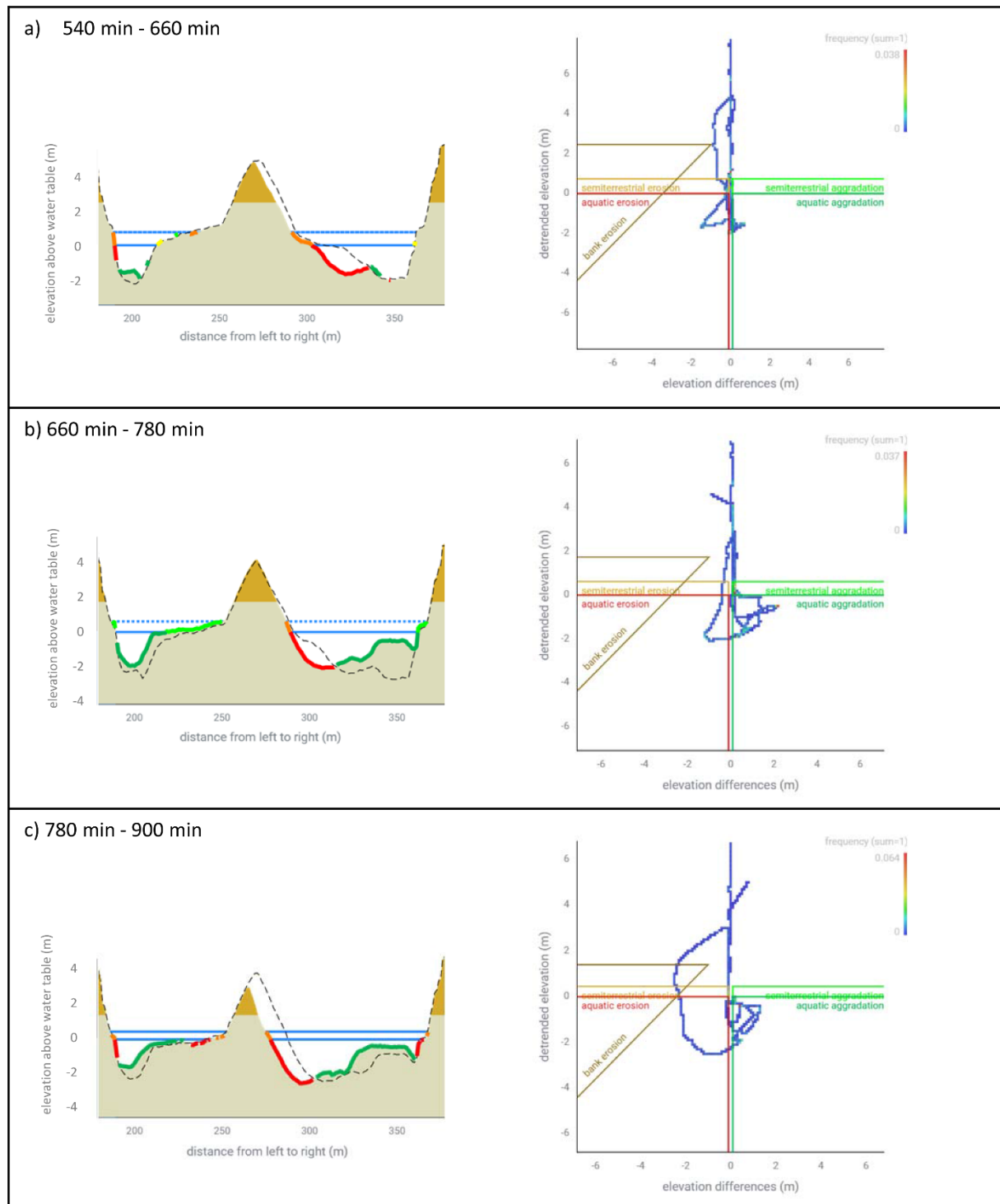


Figure 54. Morphodynamics in a cross section displayed in cross-sectional view and in a diagram showing the frequency of elevation changes in different vertical positions in relation to the water table, for the model time intervals a) 540 min – 660 min, b) 660 min – 780 min, and c) 780 min – 900 min.

- Bare sediment in semiterrestrial zone created through deposition
- Deposition in aquatic zone (m)
- Bare sediment in semiterr. habitats created from decreased water level

- Bare sediment in semiterrestrial zone created through erosion
- Erosion in aquatic zone (m)

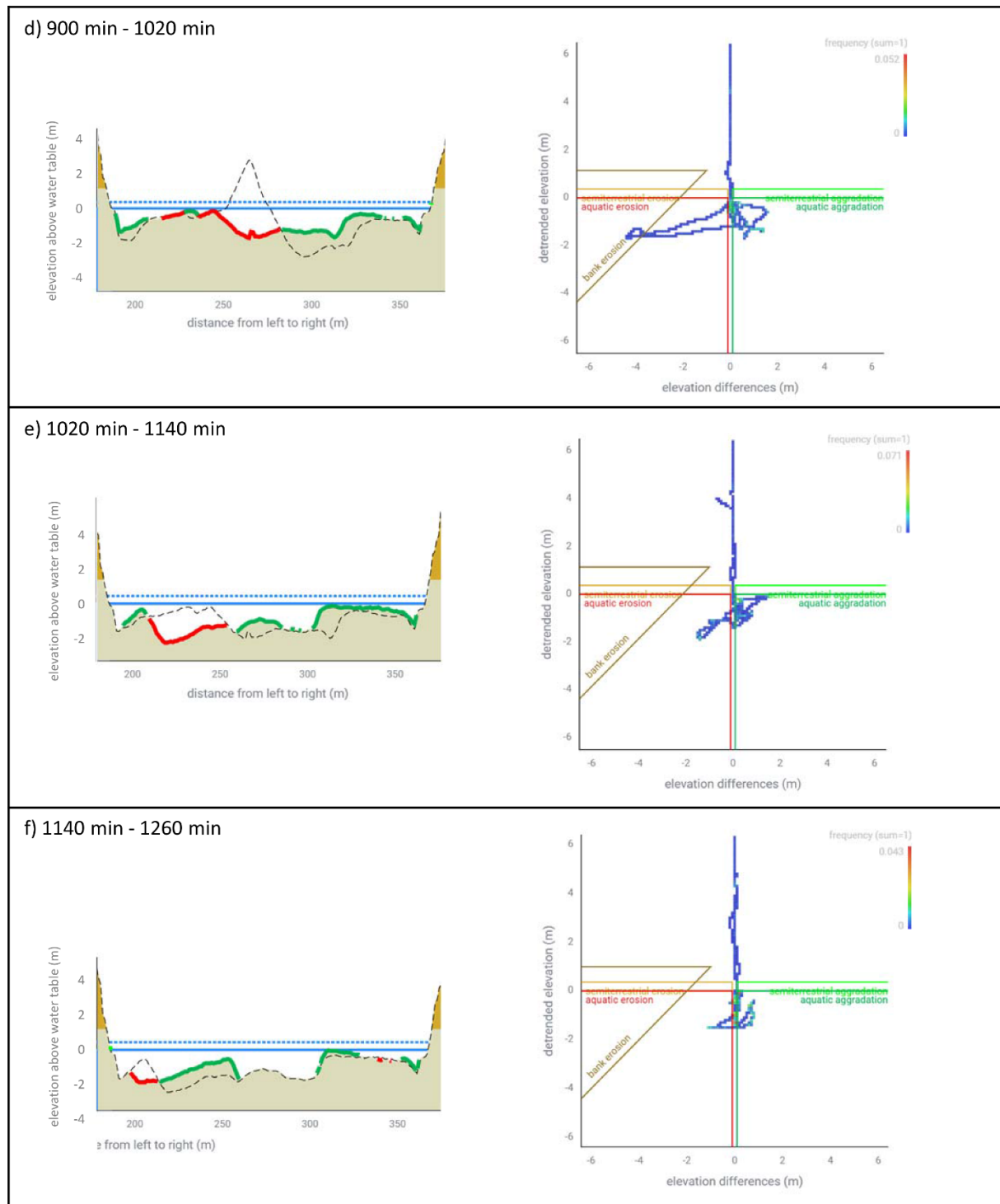


Figure 55. Morphodynamics in a cross section displayed in cross-sectional view and in a diagram showing the frequency of elevation changes in different vertical positions in relation to the water table, for the model time intervals a) 900 min – 1020 min, b) 1020 min – 1140 min, and c) 1140 min – 1260 min.

— Bare sediment in semiterrestrial zone created through deposition  
 — Deposition in aquatic zone (m)  
 — Bare sediment in semiterr. habitats created from decreased water level

— Bare sediment in semiterrestrial zone created through erosion  
 — Erosion in aquatic zone (m)

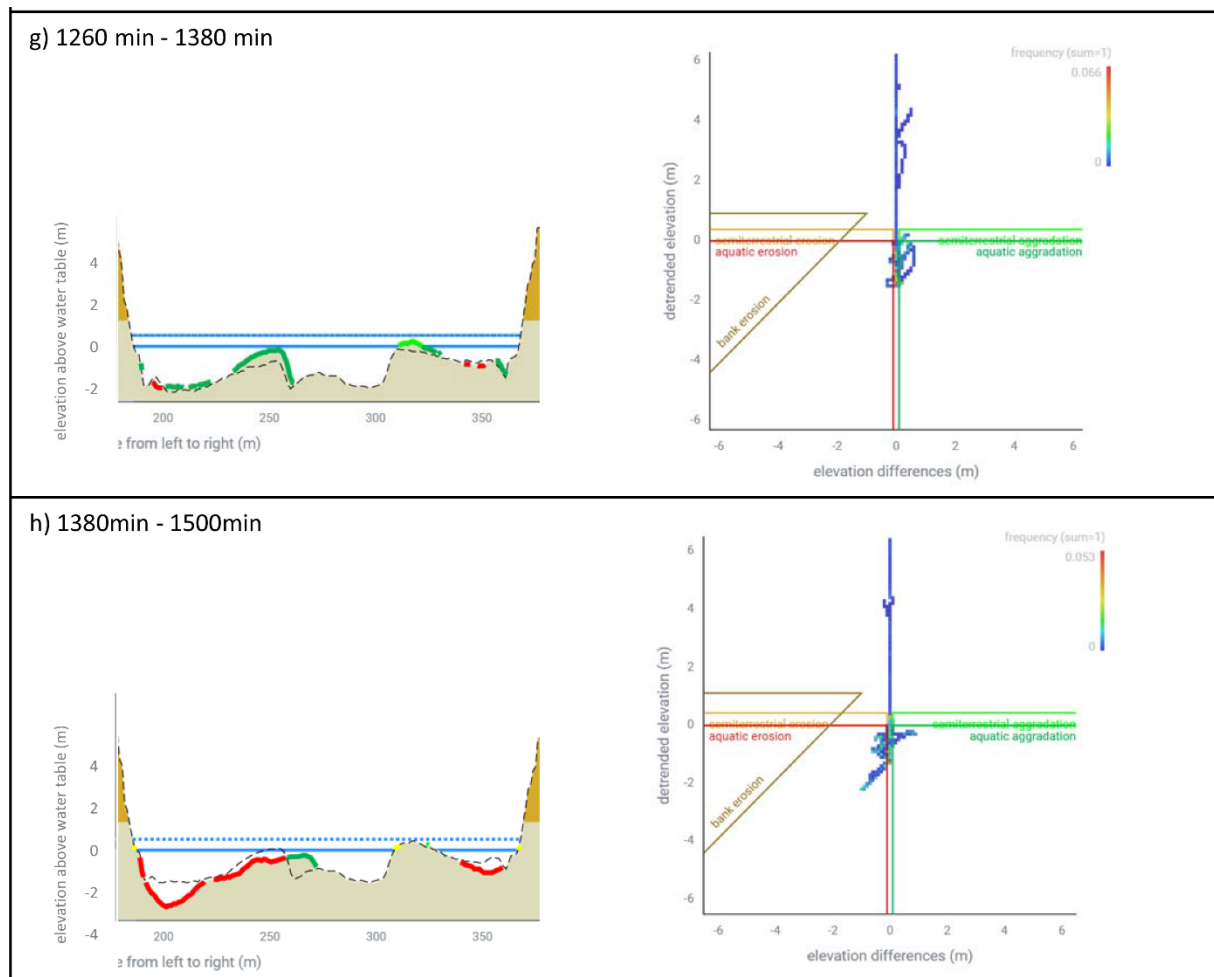


Figure 56. Morphodynamics in a cross section displayed in cross-sectional view and in a diagram showing the frequency of elevation changes in different vertical positions in relation to the water table, for the model time intervals a) 1260 min – 1380 min, and b) 1380 min – 1500 min.

Figure 57 shows the frequency diagram for all analysed 22 cross sections (50 m interval) at once for the time period between 1620 min and 1860 min, showing that larger elevation changes were caused by aggradation, to a large part in the aquatic zone. The time period was selected as it is towards the end of bedload supply, and the duration approximately corresponds to the time needed by the river to approximately supply the annual yield of bedload ( $\sim 45000 \text{ m}^3$  in nature). As in the smaller scale measure, bare sediment surfaces are formed in both the aquatic and semiterrestrial zone. As the banks were already eroded, no more bank erosion occurred in fine sediment layers over a depth of more than 1m. If the channel would also be allowed to migrate, such as possible in Type C sections proposed in the EU-Interreg V-A SI-AT goMURra project, bank erosion would repeatedly occur and better provide habitats also for bank-nesting birds. Figure 57 shows a more diverse pattern of frequency than the respective diagram of the smaller-scale measure in Figure 46, where most frequencies of occurrence are in the no morphodynamics range (defined here between -0.1 m and 0.1m elevation change). Most important, when using the annual yield of sediment supply ( $45000 \text{ m}^3 \text{ a}^{-1}$  in the

channelized section according to findings in the goMURra project) to derive the nature time scale, the smaller measure would provide such habitats for one year until all the sediment (roughly 40000 m<sup>3</sup>) was supplied, while in the larger measure the model time at the end of the bedload supply (1920 min) approximately corresponds to 8 years considering the supply of about 363000 m<sup>3</sup>.

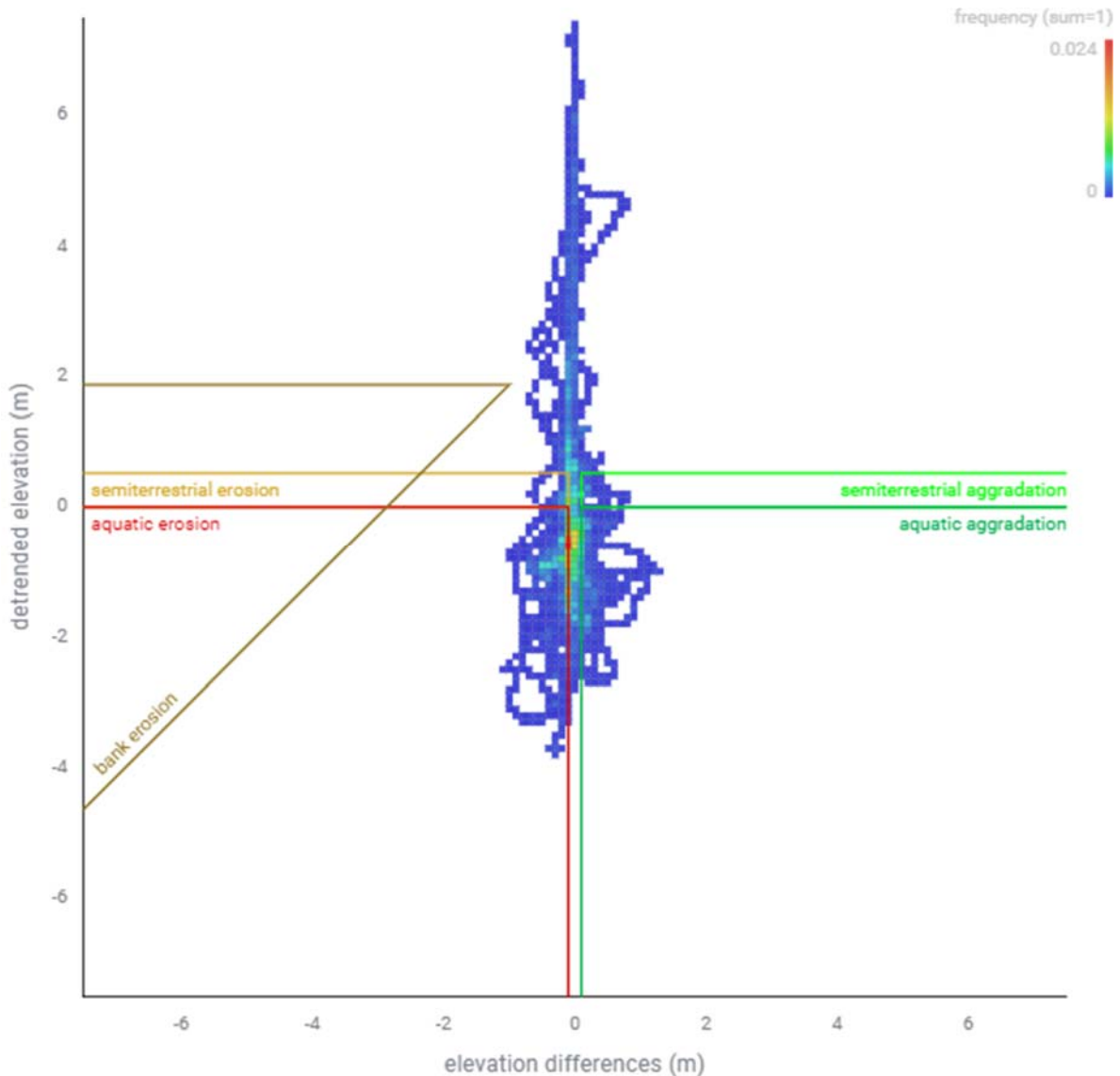


Figure 57. Frequency of occurrence of elevation changes in different elevations for the investigated larger-scale measure.

Moreover, the large amount of sediment stored in the large-scale measure causes a new creation of semiterrestrial habitats also beyond the period of bedload supply (Figure 58).

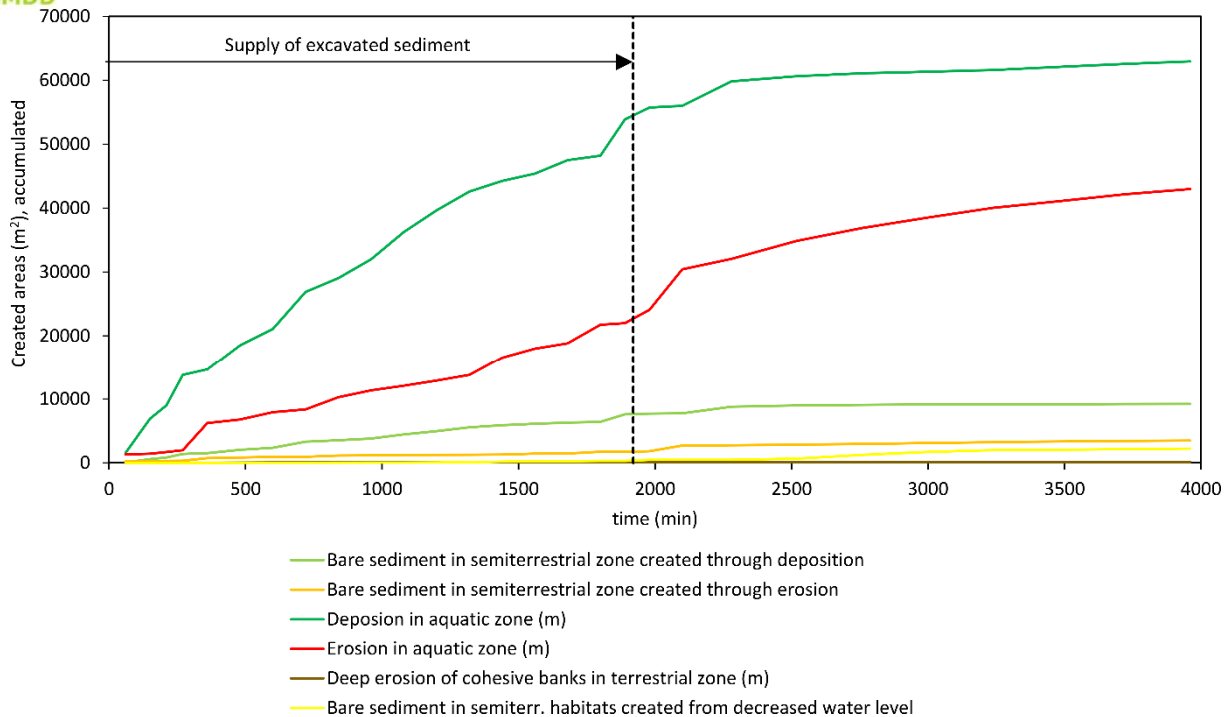


Figure 58. Cumulative provision of habitats potentially of increased usability for rejuvenation of riverine species in the larger-scale measure.

In Figure 59, the created semiterrestrial habitats were estimated for the morphodynamics of one year in nature, based on the time needed to transport annual bedload yields in the upstream channelized section in the model and in nature. At the status quo, only very little areas are created in the semiterrestrial zone, and probably in nature the provision of semiterrestrial habitats would be even less as the model showed more bank erosion near the bedrock sill than in nature. Negligible areas of semiterrestrial zone are created through deposition, a quite large proportion of new semiterrestrial area simply resulted from the lowering of the water surface as a consequence of incision. The dynamics of the planned smaller-scale measure increased the provision of habitats in the semiterrestrial zone, both through erosion and deposition. The larger-scale measure provides most semiterrestrial habitats. Again, it needs to be considered that these areas are estimated to be provided annually, while the bedload is supplied to the smaller measure for one year only. In the larger measure bedload is supplied for 8 years and dynamics continue based on the larger storage after the supply ended.

Note that in the model the bedload was supplied at the carrying capacity of the upstream channelized section, which is higher than the carrying capacity of natural or restored rivers. The results of the EU-Interreg V-A SI-AT project goMURra-measures showed that the bedload demand of wider and more curved channels is significantly reduced ( $\sim 20000 \text{ m}^3 \text{ a}^{-1}$  in the measure Type C instead of  $45000 \text{ m}^3 \text{ a}^{-1}$  in the channelized Mura River), so that less bedload supply is sufficient to maintain a more natural morphology. Hence, once the morphology developed, less annual bedload supply is required while the excavations for the larger measures provide more material, which strongly increases the time the material can be replenished.

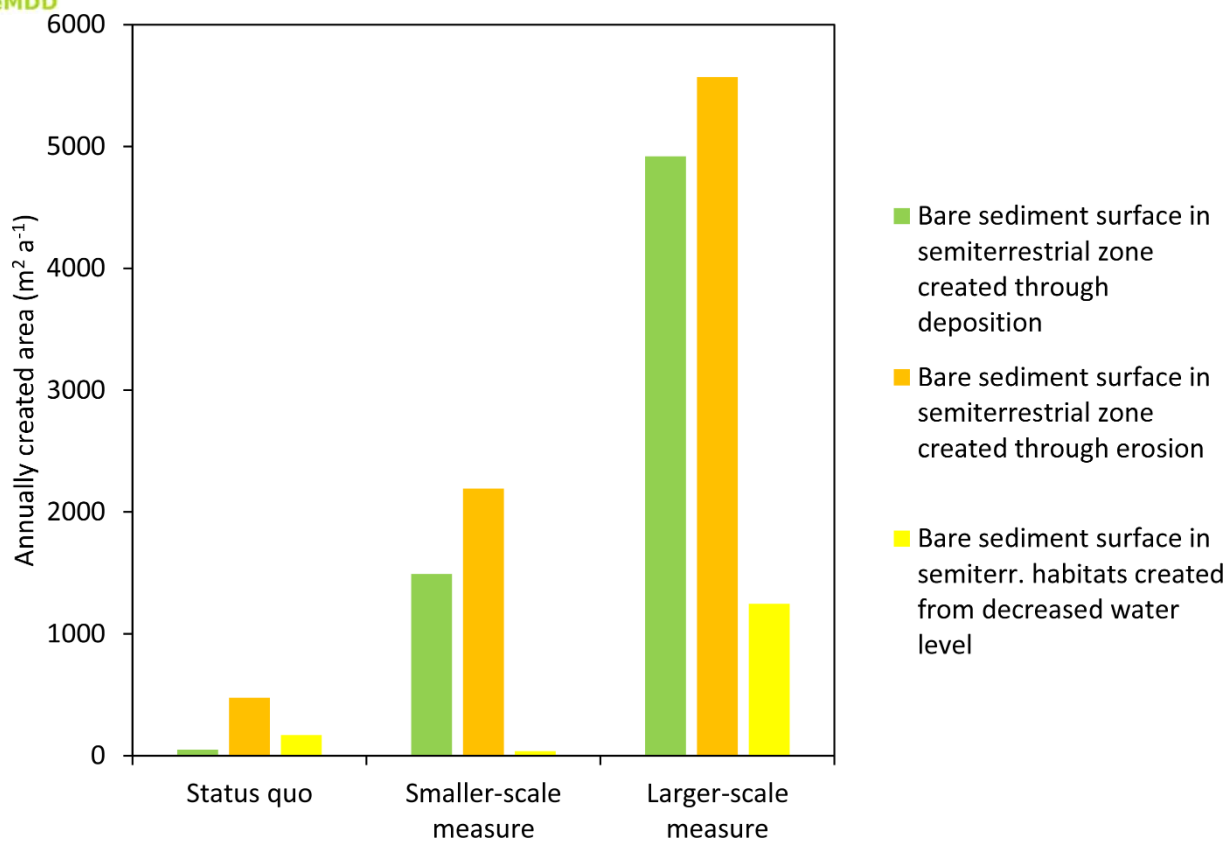


Figure 59. Bare sediment surfaces created annually in the status quo, in the smaller-scale measure and in the larger-scale measure, calculated for a period corresponding to one year of bedload supply. Note that in the smaller-scale measure, all bedload supply may eventually be consumed within one year only.

## V. Summary, conclusions & recommendations for action

The Mura River at the border between Austria and Slovenia has been severely affected by channelization and the reduction of sediment supply from the catchment. While the narrowing and bank protection had immediate negative impacts on habitat availability (loss of gravel bars and of natural eroding banks), the situation was aggravated because the increased transport capacity in the narrower and steeper channel and the reduction of sediment supply caused a strong imbalance in the sediment budget, resulting in channel incision. The channel incision was accompanied by a lowering of the water levels, which increasingly disconnected the floodplain and the mill channels from the river. In addition, the channel incision threatened to reach the tertiary sediment below the gravel bed, which would lead to a loss of gravel and - depending on the erodibility of the tertiary sediment - eventually to a sudden riverbed breakthrough. In that case, tertiary fines would be washed out in suspension, which would result in a drop of the bed by several meters, which probably cannot be restored by ecologically oriented renaturation measures.

The countermeasures implemented according to the basic water management concept completed in 2001 initially had a stabilizing effect on the riverbed and provided habitat. However, due to the negligible bedload input from upstream in the widening section at Gosdorf, there was only a low hydraulic load on the banks and only little bedload input derived from bank erosion, so that the effect of the measure lasted for a shorter period than expected. An updated analysis of the bed levels in D.T1.2.3 (Klösch et al., in prep.) showed that channel incision resumed unexpectedly quickly after a short stabilisation phase. Currently, the average height of the riverbed is below the level before the implementation of the countermeasure. The reduced distance to the tertiary as well as the high pressure on biodiversity requires an immediate and effective restoration measure.

In the bilateral EU Interreg V-A SI-AT project goMURra, bedload supply, channel width and channel slope were identified as the most important parameters determining the sediment balance of the Mura River. Depending on the local spatial constraints, several types of measures were derived that aim at a dynamic equilibrium with stabilised bed levels. The largest measure type, type C, makes the greatest use of the floodplain with the greatest curvature (thus the lowest channel gradient) and the greatest width, resulting in the lowest bedload transport capacity, while the ecological benefit is the greatest (Klösch et al., 2021).

Considering the outcome of the goMURra project, the restoration measure implemented in lifelineMDD was designed. First, a large-scale measure was planned that took into account the need to increase the curvature of the main channel and the width. Subsequently, the planner devised a smaller measure, taking into account the available budget for restoration costs, but with the overall aim of continuing the restoration works towards the larger measure beyond the end of the project lifelineMDD.

In the laboratory, a model was created at a plan view scale of 1:110, which included the restored section at Gosdorf and parts of the upstream and downstream channelized sections as inflow and outflow sections. The laboratory model first reconstructed the incising trend of the bed on the Mura River in its current state without bedload supply. Subsequently, the two variants of restoration (the small-scale measure to be implemented in lifelineMDD and the large-scale measure) were tested for their effects on morphodynamics. In both measures, the sediment excavated during restoration was provided as a supply from upstream at the level of the carrying capacity of the upstream, channelized river. The excavation of the smaller measure provided about 40000 m<sup>3</sup>, that of the larger measure about 360000 m<sup>3</sup>.

Bare sediment surfaces, which are formed in the channel by the emergence of bars above the water surface or by erosion of banks or bars, are crucial for the rejuvenation of many river species. Given the limited availability of such habitats under heavy channelization, they act as 'bottleneck habitats' (e.g. Cantin and Post, 2018), limiting the overall abundance of a species. In the analyses of the laboratory model runs, special attention was therefore paid to the corresponding habitats by defining a semi-terrestrial zone based on the frequency of flooding and analysing the morphodynamics - and thus the creation of bare sediment surfaces - in this zone.

Compared to the status quo, the small-scale measure already showed positive effects by raising bed levels and triggering habitat-relevant morphodynamics. After the entire bedload was added, the average bed elevation in the entire Gosdorf section rose by 0.33 m. Within one year, habitats with bare sediment surfaces formed on about 3700 m<sup>2</sup>. The amount of sediment supplied (40000 m<sup>3</sup>) roughly corresponds to the annual sediment transport capacity of the upstream channelized stretch (45000 m<sup>3</sup> a<sup>-1</sup>). Considering the larger width in the restored section (115 m wetted width at mean discharge compared to 76 m in the channelized section), a lower sediment transport capacity can be expected in the restored section, so that the supplied bedload can stabilise the bed for a longer period than one year.

In the larger measure, the bedload supply of approx. 360000 m<sup>3</sup> caused an average increase of bed elevation in the entire Gosdorf section of approx. 2.5 m. Just before all sediment was replenished, the annual formation of bare sediment areas amounted to approx. 10500 m<sup>2</sup> per year. Since the amount of bedload supply is a multiple of the annual bedload transport capacity, morphodynamics of this magnitude are present over several years, in contrast to the small-scale measure. As the wetted width at the assumed bed-forming discharge increased from 76 m in the channelized section to approximately 160 m in the restored section and the slope decreased due to induced curvature, the bedload transport capacity is greatly reduced, as derived for different measure types in EU Interreg V-A SI-AT project goMURra, so that sediment is stored within the restored section for a long period after sediment delivery ceases. Tracking of individual particles revealed heavy burial and thus a large vertical and lateral exchange of transported sediment, which contrasts strongly with transport in the channelized state.

The status quo studied showed that in the absence of sediment supply, only a very small amount of bar-related habitats would develop, even if bank protections are already removed. This finding underlines the correlations described in the literature, according to which lateral dynamics depend on bedload supply. In sediment-starving rivers, as is most pronounced at the upper end of the Mura River in the TBR MDD, the removal of bank protection is not sufficient to trigger a widening, and bedload stored in the banks would not be sufficiently mobilised to supply bedload to the channel.

The results show that the small-scale measure implemented under lifecycleMDD develops geomorphological features that are relevant as habitat for the rejuvenation of riverine species. However, given the limited increase in width and the lack of curvature of the main channel, the reduction in bedload transport capacity in the restored section remains limited. As a result, the sediment supply, which is roughly equivalent to one year's bedload yield of the channelised Mura River, will be quickly consumed, and the creation of new habitats in the semiterrestrial zone is unlikely to last long after the sediment supply ends - possibly no longer than one year. In the larger-scale measure, the amount of sediment excavated and thus the amount of sediment for replenishment is much greater, while at the same time bedload transport capacity is greatly reduced, resulting in a greatly extended life of the measure, after which sediment replenishment from other resources must continue. The annual creation of new habitats in the semiterrestrial zone was found to be about three times higher than in the smaller measure, but is secured for several years.

The small-scale measure to be implemented in Gosdorf is a first step in the right direction. The bed is temporarily raised and habitats are created. However, this small-scale measure is limited in its effectiveness and therefore requires a continuation of restoration actions. The investigations in this project and in the goMURra project (EU Interreg V-A SI-AT) showed that the efficiency of measures per unit of excavated and replenished sediment increases with the size of the measure, if the measures consider width and slope (slope is adjustable via curvature) as the main underlying parameters. With increasing size, the laboratory experiments showed that the bedload transport capacity falls far below the bedload transport capacity of the upstream channelized section. The sediment was then stored for a longer period of time, which extended the lifetime of the measure far beyond the period of sediment supply.

In the laboratory model, the bedload in both measure variants was replenished with the transport capacity of the channelized section upstream. When implementing the measure, river managers can eventually supply bedload at a lower rate to account for the reduced bedload transport capacity in the restored stretch. However, a minimal 'pulse' of bedload supply is required to allow sedimentation and associated creation of bar-related habitats.

Given the limited length of the inlet section in the model, the stabilising effect of the measure on the upstream section could not be taken into account. In practice, the raising bed levels in the restored section would also have a stabilising effect upstream by reducing the energy slope there and thus also the erosion rate of the replenished sediment (e.g. deposits dumped into the channel) below the former bedload transport capacity of

the channelized section. As a result, some of the replenished bedload would be deposited upstream in the channelized section, but where the narrow channel impedes the emergence of bars. To make better use of the bedload, it is recommended to increase not only the width and curvature but also the longitudinal extent of the restoration measures.

Small side channels run the risk of increasing disconnection from the main channel as the channel aggrades. Such an aggrading trend was detected in the side channel of the smaller-scale measure, while in the larger-scale measure the shift of the main channel (initially triggered by the inlet structure, then maintained by its own dynamics further downstream) ensured dynamics over the entire width.

As the length of a measure increases, more sediment is made available from excavation works, while the demand on bedload supply remains the same. Again, the recommendation is to increase the width and length of the restoration measures to increase the efficiency of the bedload used for restoration. A low annual bedload demand due to decreased bedload transport capacity and a great volume of bedload made available from initiation works of a large measure should maximise the life of the measure and best bridge the period until the permeability of the upstream barriers is improved. Including restoration on the opposite, Slovenian side would allow more curvature of the main channel over a longer distance, provide more excavated material that can be used as sediment supply, and offer greater ecological benefits. Including both sides of the floodplain for restoration would facilitate the development of measures such as Type B and Type C, as recommended in the EU Interreg V-A SI-AT project goMURra. The large-scale measure tested in the hydromorphological model should be recognised as the minimum size for the effectiveness of the measure to achieve the required morphodynamics and provision of ecosystem services. From scientific point of view, it is recommended to also test the measure types of goMURra with hydromorphological laboratory modelling.

## VI. References

- Austrian-Slovenian Standing Committee for the Mur River (2001), Basic Water Management Concept—Phase I, report, Vienna.
- Biedenharn DS, Copeland RR, Thorne CR, Soar PJ, Hey RD, Watson CC (2000). Effective Discharge Calculation: A Practical Guide. US Army Corps of Engineers, Engineer Research and Development Center, Washington DC.
- Cantin, A. and Post, J.R. (2018), Habitat availability and ontogenetic shifts alter bottlenecks in size-structured fish populations. *Ecology*, 99: 1644-1659.  
<https://doi.org/10.1002/ecy.2371>
- Church, M. (2006). Bed material transport and the morphology of alluvial river channels. *Annu. Rev. Earth Planet. Sci.*, 34, pp. 325-354.
- Habersack H, Nachtnebel HP, Hengl M, Poppe M, Schneider J, Fazarinc R (2001b). Flussmorphologie. Endbericht des Themenbereichs 1.4 des Wasserwirtschaftlichen Grundsatzkonzepts für die Grenzmur – Phase I, im Auftrag der Ständigen österreichisch-slowenischen Kommission für die Mur.
- Habersack H, Klösch M, Blamauer B (2013). Geschiebetransport und Seitenerosion an der Grenzmur. WP 3.1: Geschiebe- und Schwebstoffmonitoring, EU Interreg SI-AT Projekts DRA-MUR-CI.
- Hengl H, Habersack H, Nachtnebel HP, Schneider J, Hunziker R, Mikos M (2001). Geschiebetransportmodell. Endbericht des Themenbereichs 1.6 des Wasserwirtschaftlichen Grundsatzkonzepts für die Grenzmur – Phase I, im Auftrag der Ständigen österreichisch-slowenischen Kommission für die Mur.
- Julien, P.Y. (2002): *River mechanics*. Cambridge University Press.
- Julien, P.Y. (2010): *Erosion and sedimentation*. Cambridge University Press.
- Jungwirth M, Zauner G, Pinka P, Hinterhofer M, Holzer G, Krusnik C, Melcher A, Povz M, Schlager E, Unfer G, Wiesner C, Zitek A (2001). Fischbestand Mur. Endbericht des Themenbereichs 2.1 des Wasserwirtschaftlichen Grundsatzkonzepts für die Grenzmur – Phase I, im Auftrag der Ständigen österreichisch-slowenischen Kommission für die Mur.
- Klösch M, Hornich R, Baumann N, Puchner G, Habersack H (2011). Mitigating Channel Incision via Sediment Input and Self-Initiated Riverbank Erosion at the Mur River, Austria. In: Bennett S. J., Castro J. M., Simon A., *Stream Restoration in Dynamic Fluvial Systems: Scientific Approaches, Analyses, and Tools* 194; American Geophysical Union; ISBN 978-0-87590-483-2
- Klösch, M., Tritthart, M., Beikircher, U., Dunst, R., Eder, M., Habersack, H. (2021) Grenzüberschreitender Managementplan zur innovativen nachhaltigen Bewirtschaftung der Grenzmur und zur Verbesserung des Hochwasserschutzes - D.T1.3.2 Sedimenttransportstudie. EU Interreg V-A SI-AT goMURra.

Klösch, M., Dunst, R., Habersack, H. (in prep.). Sediment balance and transport study. EU Interreg Danube Transnational project lifelineMDD, Deliverable D.T1.2.3.

Klösch M, Bertrand M, Boz B, Carolli M, Chouquet I, Dunst R, Egger G, Fragola G, Gaucher R, Gmeiner Ph, Goltara A, Hauer C, Holzapfel P, Humar N, Langendoen EJ, Javornik L, Liébault F, Maldonaldo E, Marangoni N, Molnar P, Pessenlehner S, Pusch M, Recking A, Rossi D, Rozman D, Šantl S, Stephan U, Habersack H (2019). D.T2.3.1. Technical notes on tools to support planning and design of hydromorphological management and restoration measures, Delovni sklop 2, EU-Interreg Alpski prostor, projekt HyMoCARES.

Kobus, H. (1984): Wasserbauliches Versuchswesen. DVWK-Schrift 39. Berlin (in German).

Marti C, Bezzola GR (2009). Bed Load Transport in Braided Gravel-Bed Rivers. In Braided Rivers (eds I. Jarvis, G. H. Sambrook Smith, J. L. Best, C. S. Bristow and G. E. Petts). doi:10.1002/9781444304374.ch9

Mueller ER, Pitlick J (2014). Sediment supply and channel morphology in mountain river systems: 2. Single thread to braided transitions, J. Geophys. Res. Earth Surf., 119, 1516–1541, doi:10.1002/2013JF003045.

Novak, P., Guinot, V., Jeffrey, A., & Reeve, D.E. (2010): Hydraulic modelling – An introduction. Principle methods and applications. Spon Press.

Schumm SA (1985). Patterns of alluvial rivers. Annual Review of Earth and Planetary Sciences 13:1, 5-27

Senfter, S., Unterlercher, M., Zupancic, G., Klösch, M., Habersack, H., Ulaga, F. (2021). Grenzüberschreitender Managementplan zur innovativen nachhaltigen Bewirtschaftung der Grenzmur und zur Verbesserung des Hochwasserschutzes - D.T1.3.1 Maßnahmenkonzept Grenzmur. EU Interreg V-A SI-AT goMURra.

Wagner B, Hauer C, Schoder A, Habersack H (2015). A review of hydropower in Austria: Past, present and future development. RENEW SUST ENERG REV. 2015; 50: 304-314

Zupancic, G., Klösch, M., Unterlercher, M., Ulaga, F., Ristic, M. (2021). Grenzüberschreitender Managementplan zur innovativen nachhaltigen Bewirtschaftung der Grenzmur und zur Verbesserung des Hochwasserschutzes - D.T1.3.1 Measure effectiveness assessment. EU Interreg V-A SI-AT goMURra.